

The role of arginine 204 in *Candida glabrata* tRNA nucleotidyltransferase

Gabriele Colasurdo

A Thesis

In The Department

of

Chemistry and Biochemistry

Presented in Partial Fulfillment of the Requirements

for the Degree of Master of Science

(Chemistry) at Concordia University

Montreal, Quebec, Canada

March 2011

© Gabriele Colasurdo, 2011

CONCORDIA UNIVERSITY

School of Graduate Studies

This is to certify that the thesis prepared

By: Gabriele Colasurdo

Entitled: The role of arginine 204 in *Candida glabrata* tRNA nucleotidyltransferase

and submitted in partial fulfillment of the requirements for the degree of

Master of Science (Chemistry)

complies with the regulations of the University and meets the accepted standards with respect to originality and quality.

Signed by the final examining committee:

Judith Kornblatt Chair
Peter Pawelek Examiner
Joanne Turnbull Examiner
Paul Joyce Supervisor

Approved by

Heidi Muchall
Chair of Department or Graduate Program Director

April 6, 2011

Brian Lewis
Dean of Faculty

ABSTRACT

The role of arginine 204 in *Candida glabrata* tRNA nucleotidyltransferase

Gabriele Colasurdo

The enzyme ATP(CTP):tRNA nucleotidyltransferase is required for protein synthesis in eukaryotes. It allows for the step-wise addition of a specific cytidine-cytidine-adenosine (CCA) sequence to the 3' ends of tRNAs without the use of a nucleic acid template. Crystal structures of the eubacterial and archeal enzymes have been solved both in the presence and absence of model substrates. Based on these studies and primary sequence comparisons, roles for a number of conserved residues have been proposed. Here, we examine the role of an arginine residue in the conserved EDxxR motif. In bacteria, this residue helps nucleotide selection by altering its orientation in space to make distinct hydrogen bonds first with CTP and then with ATP as part of a dynamic amino acid template (Li et al., 2002). We found that changing this arginine (Arg204) in the *C. glabrata* enzyme to alanine, glutamate, or glutamine, results in variant enzymes unable to support *in vivo* growth. Although biophysical experiments show differences between native and variant enzymes, Arg204's primary role is not in defining the enzyme's overall structural integrity. As expected, *in vitro* nucleotide incorporation experiments show a decrease in nucleotide incorporation efficiency at all positions, decreased specificity at position 75, and an increase in specificity at position 76 (compared to the native enzyme). Along with its suggested dynamic role during nucleotide binding, the results shown here suggest that Arg204 in *C. glabrata* tRNA nucleotidyltransferase also plays a role in orienting residues in the binding pocket while altering the pocket's size to aid in discrimination between nucleotides at the different positions.

Table of Contents

List of Figures	viii
List of Tables	xii
List of Abbreviations	xv
1. Introduction	1
1.1 Transfer RNA (tRNA)	1
1.2 ATP(CTP):tRNA nucleotidyltransferase	2
1.3 Nucleotidyltransferase superfamily	2
1.4 Classes of nucleotidyltransferase superfamilies	3
1.5 Structural properties of class II tRNA nucleotidyltransferases.....	6
1.6 Roles of conserved Motifs	10
1.7 The role of arginine 244 in <i>Candida glabrata</i> tRNA nucleotidyltransferase ...	16
1.8 An alternate mechanism of substrate recognition by class II tRNA nucleotidyltransferases.....	18
1.9 Rationale	19
2. Materials and Methods	23
2.1 Strains, Buffers, Growth Media, and Solutions	23
2.2 Construction of expression system	26
2.2.1 Generation of products and ligation into pGEX-2T	26
2.3 Expression and purification of tRNA nucleotidyltransferase	27
2.3.1 Protein expression.....	27
2.3.2 Cell lysis.....	27
2.3.3 Glutathione Sepharose Fast Flow 4B chromatography.....	27
2.3.4 Purification and thrombin cleavage of GST-tagged tRNA nucleotidyl- transferase	28
2.3.5 Sodium dodecyl sulfate polyacrylamide gel electrophoresis (SDS-PAGE)	29
2.3.6 Determination of protein concentration	30
2.4 Biophysical characterization of tRNA nucleotidyltransferase.....	30
2.4.1 Secondary structure determination by circular dichroism	30
2.4.2 Temperature denaturation monitored by circular dichroism.....	31

2.4.3	Tertiary structure determination by fluorescence spectroscopy	31
2.5	Enzyme activity assays	32
2.5.1	Agarose gel electrophoresis	32
2.5.2	Large scale isolation of plasmids G73 and pmBSDCCA from <i>E. coli</i>	32
2.5.3	Preparation of template for <i>in vitro</i> run-off transcription	33
2.5.4	Preparation of <i>in vitro</i> run-off transcribed tRNA with specific 3'ends	34
2.5.5	Urea denaturing polyacrylamide sequencing gels	35
2.5.6	Standard activity assays with various [α - 32 P] GTP transcribed tRNA	36
2.5.7	Time course assays with the various tRNA substrates	38
3.	Results	39
3.1	Expression and purification of native and variant enzymes	39
3.2	Biophysical characterization of tRNA nucleotidyltransferase	42
3.2.1	Secondary structure determination by circular dichroism	42
3.2.2	Thermal denaturation of native and variant enzymes monitored by circular dichroism (CD) spectroscopy.....	44
3.2.3	Tertiary structure characterization by fluorescence spectroscopy	46
3.3	Enzyme assays	49
3.3.1	Run-off transcription assays.....	49
3.3.1.1	Restriction enzyme digests of G73 and pmBsDCCA plasmids.....	49
3.3.1.2	Run-off transcription.....	50
3.3.1.3	Standard and modified tRNA nucleotidyltransferase assays	50
3.3.1.3.1	Assays with the tRNA-N substrate (native and single variant enzymes)	50
3.3.1.3.2	Assays with the tRNA-NC substrate (native and single variant enzymes).....	55
3.3.1.3.3	Assays with the tRNA-NCC substrate (native and single variant enzymes)	57
3.3.1.3.4	Double variant enzyme assays (with tRNA-N, -NC, and -NCC substrates).....	59
3.3.1.4	Time-course assays under standard conditions with tRNA nucleotidyltransferase	62
3.3.1.4.1	Assays with the tRNA-N substrate	62
3.3.1.4.2	Assays with the tRNA-NC substrate.....	70
3.3.1.4.3	Assays with the tRNA-NCC substrate.....	77

3.3.1.4.4	Assays with the tRNA-NCCA substrate	84
3.3.1.5	Time-course assays of tRNA nucleotidyltransferases using the tRNA-NCC template as a substrate with ATP alone	84
3.3.1.6	Time-course assays of tRNA nucleotidyltransferases using the tRNA-NCC template as a substrate with CTP alone	91
3.3.1.7	Modified assays of tRNA nucleotidyltransferase supplied with GTP or UTP alone	97
3.3.1.7.1	Supplied with GTP alone	97
3.3.1.7.2	Supplied with UTP alone	100
4.	Discussion.....	103
4.1	Role of arginine 204 in <i>Candida glabrata</i> tRNA nucleotidyltransferase	103
4.2	Arginine 204 is required for cell viability.....	104
4.3	Substitution of arginine 204 by Ala, Glu, or Gln suggests its primary role is not in defining the enzymes overall structural integrity.....	105
4.3.1	Secondary structure.....	105
4.3.2	Tertiary structure.....	108
4.3.3	Thermal stability	111
4.3.4	Summary	112
4.4	Substitution arginine 244 to Ala, in combination with arginine 204 to either Glu or Gln does not significantly alter the higher order structure of the enzyme.....	113
4.5	Ability of native and variant enzymes to use specific tRNA substrates	114
4.5.1	tRNA-NCC substrate	115
4.5.2	tRNA-NC substrate.....	117
4.5.3	tRNA-N substrate.....	119
4.5.4	Ability of the double variants in utilizing the three tRNA substrates.....	121
4.5.4.1	tRNA-NCC substrate	121
4.5.4.2	tRNA-NC substrate.....	123
4.5.4.3	tRNA-N substrate.....	124
4.5.5	Ability of the enzymes to extend further than tRNA- NCCA	124
4.5.6	Ability of the enzymes to utilize GTP or UTP	125
4.6	Linking biophysical and enzyme assay data	127

4.7	An updated proposed mechanism involving arginines 204 and 244	131
4.8	Conclusion	134
4.9	Future work	135
5.	References	136

List of Figures

		Page
Fig. 1-1	Classical secondary structure of transfer RNA	1
Fig. 1-2	Sequence alignment of some class II tRNA nucleotidyltransferases	6
Fig. 1-3	Crystal structures of 4 different class II tRNA nucleotidyltransferases	7
Fig. 1-4	Model of <i>Candida glabrata</i> tRNA nucleotidyltransferase	9
Fig. 1-5	The role of motif A during CCA-addition	10
Fig. 1-6	Nucleotide binding profile of class II tRNA nucleotidyltransferases	12
Fig. 1-7	Hydrogen bond donor-acceptor patterns for nucleotides in class II tRNA nucleotidyltransferases	14
Fig. 1-8	Model of helices G and J during extension with an incoming ATP	16
Fig. 1-9	Viability of <i>Candida glabrata</i> tRNA nucleotidyltransferase strains with substitutions at Arg204	20
Fig. 1-10	Close up model of domain D of <i>C. glabrata</i> tRNA nucleotidyltransferase.	21
Fig. 3-1	Coomassie blue-stained SDS-PAGE of purified native and variant nucleotidyltransferases	40
Fig. 3-2	Coomassie blue-stained SDS-PAGE representing the stepwise purification of the alanine variant of tRNA nucleotidyltransferase	40
Fig. 3-3	SDS-PAGE (Coomassie blue-stained) representing the stepwise removal of free GST after thrombin cleavage	41
Fig. 3-4	Far-UV CD spectra of native & variant tRNA nucleotidyltransferases	42
Fig. 3-5	Overlaid Far-UV CD spectra of native & variant tRNA nucleotidyltransferases	43
Fig. 3-6	Temperature denaturation of native & variant enzymes monitored by circular dichroism spectroscopy	45
Fig. 3-7	Emission spectra of native & variant tRNA nucleotidyltransferases	46
Fig. 3-8	Overlaid spectra of native & variant tRNA nucleotidyltransferases	47
Fig. 3-9	Agarose gel of digested G73 and pmBsDCCA plasmids	49
Fig. 3-10	Autoradiogram of run-off transcription products separated on a 20% polyacrylamide 7 M urea denaturing sequencing gel	50
Fig. 3-11	Denaturing polyacrylamide gel showing assays under standard conditions using substrate tRNA-N (native and single variants)	54
Fig. 3-12	Denaturing polyacrylamide gel showing assays under standard conditions using substrate tRNA-NC (native and single variants)	56
Fig. 3-13	Denaturing polyacrylamide gel showing assays under standard conditions using substrate tRNA-NCC (native and single variants)	58

Fig. 3-14	Denaturing polyacrylamide gel showing assays under standard conditions using substrate tRNA-N (double variants)	59
Fig. 3-15	Denaturing polyacrylamide gel showing assays under standard conditions using substrate tRNA-NC (double variants)	60
Fig. 3-16	Denaturing polyacrylamide gel showing assays under standard conditions using substrate tRNA-NCC (double variants)	61
Fig. 3-17	Denaturing polyacrylamide gel showing a time-course assay under standard conditions using substrate tRNA-N (Arg204)	64
Fig. 3-18	Denaturing polyacrylamide gel showing a time-course assay under standard conditions using substrate tRNA-N (R204A)	65
Fig. 3-19	Denaturing polyacrylamide gel showing a time-course assay under standard conditions using substrate tRNA-N (R204E)	66
Fig. 3-20	Denaturing polyacrylamide gel showing a time-course assay under standard conditions using substrate tRNA-N (R204Q)	67
Fig. 3-21	Denaturing polyacrylamide gel showing a time-course assay under standard conditions using substrate tRNA-N (R244A-R204E)	68
Fig. 3-22	Denaturing polyacrylamide gel showing a time-course assay under standard conditions using substrate tRNA-N (R244A-R204Q)	69
Fig. 3-23	Denaturing polyacrylamide gel showing a time-course assay under standard conditions using substrate tRNA-NC (Arg204)	71
Fig. 3-24	Denaturing polyacrylamide gel showing a time-course assay under standard conditions using substrate tRNA-NC (R204A)	72
Fig. 3-25	Denaturing polyacrylamide gel showing a time-course assay under standard conditions using substrate tRNA-NC (R204E)	73
Fig. 3-26	Denaturing polyacrylamide gel showing a time-course assay under standard conditions using substrate tRNA-NC (R204Q)	74
Fig. 3-27	Denaturing polyacrylamide gel showing a time-course assay under standard conditions using substrate tRNA-NC (R244A-R204E)	75
Fig. 3-28	Denaturing polyacrylamide gel showing a time-course assay under standard conditions using substrate tRNA-NC (R244A-R204Q)	76
Fig. 3-29	Denaturing polyacrylamide gel showing a time-course assay under standard conditions using substrate tRNA-NCC (Arg204)	78
Fig. 3-30	Denaturing polyacrylamide gel showing a time-course assay under standard conditions using substrate tRNA-NCC (R204A)	79
Fig. 3-31	Denaturing polyacrylamide gel showing a time-course assay under standard conditions using substrate tRNA-NCC (R204E)	80
Fig. 3-32	Denaturing polyacrylamide gel showing a time-course assay under standard conditions using substrate tRNA-NCC (R204Q)	81

Fig. 3-33	Denaturing polyacrylamide gel showing a time-course assay under standard conditions using substrate tRNA-NCC (R244A-R204E)	82
Fig. 3-34	Denaturing polyacrylamide gel showing a time-course assay under standard conditions using substrate tRNA-NCC (R244A-R204Q)	83
Fig. 3-35	Denaturing polyacrylamide gel showing time-course assays under standard conditions using substrate tRNA-NCCA	84
Fig. 3-36	Denaturing polyacrylamide gel showing a time-course assay in the absence of CTP using substrate tRNA-NCC (Arg204)	85
Fig. 3-37	Denaturing polyacrylamide gel showing a time-course assay in the absence of CTP using substrate tRNA-NCC (R204A)	86
Fig. 3-38	Denaturing polyacrylamide gel showing a time-course assay in the absence of CTP using substrate tRNA-NCC (R204E)	87
Fig. 3-39	Denaturing polyacrylamide gel showing a time-course assay in the absence of CTP using substrate tRNA-NCC (R204Q)	88
Fig. 3-40	Denaturing polyacrylamide gel showing a time-course assay in the absence of CTP using substrate tRNA-NCC (R244A-R204E)	89
Fig. 3-41	Denaturing polyacrylamide gel showing a time-course assay in the absence of CTP using substrate tRNA-NCC (R244A-R204Q)	90
Fig. 3-42	Denaturing polyacrylamide gel showing a time-course assay in the absence of ATP using substrate tRNA-NCC (Arg204)	91
Fig. 3-43	Denaturing polyacrylamide gel showing a time-course assay in the absence of ATP using substrate tRNA-NCC (R204A)	92
Fig. 3-44	Denaturing polyacrylamide gel showing a time-course assay in the absence of ATP using substrate tRNA-NCC (R204E)	93
Fig. 3-45	Denaturing polyacrylamide gel showing a time-course assay in the absence of ATP using substrate tRNA-NCC (R204Q)	94
Fig. 3-46	Denaturing polyacrylamide gel showing a time-course assay in the absence of ATP using substrate tRNA-NCC (R244A-R204E)	95
Fig. 3-47	Denaturing polyacrylamide gel showing a time-course assay in the absence of ATP using substrate tRNA-NCC (R244A-R204Q)	96
Fig. 3-48	Denaturing polyacrylamide gel of 30 minute assays using substrate tRNA-N with only GTP present	98
Fig. 3-49	Denaturing polyacrylamide gel of 30 minute assays using substrate tRNA-NC with only GTP present	98
Fig. 3-50	Denaturing polyacrylamide gel of 30 minute assays using substrate tRNA-NCC with only GTP present	99
Fig. 3-51	Denaturing polyacrylamide gel of 30 minute assays using substrate tRNA-N with only UTP present	101

Fig. 3-52	Denaturing polyacrylamide gel of 30 minute assays using substrate tRNA-NC with only UTP present	101
Fig. 3-53	Denaturing polyacrylamide gel of 30 minute assays using substrate tRNA-NCC with only UTP present	102
Fig. 4-1	Close-up of <i>C. glabrata</i> tRNA nucleotidyltransferase model showing Tyr135	106
Fig. 4-2	Model of <i>C. glabrata</i> tRNA nucleotidyltransferase showing fluorophores	109
Fig. 4-3	Schematic mechanism of proposed nucleotide addition in <i>C. glabrata</i> tRNA nucleotidyltransferase	133

List of Tables

	Page	
Table 2-1	Components for buffers, growth media, and solutions	23
Table 2-2	List of chemicals, restriction enzymes, and manufacturers	25
Table 2-3	Construction of tRNAs with specific 3' ends	34
Table 3-1	Melting temperature (T_m) analysis of native and variant enzymes	45
Table 3-2	Peak wavelength and intensity of all studied tRNA nucleotidyltransferases	48
Table 3-3	Fragment sizes (in base pairs) after digestion of G73 and pmBsDCCA plasmids	50
Table 3-4	Percentages of products obtained using tRNA-N as the substrate for standard assays (native and single variants)	54
Table 3-5	Percentages of products obtained using tRNA-NC as the substrate for standard assays (native and single variants)	56
Table 3-6	Percentages of products obtained using tRNA-NCC as the substrate for standard assays (native and single variants)	58
Table 3-7	Percentages of products obtained using tRNA-N as the substrate for standard assays (double variants)	60
Table 3-8	Percentages of products obtained using tRNA-NC as the substrate for standard assays (double variants)	61
Table 3-9	Percentages of products obtained using tRNA-NCC as the substrate for standard assays (double variants)	61
Table 3-10	Percentage of resulting tRNAs from a time-course assay with tRNA-N under standard conditions (Arg204)	64
Table 3-11	Percentage of resulting tRNAs from a time-course assay with tRNA-N under standard conditions (R204A)	65
Table 3-12	Percentage of resulting tRNAs from a time-course assay with tRNA-N under standard conditions (R204E)	66
Table 3-13	Percentage of resulting tRNAs from a time-course assay with tRNA-N under standard conditions (R204Q)	67
Table 3-14	Percentage of resulting tRNAs from a time-course assay with tRNA-N under standard conditions (R244A-R204E)	68
Table 3-15	Percentage of resulting tRNAs from a time-course assay with tRNA-N under standard conditions (R244A-R204Q)	69
Table 3-16	Percentage of resulting tRNAs from a time-course assay with tRNA-NC under standard conditions (Arg204)	71
Table 3-17	Percentage of resulting tRNAs from a time-course assay with tRNA-NC under standard conditions (R204A)	72
Table 3-18	Percentage of resulting tRNAs from a time-course assay with tRNA-NC under standard conditions (R204E)	73
Table 3-19	Percentage of resulting tRNAs from a time-course assay with tRNA-NC under standard conditions (R204Q)	74
Table 3-20	Percentage of resulting tRNAs from a time-course assay with tRNA-NC under standard conditions (R244A-R204E)	75

Table 3-21	Percentage of resulting tRNAs from a time-course assay with tRNA-NC under standard conditions (R244A-R204Q)	76
Table 3-22	Percentage of resulting tRNAs from a time-course assay with tRNA-NCC under standard conditions (Arg204)	78
Table 3-23	Percentage of resulting tRNAs from a time-course assay with tRNA-NCC under standard conditions (R204A)	79
Table 3-24	Percentage of resulting tRNAs from a time-course assay with tRNA-NCC under standard conditions (R204E)	80
Table 3-25	Percentage of resulting tRNAs from a time-course assay with tRNA-NCC under standard conditions (R204Q)	81
Table 3-26	Percentage of resulting tRNAs from a time-course assay with tRNA-NCC under standard conditions (R244A-R204E)	82
Table 3-27	Percentage of resulting tRNAs from a time-course assay with tRNA-NCC under standard conditions (R244A-R204Q)	83
Table 3-28	Percentage of resulting tRNAs from a time-course assay with tRNA-NCC in the absence of CTP (Arg204)	85
Table 3-29	Percentage of resulting tRNAs from a time-course assay with tRNA-NCC in the absence of CTP (R204A)	86
Table 3-30	Percentage of resulting tRNAs from a time-course assay with tRNA-NCC in the absence of CTP (R204E)	87
Table 3-31	Percentage of resulting tRNAs from a time-course assay with tRNA-NCC in the absence of CTP (R204Q)	88
Table 3-32	Percentage of resulting tRNAs from a time-course assay with tRNA-NCC in the absence of CTP (R244A-R204E)	89
Table 3-33	Percentage of resulting tRNAs from a time-course assay with tRNA-NCC in the absence of CTP (R244A-R204Q)	90
Table 3-34	Percentage of resulting tRNAs from a time-course assay with tRNA-NCC in the absence of ATP (Arg204)	92
Table 3-35	Percentage of resulting tRNAs from a time-course assay with tRNA-NCC in the absence of ATP (R204A)	92
Table 3-36	Percentage of resulting tRNAs from a time-course assay with tRNA-NCC in the absence of ATP (R204E)	93
Table 3-37	Percentage of resulting tRNAs from a time-course assay with tRNA-NCC in the absence of ATP (R204Q)	94
Table 3-38	Percentage of resulting tRNAs from a time-course assay with tRNA-NCC in the absence of ATP (R244A-R204E)	95
Table 3-39	Percentage of resulting tRNAs from a time-course assay with tRNA-NCC in the absence of ATP (R244A-R204Q)	96
Table 3-40	Percentage of resulting tRNAs from a 30 minute assay starting with tRNA-N and only GTP present	98
Table 3-41	Percentage of resulting tRNAs from a 30 minute assay starting with tRNA-NC and only GTP present	99
Table 3-42	Percentage of resulting tRNAs from a 30 minute assay starting with tRNA-NCC and only GTP present	99
Table 3-43	Percentage of resulting tRNAs from a 30 minute assay starting with tRNA-N and only UTP present	101

Table 3-44	Percentage of resulting tRNAs from a 30 minute assay starting with tRNA-NC and only UTP present	102
Table 3-45	Percentage of resulting tRNAs from a 30 minute assay starting with tRNA-NCC and only UTP present	102
Table 4-1	Summary of nucleotide incorporation results when the native and variant tRNA nucleotidyltransferase enzymes were supplied with the tRNA-N substrate	128
Table 4-2	Summary of nucleotide incorporation results when the native and variant tRNA nucleotidyltransferase enzymes were supplied with the tRNA-NC substrate	128
Table 4-3	Summary of nucleotide incorporation results when the native and variant tRNA nucleotidyltransferase enzymes were supplied with the tRNA-NCC substrate	128
Table 4-4	Summary of biophysical results compared to the native enzyme	129

List of Abbreviations

A.U.	Absorbance units
AMP	Adenosine monophosphate
APS	Ammonium persulfate
Asp	Aspartic acid / Aspartate
Arg	Arginine
ATP	Adenosine triphosphate
CaCl ₂	Calcium chloride
CCA	Cytidine-Cytidine-Adenosine
CD	Circular Dichroism
CMP	Cytidine monophosphate
CTP	Cytidine triphosphate
dH ₂ O	Distilled water
DNA	Deoxyribonucleic acid
EDTA	Ethylene diamine tetra-acetic acid
FOA	5-fluoro-orotic acid
Gln	Glutamine
Glu	Glutamic acid / Glutamate
GMP	Guanosine monophosphate
GST	Glutathione-S-transferase
GTP	Guanosine triphosphate
HCl	Hydrochloric acid
His	Histidine
IPTG	Isopropyl- β -D-Thiogalactopyranoside
k _{cat}	Turnover number
kDa	Kilodaltons
K _M	Michaelis-Menton constant
Leu	Leucine
mdeg	Millidegrees
NTP	Nucleotide triphosphates
O.D.	Optical density
PAGE	Polyacrylamide gel electrophoresis
PBS	Phosphate buffered saline
PDB	Protein data bank
RNA	Ribonucleic acid
Rpm	Rotations per minute
SC	Synthetic complete
SDS	Sodium dodecyl sulfate
TBE	Tris-Boric acid-EDTA
TdT	Terminal deoxynucleotidyl transferase
TEMED	Tetramethylethylenediamine
T _m	Melting temperature
tRNA	Transfer ribonucleic acid
Tyr	Tyrosine

UMP	Uracil monophosphate
Ura	Uracil
UTP	Uracil triphosphate
UV	Ultraviolet
Xg	Centrifugal force (times the force of gravity)
YT	Yeast tryptone

1. Introduction

1.1 Transfer RNA (tRNA)

During protein synthesis a specific transfer RNA (tRNA) directly carries each activated amino acid to the ribosome. Therefore, the sequence and structure of the transfer RNA is important for correct protein synthesis. Transfer RNAs can be folded into a clover-leaf secondary structure as shown (Figure 1-1) ending with the single-stranded cytidine-cytidine-adenosine (CCA) sequence required for amino acid attachment.

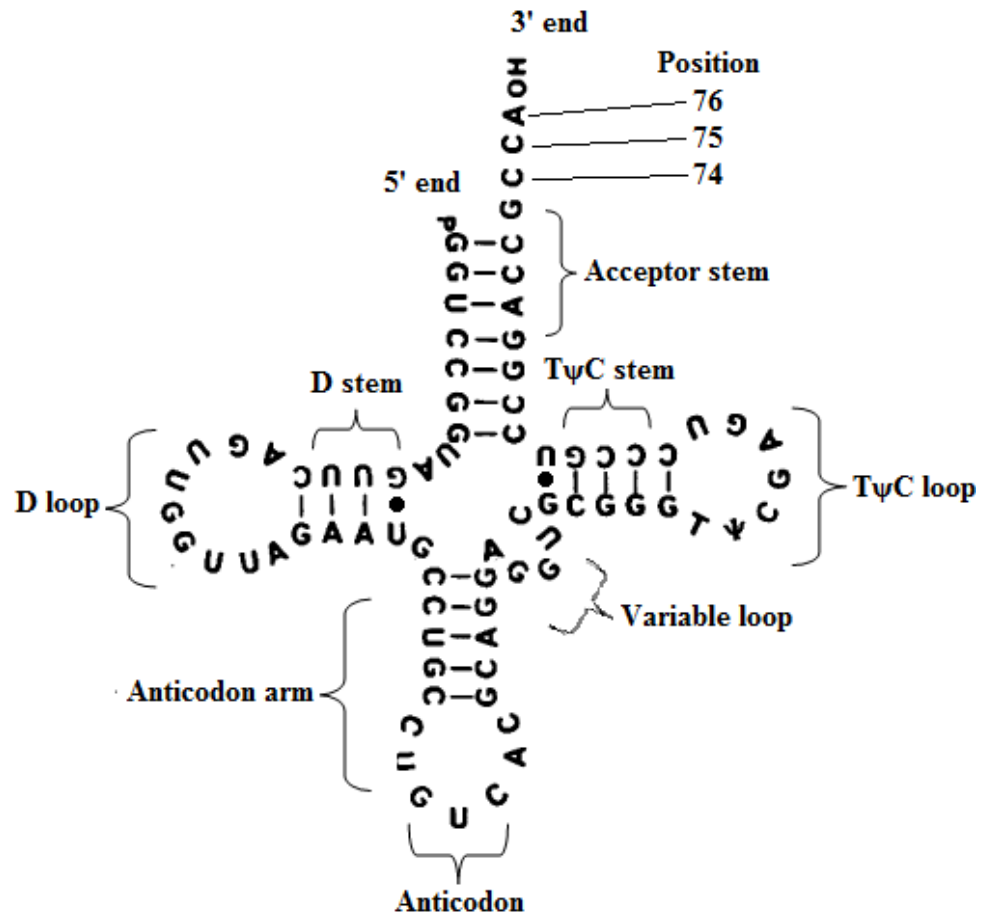


Fig. 1-1. Classical secondary structure of transfer RNA. This is the structure of the tRNA^{Asp} from *Bacillus subtilis*. Dashes (—) represent standard Watson-Crick base pairs, while dots (●) indicate non-standard base pairs. This figure was acquired and modified from Yamada *et al.* (1983). The terminal CCA sequence is numbered according to the standard system for tRNAs.

Although all mature tRNAs contain this 3' terminal CCA sequence required for aminoacylation, this sequence is not found in all tRNA genes and therefore must be added post-transcriptionally by tRNA nucleotidyltransferase in some cases (Hecht *et al.*, 1959; Deutscher, 1973b; Deutscher, 1990). The ability of tRNA nucleotidyltransferase to incorporate specifically AMP and CMP residues into tRNAs that are either completely or partially missing this 3' terminal CCA sequence (Deutscher, 1973b; Deutscher, 1982) will be addressed in this thesis.

1.2 ATP(CTP):tRNA nucleotidyltransferase

For many years, tRNA nucleotidyltransferase has been of considerable interest because of its ability to add a precise nucleotide sequence, always C74, C75, A76 (numbering according to the classical tRNA secondary structure), without a nucleic acid template (Yue *et al.*, 1996; Li *et al.*, 2002). While two other enzymes, poly(A) polymerase (PAP) and terminal deoxynucleotidyltransferase (TdT), are able to add nucleotides without the assistance of a nucleic acid template (Yue *et al.*, 1996; Li *et al.*, 2002), they add varying length chains of a single nucleotide (adenosine and deoxythymidine, respectively) to RNA and DNA, respectively. Although each of these enzymes adds different nucleotides to different templates they all are members of the nucleotidyltransferase superfamily and share some common features.

1.3 Nucleotidyltransferase superfamily

All of the nucleotidyltransferase superfamily enzymes have a characteristic conserved active site motif and use nucleoside triphosphates (NTPs) as substrates (Avarind and Koonin, 1999). The active site motif consists of three carboxylic amino

acids (aspartic acid or glutamic acid) as a triad required for binding two divalent cations (Joyce and Steitz, 1994; Martin and Keller, 1996). Members of this superfamily have a single active site near the amino terminus of the protein. All enzymes in this superfamily likely achieve catalysis by the same conserved mechanism. Initial coupling of the NTP (or dNTP) by the terminal hydroxyl group of the nucleic acid substrate occurs first and results in the elimination of pyrophosphate from the original triphosphate substrate (Holm and Sander, 1995), before addition of the resulting monophosphate.

1.4 Classes of nucleotidyltransferase superfamilies

The nucleotidyltransferase superfamily has been divided into two classes (class I and class II) based on conserved motifs and the presence or absence of a well-conserved 25 kDa amino-terminal domain (Yue *et al.*, 1996). The class I nucleotidyltransferases (lacking the conserved 25 kDa amino-terminal domain) include archeal tRNA nucleotidyltransferases, eukaryotic poly(A) polymerases, and related enzymes such as DNA polymerase β (Pol β), terminal deoxynucleotidyl transferase (TdT), and 2'-5' oligo(A) synthase (Martin and Keller, 2004). Class II enzymes (with the conserved amino-terminal domain) include eukaryotic and eubacterial tRNA nucleotidyltransferases. The conservation of the amino terminus in class II tRNA nucleotidyltransferases allowed the identification of conserved motifs labeled A-E (Li *et al.*, 2002) which are absent in the class I enzymes. This study examines the role of arginine 204 of the class II *Candida glabrata* ATP(CTP):tRNA nucleotidyltransferase. Arg204 is conserved in all class II ATP(CTP):tRNA nucleotidyltransferases and is part of Motif D (Fig. 1-2). This motif has a conserved sequence (E/D)D**xzRzzRzz**RF where R204 is in bold, x is any amino acid and z represents a hydrophobic residue.

```

SC -----MLRSTISLLMNSAAQKTMNSN----- 22
CG -----MFKAIRRVFT----- 10
KL -----MFKMV----- 5
LA MRLSFKTVTNVVVVLPRGRTRSIINFTLFPTITSNLVLP-----LLRTPKTPS----FH 51
AT MRLSSLPIN-TLINLP--KSLFLISPFRFRNLNRSLTVASRISSTLLRVSGVSSRPCGYW 57
AA -----
TM -----
HS -----MLRCLYHWHRPVLNRRWSRLCLLK----- 24
BS -----
EC -----

SC -----FVLNAPKITLTKVEQNICNLLNDYTDLYNQKYHNKPEPLTL 63
CG -----MIPRIQLTEKETRICNLLKDYTAHYNLSLHYGQ-EPLTL 47
KL -----ASKIQLNKVESEICTLVKEFCSHYNKANAET-EPLVA 41
LA SSLSSPMS-----SHKVRDNIQLSDVEKRIFDRLLATLRFN-----LQTHL 93
AT FSTNAAMTNVGEEDKQSIPISELKENIELTDKERKIFDRLLSTLRYCN-----LDTQL 110
AA -----MVGQIAKEMG-----LRA 13
TM -----XQIFRDVSKLLVERVDPKILNLFRLLGKFGDEVN-----XPV 37
HS -----QYLFTMKLQSPFQSLFTEGLKSLTELFVKEN-----HEL 59
BS -----MKPPFQEALGIIQQLKQHG-----YDA 22
EC -----MKI 3

```

Motif A

```

SC RITGGWVRDKLLGQGSDDLDTAINVMSGEQFATGLNEYLQQHYAKYGAKPHNIHKIDKNP 123
CG RITGGWVRDKLLGQGSDDLDTAINIMSGEEFATGLNGYLLEHFDKYGVKPHSIHKIDKNP 107
KL RITGGWVRDKLLGNDSNDLDTAINNMTGEQFAEKLC AFLQDR----GLETHSLHTIDKNP 97
LA RVAGGWVRDKLLGKECYDIDIALDKMMGTEFVDKVVREYLLSI----GEEAQGVCVIESNP 149
AT RVAGGWVRDKLLGKESDDIDIAIDNMSGSEFLDKFKEYLSSR----DEEVQGDVTIERNP 166
AA YIVGGVVRDILLGKEVWDVDFVVEGN-AIELAKELARRHGVN-----VH 56
TM YVVGGFVRDLLLGKIKNLDIDIVVEGN-ALEFAEYAKRFLPGK-----LV 80
HS RIAGGAVRDLLNGVKPQDIDFATTAT-----PTQMKEMFQSAG-----IRMIN 102
BS YFVGGAVRDLLGRPIGDVDLATSAL-----PEDVMAIFPKT-----I 60
EC YLVGGAVRDALLGLPVKDRDWWVVVGS-----TPQEMLDAG-----YQ 40

```

. . * * * * * * * * . .

Flexible loop

Motif B

```

SC ESKKHLETATTKLFGVEVDFVNLRSKYEKLSRIPKVC-FGTPEEDALRRDATLNALFY 181
CG ESKKHLETATTKLFDVEVDFVNLRSKYEKLSRIPKVC-FGTPEEDALRRDATLNALFY 165
KL SKSKHLETCTTKLFDVPVDFVNLRSKYEKLSRIPKVC-FGTPYDDAMRRDATLNAMFY 155
LA DQSKHLETARMRLFDMWIDFVNLRSKYEKLSRIPKVC-FGTPEEDALRRDATLNALFY 208
AT DQSKHLETAKLRIYDQWIDFVNLRSKYEKLSRIPKVC-FGTAKDDAFRRDLTINSLFY 224
AA PFPEFGTAHLKIG-KLKLKELFATARRE-TYPRPGAYPKVE-PASLKEDLIRRDFTINAMAI 113
TM KHDKFXASLFLKGLRIDDIATARLE-YYESPALKLPDVE-XSTIKKDLYRRDFTINAXAI 138
HS NRGEKHGTITARLHEENFEITTLRID-VTTDG-RHAEVEFTTDWQKDAERRDLTINSMFL 160
BS DVGSKHGTVVVVHKGKAYEVTTFFKTDGDYEDYRRPESVTFVRSLEEDLKRRDFTMN---- 116
EC QVGRDFPVFLHPQTHEEYALARTERKSGSGYTGFTCYAAPDVTLEDDLKRRDLTIN---- 96

```

. * * * * * *

	Motif C	Motif D	
SC	NIHKGEVEDFTKR--GLQDLKDGVLRTPLPAKQ	TFLDDPLRVLRRLIRFASR---FNFTID	236
CG	NICQDAVEDFTKR--GWQDLQDGVLRTPLPARQ	TFLDDPLRVLRRLIRFASR---FNFNIE	220
KL	NITIEDKIEDFTKK--GFQDLNDGILRTPLPPRQ	TFIDDDPLRVLRRLIRFASR---FNFQID	210
LA	NINTDSVEDFTKR--GISDLKSGKIVTPLPPKAT	TFLDDPLRVVRAIRFGAR---FEFTLD	263
AT	NINSGAVEDLTER--GIDDLKSGKIVTPLPAKAT	TFLDDPLRVLRRAVRFGAR---FGFTLD	279
AA	SVNLEDYGTLLIDYFGGLRDLKDKVIRVLHP--	VSFIEDPVRILRALRFAGR---LNFKLS	168
TM	KLNPKDFGLLIDFFGGYRDLKEGVIRVLHT--	LSFVDDPTRILRAIRFEQR---FDFRIE	193
HS	GFDG----TLFDYFNGYEDLKNKKVRFVGHAKQ	RIQEDYLRILRYFRFYGR---IVDKPG	213
BS	AIAMDEYGTIIDPFGGREAIRRRIIRTVGEAEK	RFREDALRMMRAVRFVSE---LGFALA	173
EC	ALAQDDNGEIIDPYNGLGDLQNRLLRHVSP---	AFGEDPLRVLRVARFAARYAHLGFRIA	153
	. : . * : . :	: :* *::* ** . :	

Motif E

SC	PEVMAEMGDPQINVAFNSKISR	ERVGVEMEKILV	GGTPLLALQLIQRAHLENVIFFWH--	294
CG	AGVLKEMHDPEINEAFNNKISR	ERIGVEMEKILV	GNPILGLKLIQRTHLENVIFLWH--	278
KL	PQTYQAMRDPGIHQSFNHKISK	GRVYTEMHKTLS	SANPFYALDLIQGAHLSRVIFTTN--	268
LA	EDLKQAAACDEVKDALAAKISR	ERIGTEIDLMS	GNQPVKAMTYICDLTIFWIVFSLPPT	323
AT	EELKEAASSEEVRVALGEKISR	ERIGNEIDLMS	GNGPVSAVTYLSDLKLFVSVFALPSS	339
AA	RSTEKLLK-QAVNLGLLKEAPR	GRLINEIKLAL	REDRFLEILELYRKYRVLEEIEEGF--	225
TM	ETTERLLK-QAVEEGYLERTTG	PRLRQELEKILE	EKNPLKSIRRXAQFDVIKHLFPKT--	250
HS	DHDPETLEAIAENAKGLAGISG	ERIWVELKKILV	GNHVNHLIHLIYDLDVAPYIGLPAN-	272
BS	PDTEQAIV---QNAPLLAHISV	ERMTMEMEKLL	GGPFAARALPLLAETGLNAYLPGLAG-	229
EC	DETLALMR-EMTHAGELEHLTP	ERVWKETESAL	TRNPQVFFQVLRDCCGALRVLPFEID-	211
	. . * : * . :	. . . :		

SC	NDSSVVKFNEENCQDMDKINH	VYNDNILNSHLKSF	IELYPMFLEKLPILREKIG-RSPGF	353
CG	GDQSVIEYNRKNWPQTKDVED	IYKKGIFNHHLKNF	IHHYKDFLSRYLKLQRAIETKDKSF	338
KL	ESS-----PEIESIYEN--	LDQHLKSVVETI	PKLLKSHTTFASVFP----GM	309
LA	FEPAISDGGERLCISQLDIS	WNLIHLLGKTTFT	DEQRRLTYAAMFLPLRNTIYREKKAK	383
AT	AEPSPPENCGSLSSQSYLEAM	WSLLKTPRPGKFS	GEQRRLALYAAMFLPFRKTVYKDTKKG	399
AA	-----QWNEKVLQKLYAL	RKVVVDWHALEF		249
TM	-----YYTPSXDEKXENL	FRNIPWWEENF		274
HS	-----ASLEEFDKVSKN	VDG-----		287
BS	-----KEKQLRLAAAYR	WPWLAA		247
EC	-----ALFGVPAPAKWH	PEIDTGIHTLMTLS		237

SC	QQNFILSAILSPMANLQI	IGNPKKKINNLVSV	TESIVKEGLKLSKNDAAVIAKTVD	SICS 413
CG	QQNFLLASILIPMADLKI	IALPKKKLNNTLP	VSESIVREGLKFNKASSIVVARC	VENIAA 398
KL	QEPLILSLVLSGFKGLK--	GPDPKPKNSIPL	AGVITKEGLNFPNTQVDNVIAC	VESEDS 367
LA	KVPVVNYIFRESLKRKAK	PETVLDLHRASNK	FSLIPLCLVSNEDVQIVGHDW	MTELID- 442
AT	SIPVVNHIKFKFSMKRKT	SDAETVMNIHQ	TTERFRSLIPSLEVKKDVELDEL	TWAADILEH 459
AA	SEERIDYGWLYLLILIS	NLDYERGHKHF	LEEMSAPSWVRETYKFMKFKL	GLSKEEL----- 304
TM	G--EVDRFYAVLHVFL	EYDDESWEKVR	DRYSLRRNLINERHVEKS	SAPALLEXL----- 327
HS	----FSPKPVTLASL	FKVQDDVTKLDL	RKIAKEEKNLGLFIVKNRK	DLIKATD----- 338
BS	REERWALLCHALGVQ	ESRPFRAWKLP	NKVVDEAGAILTALADI	PRPEAWTNEQLFS--- 304
EC	MAAMLSPQVDVRFAT	LCHDLGKGLT	PELWPRHHGHGPAGVK	LVEQLCQRLRVPNEIRD- 296

SC	YEEILAK--FADRSQ	LKKSEIGIFLRN	FNGEWETAHFASLSDAFLKIP	KLETKKIEL--- 468	
CG	YNSMVEK--YLQSGDL	KRSEVGTFLREL	RGDWEIVHYVSLMDQYLK	YSRKDNVFN--- 452	
KL	YHNLVK-----	NGKSMKRSEL	GFALRKLGNWQMVHFYNL	CLDYLRHGDEP----- 413	
LA	-----VPVSSRVR	VLTGFLREL	RDFWRVALLISILLHP-ID	VNDTEDE---SS 487	
AT	WKSITLNDPVI	PATSKIRVLT	GFLLRDIKDFWRVSL	LSLLSATVDGSNDHQ	DIGQLDF 519
AA	-----KKAKENY	EVYRLLKPLH--	TSVLLLLMLEELKE-----		336
TM	-----SERVPAS	FVYPLVKGVS	NETICHFLAYLSGEKEG-----		361
HS	-----SSDPLK	PYQDFIIDS	REPTATTRVCELLKYQ	GEH----- 372	
BS	-----AGLERAL	SVETVRAAFT	GAPPGPWHEKLR	RRRFAS----- 338	
EC	-----LARLVAE	FHDLIHTF	PMLNPKTIVKLFDS	IDAURKP----- 332	

```

SC      ----LFQNYNEFYYSIFDNNLNNCHELKPIVDGKQMAKLLQMKPGP-WLGKINNEAIRWQ 523
CG      ----IIDKYDRFWNYIQEQNLQSDSKMVP IIDGKRMVKILETKPGP-WLGKINDEVILWQ 507
KL      -----IPHYDEFYKHVHDCCKLDDVYTLKHIINGKELAKLLDRKPGI-WMGETLDRILIWQ 467
LA      QLSKRRDLFNTVENSVIKLGLEKVVDVKQLINGKDVMSVLQLKGGP-MVKEWLDKAMACN 546
AT      QLERMRETYLTVEATIHGLGLDKIWDAPLVNGREIMQIAELKGGSRILIREWQQKLLTWQ 579
AA      ---KIKLYLEKLRKVKLPKEKIEELKKQGLK-GKELGERIEELKREIMN----- 381
TM      ---LFKSYLLKIKNTKLEKINGEYLIRKGITSGKIIIGEVLEKILXKKLDGDTRDEEEILE 418
HS      ---CLLKEMQQWSIPFPVSGHDIR-KVGISSGKEIGALLQQLREQ-----WK 416
BS      -----LPIKTKGELAVNGKDVIEVWGKPAWPVKEALDAIWRVAVNGEVENE----K 386
EC      -----QRVEQLALTSEADVRGRTGFESADYPQGRWLREAWVAQSVPTKAVVEAGFKGVE 387
          *      :      :
SC      FDNPTGTDQELITHLKAILPKYL--- 546
CG      FDHPQGTEQELISFIKSILPNYLQ-- 531
KL      LDNPDISKETFIEENLNDIVHLP---- 489
LA      LPIP-----QELQRNVLIG----- 560
AT      LAYPNGTAECKEWMRDIKAKRQRIE 605
AA      -----KIKLAAALE----- 390
TM      EVLASLETEGKLAAALEHHHHHH--- 441
HS      KSGYQMEKDELLSYIKKT----- 434
BS      ERIYAWLMERNRTREKNC----- 404
EC      IREELTRRRRIA AVASWKEQRCPKPE- 412

```

Fig. 1-2. Sequence alignment of some class II tRNA nucleotidyltransferases.

Alignment generated by ClustalW (Gibson *et al.*, 2007). This alignment features tRNA nucleotidyltransferase sequences from *Saccharomyces cerevisiae*, SC (EDN63144); *Candida glabrata*, CG (CAG62257); *Kluyveromyces lactis*, KL (AAG00316); *Lupinus albus*, LA (AAB03077); *Arabidopsis thaliana*, AT (NP_173680); *Aquifex aeolicus*, AA (1VFG_B); *Thermotoga maritima*, TM (3H37A); *Homo sapiens*, HS (BAB70662); *Bacillus stearothermophilus*, BS (Q7SIB1); and *Escherichia coli*, EC (AAA23541). Protein Genbank accession numbers are in brackets. Numbers at the ends of the sequence represent the residue within the sequence. (*) Conserved in all sequences, (:) Similar, and (.) Weakly similar. Motifs A-E were identified from Li *et al.* (2002). The amino acids corresponding to arginine 204 of *Candida glabrata* are in bold. The approximate location of the flexible loop region (Tomita *et al.*, 2004; Betat *et al.*, 2010) is also identified.

1.5 Structural properties of class II tRNA nucleotidyltransferases

Class II tRNA nucleotidyltransferases are said to resemble sea horses, having regions corresponding to a head, neck, body, and tail (Li *et al.*, 2002). Presently, only four class-II tRNA nucleotidyltransferase crystal structures have been solved:

Thermotoga maritima (Toh *et al.*, 2009), *Aquifex aeolicus* (Tomita *et al.*, 2004), *Homo sapiens* (Augustin *et al.*, 2003), and *Bacillus stearothermophilus* (Li *et al.*, 2002) (Figure 1-3). It is important to note that the *Aquifex aeolicus* structure shown is that of an

adenosine-adding enzyme as this organism requires two enzymes for CCA addition: one to add two CMPs and one to add the terminal AMP (Tomita *et al.*, 2001). From these crystal structures, it is clear that class II tRNA nucleotidyltransferases are predominantly alpha helical in character. No crystal structure of any tRNA nucleotidyltransferase has been solved from a fungus, protozoan or any other single-celled eukaryote.

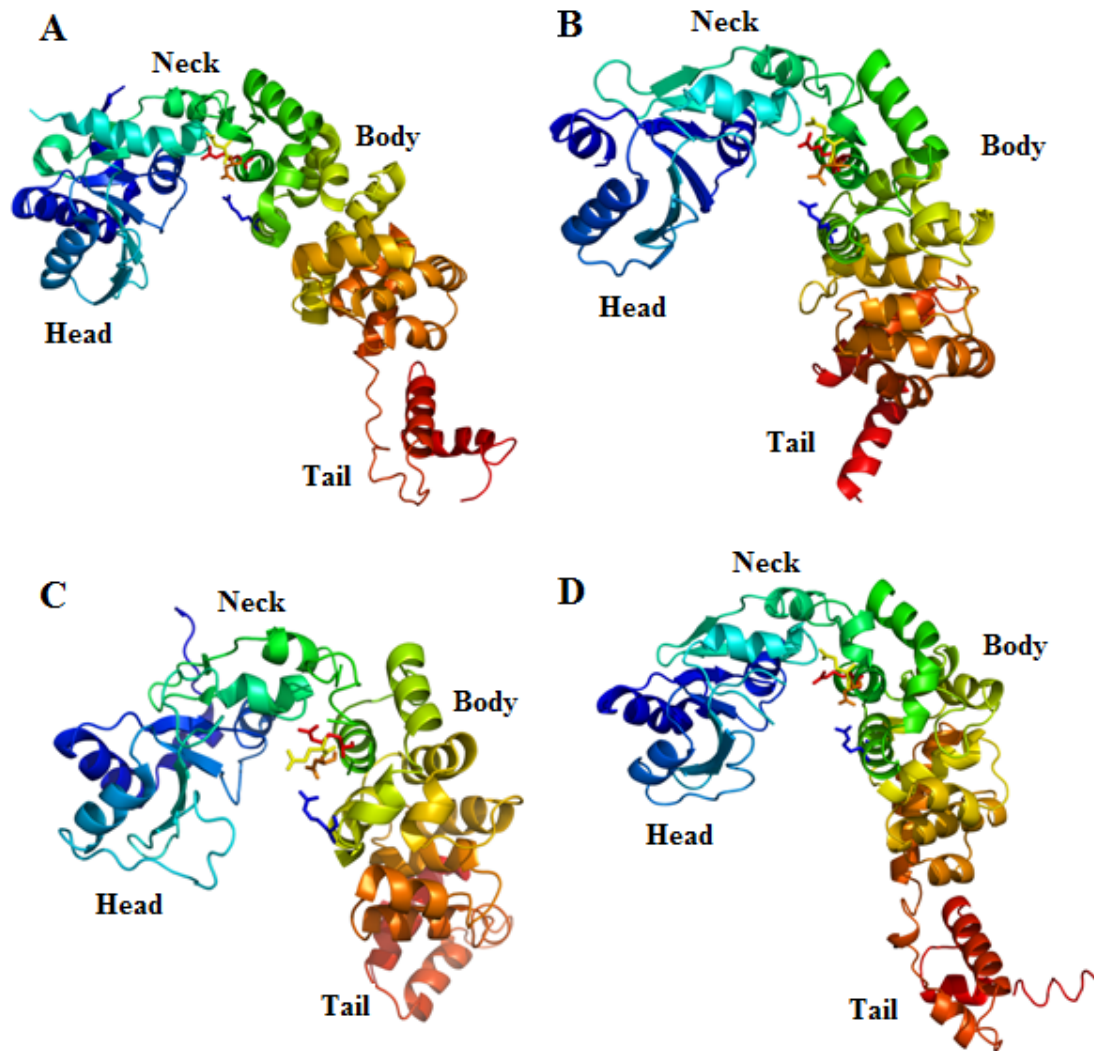


Fig. 1-3. Crystal structures of four different class II tRNA nucleotidyltransferases. Structures of tRNA nucleotidyltransferases from *Thermotoga maritima* (Toh *et al.*, 2009), *Aquifex aeolicus* (Tomita *et al.*, 2004), *Homo sapiens* (Augustin *et al.*, 2003), and *Bacillus stearothermophilus* (Li *et al.*, 2002) are labeled A-D, respectively. Active site residues belonging to motif D are shown in stick figures. Head, neck, body, and tail domains are labeled in each structure. The crystal structures were viewed with PyMol (DeLano, 2009). PDB files: 3h37, 1vfg, 1ou5, 1MIV, respectively.

As the structure and function of the *Candida glabrata* tRNA nucleotidyltransferase is being explored here, the primary sequence of this enzyme was input into the Protein Homology/analogy Recognition Engine (PHYRE) server (Kelley and Sternberg, 2009) and a model of the protein was built based on the known crystal structure of its most closely related homologue, *Homo sapiens* (Fig. 1-3C). As expected for tRNA nucleotidyltransferases, the predicted model shows a mainly alpha-helical structure with a “seahorse” conformation (Fig. 1-4). The active site is defined by portions of the head (containing motifs A and B) and neck (containing motifs D and E) of the protein (Li *et al.*, 2002). The proposed functions of each of these motifs will be discussed below (section 1.6). In addition, the body and tail domains (defining the C-terminus of the protein) are thought to recognize the top-half of the tRNA substrate, notably the acceptor stem and T ψ C stem/loop (Shi *et al.*, 1998a; Tomita *et al.*, 2004). Domain shuffling experiments between the C-terminal regions of poly(A) polymerase (which adds many adenosines) and *E. coli* tRNA nucleotidyltransferase (which adds cytidine, cytidine, and adenosine specifically) demonstrated that the tRNA is locked at the C-terminal region in tRNA nucleotidyltransferase which restricts nucleotide addition to a maximum of three residues (Betat *et al.*, 2004). Cross-linking studies (Shi *et al.*, 1998a) indicated that the tRNA remains fixed in position during nucleotide incorporation suggesting that the growing CCA terminus undergoes reorganization in the active site to make room for the next nucleotide (Yue *et al.*, 1998). This in turn suggests that the enzyme’s interaction with the tRNA’s 3’-end is not very tight (Betat *et al.*, 2010).

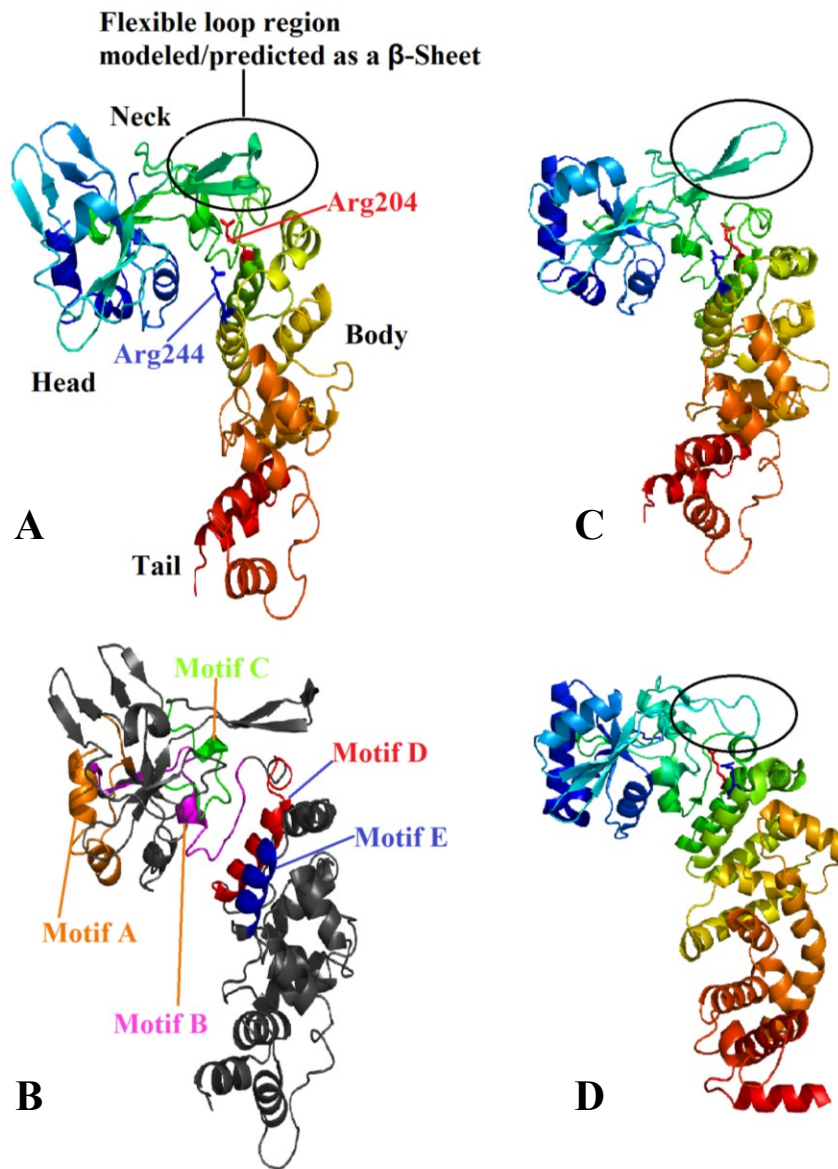


Fig. 1-4. Model of *Candida glabrata* tRNA nucleotidyltransferase. **Panel A:** *Candida glabrata* (CAG62257) primary sequence was input into the Protein Homology/analogy Recognition Engine (PHYRE) server (Kelley and Sternberg, 2009). Arginine 204 (red) and arginine 244 (blue) are labeled and displayed as sticks. Head, neck, body, and tail domains are also labeled. Also labeled is the region corresponding to the flexible loop identified in *Aquifex aeolicus* (Tomita *et al.*, 2004; Betat *et al.*, 2010). In *C. glabrata* (Panel A) and human (Panel C) this region is predicted to form a β -sheet. **Panel B:** *C. glabrata* model from Panel A showing the different structural motifs designated in Fig. 1-2. **Panel C:** *Homo sapiens* (BAB70662) primary sequence was input into the PHYRE server in order to predict the secondary structure of the flexible loop region (circled) as it was unresolved in the crystal structure (Fig 1-3). **Panel D:** *Thermotoga maritima* apo structure II (PDB file 3H38) soaked in ATP. The flexible loop region is circled. All structures were viewed with PyMol (DeLano, 2009).

1.6 Roles of conserved Motifs

Motif A (Fig. 1-2) contains two conserved aspartic acids separated by a single amino acid (DxD, where x is any amino acid) involved in coordinating metal ions involved in catalysis and in binding the triphosphate moiety of each NTP (Steitz *et al.*, 1994; Steitz, 1998; Seth *et al.*, 2002; Betat *et al.*, 2010). The two carboxylates bind and position two Mg^{2+} ions in the active site for nucleophilic attack, in addition to stabilizing the transition state of this reaction. One of the Mg^{2+} ions removes the proton from the 3'-OH group of the tRNA which in turn facilitates nucleophilic attack (by the tRNA) on the alpha phosphate group of the nucleotide. The other magnesium ion is needed to promote pyrophosphate release from the bound nucleotide (Fig. 1-5).

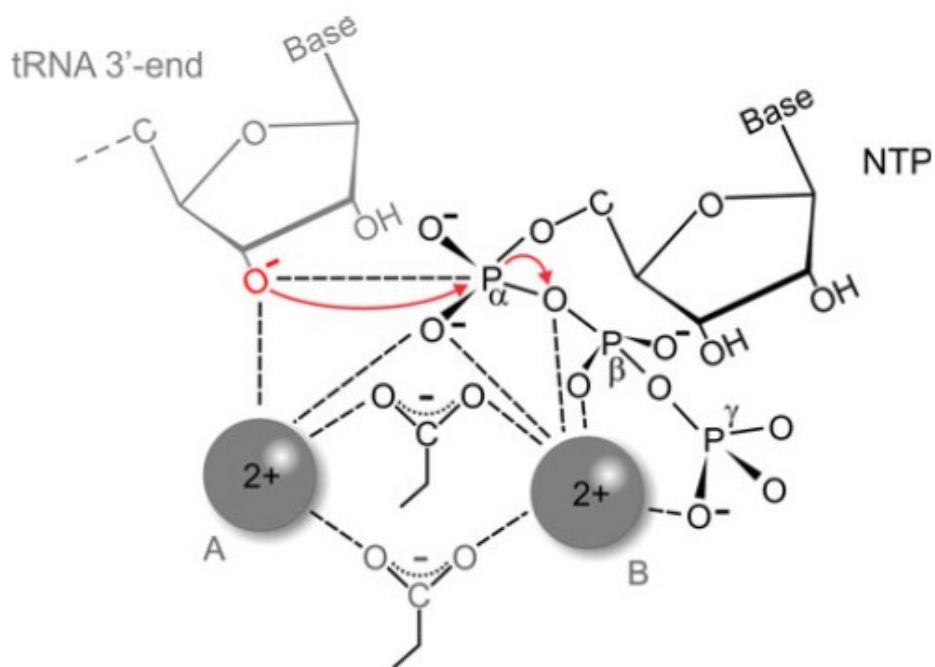


Fig. 1-5. The role of motif A during CCA-addition (Steitz, 1998; Betat *et al.*, 2010). The grey balls represent the two metal ions (Mg^{2+}) and are bound to the two carboxylates. Metal ion A deprotonates the 3'-OH group of the tRNA and activates the 3'-O⁻ attack on the α -phosphate of nucleotide. Metal ion B stabilizes the triphosphate moiety of the NTP in order to promote pyrophosphate release.

Motif B plays a critical role in discriminating between triphosphates of ribonucleotides and deoxyribonucleotides (Betat *et al.*, 2010). The arginine-arginine-aspartate (RRD) sequence in this motif recognizes the 2'-OH group of each ribonucleotide, discriminating against deoxynucleotides (Li *et al.*, 2002; Betat *et al.*, 2010). This recognition results from the central arginine residue forming a hydrogen bond with the 2'-OH group of the nucleotide. Substitution of this arginine with isoleucine resulted in the loss of discrimination against deoxynucleotides (Cho *et al.*, 2007; Betat *et al.*, 2010), further supporting the role of this motif in recognition of the sugar portion of the nucleotide triphosphate.

Motif C shows a relatively low level of sequence conservation and has had no specific role assigned to it (Betat *et al.*, 2010). It may act only as a connection between the so called head and neck domains of the proteins (Li *et al.*, 2002). In contrast, motif D plays an important role during CCA-addition. This region of the protein, including portions of both the head and neck domains, forms a nucleotide binding pocket (for one nucleotide) for the specific binding of CTP or ATP (Li *et al.*, 2002) and discriminates against UTP and GTP (Yue *et al.*, 1996; Shi *et al.*, 1998b; Betat *et al.*, 2010). Motif D and specifically the subset of three conserved amino acids EDxxR (where x represents any amino acid), were shown to form Watson-Crick-like hydrogen bonds with the incoming nucleotides in the crystal structures of the *Bacillus stearothermophilus* tRNA nucleotidyltransferase (Li *et al.*, 2002). This further explains why UTP and GTP are excluded from binding at the enzyme's active site, as they show an incompatible pattern of hydrogen bond donors/acceptors (Li *et al.*, 2002; Betat *et al.*, 2010). Complexes of the *B. stearothermophilus* enzyme with CTP show Arg157 (corresponding to Arg204 in the

C. glabrata enzyme) rotated toward CTP enabling hydrogen bonding of this arginine with both the N3 and O2 atoms of CTP (Li *et al.* 2002). Moreover, when the enzyme is associated with ATP, Arg157 hydrogen bonds with the N1 position of ATP while being stabilized by another hydrogen bond with Glu153 (corresponding to Asp200 in the *C. glabrata* enzyme) (Fig. 1-6, Li *et al.* 2002). In both complexes, Asp154 (corresponding to Asp201 in the *C. glabrata* enzyme) hydrogen bonds with either the 6-NH₂ or 4-NH₂ group of ATP or CTP, respectively (Li *et al.* 2002). The acidic residue (position 200 in the *C. glabrata* enzyme) does not interact directly with either of the bases, but plays an important role in the reorganization of the binding pocket (Li *et al.*, 2002; Betat *et al.*, 2010). This reorganization results as the glutamate and arginine residue rotates together while enlarging the binding pocket for the larger base (adenine) and switches the enzymes specificity from CTP towards ATP.

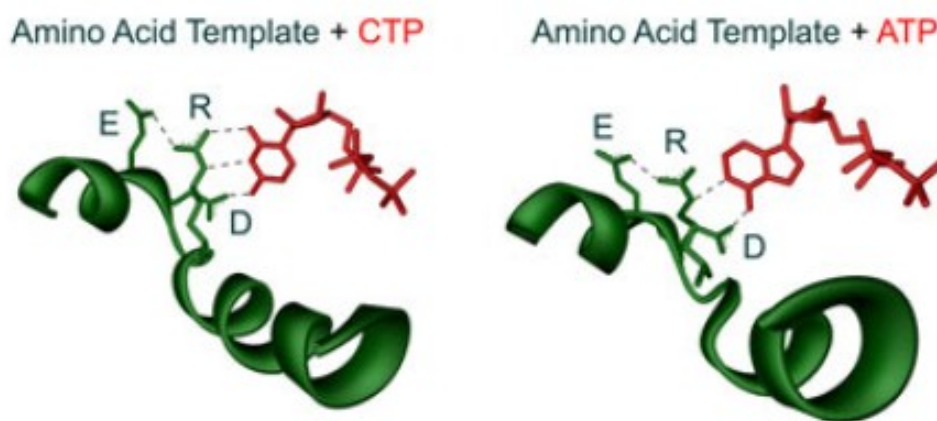


Fig. 1-6. Nucleotide binding profile of class II tRNA nucleotidyltransferases (Li *et al.*, 2002; modified from Betat *et al.*, 2010). The nucleotide binding site formed by the EDxxR motif in the *B. stearothermophilus* tRNA nucleotidyltransferase recognizes the incoming CTP and ATP by the formation of Watson/Crick-like hydrogen bonds. Three hydrogen bonds are observed for CTP binding, while only two are seen for ATP binding. The side chains of E153, D154 and R157 are shown as sticks and the incoming nucleotide in red. The helix shown represents helix G of the *B. stearothermophilus* enzyme containing motif D. R157 corresponds to R204 in the *C. glabrata* enzyme.

The importance of this dynamic amino acid template for nucleotide selection was further shown when the arginine was substituted by alanine in the *B. stearothermophilus* enzyme. This enzyme variant was unable to form two of three hydrogen bonds to CTP and one of two hydrogen bonds to ATP shown in Fig. 1-6 (Li *et al.*, 2002). Due to this, a dramatic loss of specificity was observed as the enzyme added a single CMP, GMP, AMP, or UMP nucleotide (Fig. 1-7) to a template either missing the entire 3' CCA sequence or containing only the first 3' nucleotide, CMP (Cho *et al.*, 2007). Similarly, K_m and k_{cat} determinations for these variants clearly suggested that the primary function of this arginine is to ensure nucleotide specificity and not to improve the kinetics of nucleotide incorporation (Cho *et al.*, 2007). In addition, replacement of the corresponding arginine residue by alanine in the *Escherichia coli* and *Homo sapiens* enzymes (Lizano *et al.*, 2008) demonstrated a reduced level of nucleotide incorporation to the three tRNA substrates (missing either CCA, CA, or A). Notably, the *H. sapiens* enzyme was less affected in AMP incorporation, but both enzyme variants showed similar impairment in adding the two CMP residues (Lizano *et al.*, 2008). When the variants were supplied with all four nucleotides simultaneously, a number of tRNAs were synthesized with the correct 3'-ends (-C, -CC, or -CCA) while the tRNAs which showed misincorporation were not further elongated, demonstrating that misincorporation can lead to premature termination of nucleotide addition (Lizano *et al.*, 2008). The authors suggested that the addition of two AMP nucleotides was due to the ability of ATP to still form one hydrogen bond with the aspartate residue. Furthermore, there is also evidence that the last incorporated nucleotide is inspected and identified by a few amino acids located between motifs A and B (Betat *et al.*, 2010). This mechanism is thought to work with a basic residue forming a

hydrogen bond to the O2 position of C75 of the tRNA in order to facilitate further nucleotide incorporation by re-positioning the tRNA 3' end. Evidently, if CMP is not present at that position, the next nucleotide will not be added (Neuenfeldt *et al.*, 2008; Betat *et al.*, 2010).

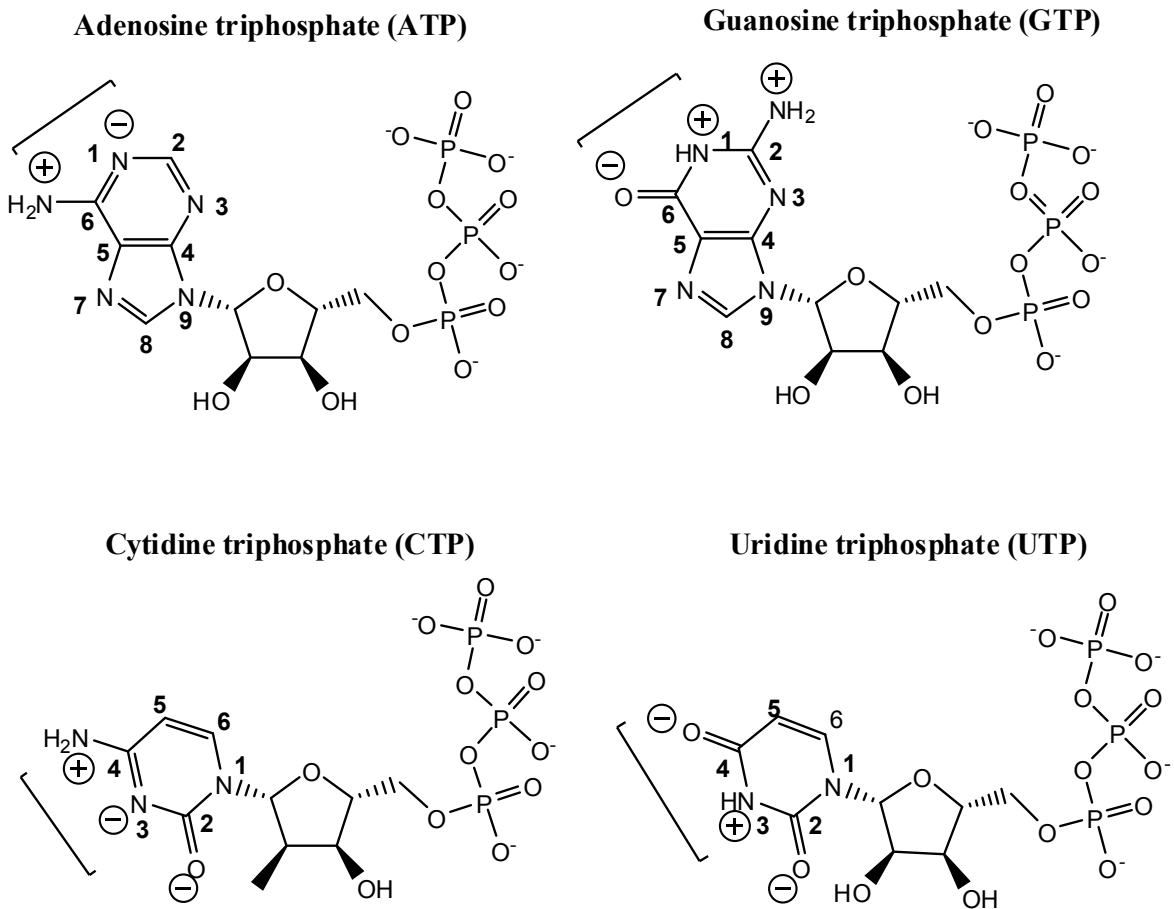


Fig. 1-7. Hydrogen bond donor-acceptor patterns for nucleotides in class II tRNA nucleotidyltransferases (as in Cho *et al.* 2003). The enzyme recognizes CTP and ATP, but discriminates against UTP and GTP through hydrogen bonds between the base and the amino acid template in motif D (EDxxR). Base pairing occurs at positions 1 and 6 (exocyclic group) of purines (ATP, GTP) and positions 3 and 4 (exocyclic group) of pyrimidines (CTP, UTP). Hydrogen bond donors are indicated by + and acceptors are indicated by - and are paired with brackets.

In contrast, replacement of either the glutamate or aspartate residue by alanine in the *E. coli* and *H. sapiens* enzymes showed less drastic results. In fact, replacing the glutamate in either enzyme left nucleotide incorporation to the three tRNA substrates unaltered (Lizano *et al.*, 2008). When the second amino acid (aspartate) was substituted to alanine, identical incorporation (compared to the native enzyme) was observed for the *E. coli* enzyme; however, the *H. sapiens* enzyme had great difficulty in adding the second CMP residue (Lizano *et al.*, 2008). To conclude, motif D seems to play a role in both specificity and/or efficiency during nucleotide incorporation.

The function of motif E is not yet fully understood but there is evidence that it may help to stabilize a helix-turn structure in motif D (Li *et al.*, 2002; Betat *et al.*, 2010) and/or might interact with the growing 3'-end of the tRNA substrate (Cho *et al.*, 2007). In class II enzymes, two invariant residues are observed (Fig. 1-2; Cho *et al.*, 2007): an arginine (R194 in Fig. 1-8, corresponding to Arg244 in the *C. glabrata* tRNA nucleotidyltransferase) and a glutamate (E198 in Fig. 1-8, corresponding to Glu248 in the *C. glabrata* tRNA nucleotidyltransferase). Both of these residues are located in helix J (Li *et al.*, 2002) and may stabilize helix G of motif D which contains the dynamic amino acid template (Fig. 1-8, Li *et al.*, 2002). In addition, both residues are thought to limit the extension of the 3' terminus (to three nucleotides) and are required for nucleotide specificity in the *B. stearothermophilus* enzyme (Cho *et al.*, 2007). Experiments to address the specific role of Arg244 in the *C. glabrata* tRNA nucleotidyltransferase were previously performed in this lab (Arthur, 2009) and are summarized in section 1.7.

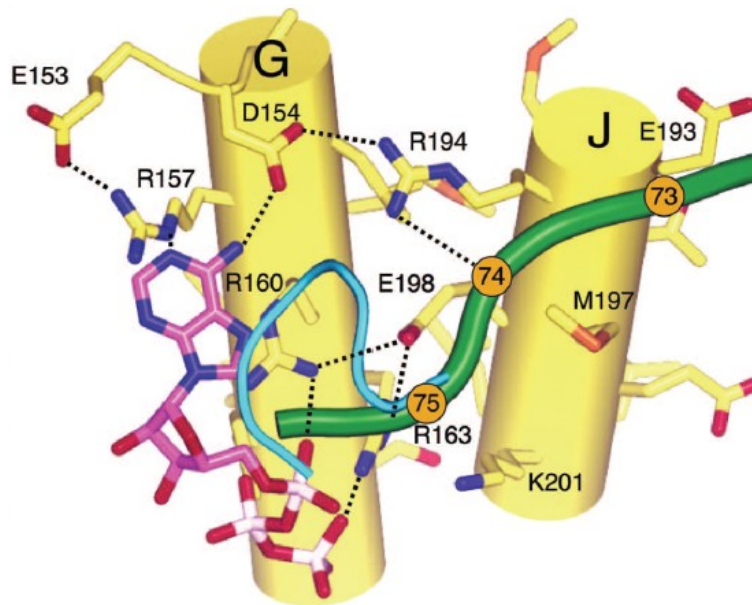


Fig. 1-8. Model of helices G and J during extension with an incoming ATP (Cho *et al.* 2007). This model is based on the crystal structure of the A adding *A. aeolicus* enzyme. Amino acid numbering corresponds to residues from the *B. stearothermophilus* enzyme. The 3' end of the tRNA is shown from the discriminator base N73, to the second position, C75. A β -turn which may also interact with the 3'-end of the tRNA is also shown. Arginines 157 and 194 corresponds to arginines 204 and 244 of the *C. glabrata* enzyme, respectively.

1.7 The role of arginine 244 in *Candida glabrata* tRNA nucleotidyltransferase (Arthur, 2009)

Changing arginine 244 of motif E in *Candida glabrata* tRNA nucleotidyltransferase to alanine, lysine, or methionine resulted in cell death (as shown with plasmid shuffling experiments). Purified native and variant proteins were characterized by far-UV circular dichroism (CD) and fluorescence spectroscopy and showed no change to the mainly α -helical secondary structure of the native enzyme, or in its tertiary structure. In addition, thermal denaturation experiments revealed an increased melting temperature for some variants, although the overall stability of the enzyme had not been majorly affected. Compared to the native enzyme, specific *in vitro* nucleotide incorporation experiments determined that the amino acid substitution resulted in a loss

of nucleotide addition at position 74, a reduction of nucleotide specificity at position 75, and an increase in nucleotide specificity at position 76. If these observations are consistent with what is happening *in vivo* then that is an obvious explanation for the cell death phenotype. Based on these results it was suggested that arginine 244 plays a specific role in orienting CTP for addition at position 75, while also discriminating against ATP binding at that position. Interestingly, the increased specificity at the third position was not observed for the lysine variant, suggesting that a positively charged residue at this position in the protein facilitates inappropriate CTP addition at position 76. Overall, it was observed that incorporation of CTP or ATP became more efficient as the size of the tRNA template increased. This was explained by the growing 3'-end of the tRNA extending further into the active site such that it could bind more efficiently or be more accessible for nucleotide addition in the absence of Arg244. Ultimately, a nucleotide addition mechanism was proposed for the *C. glabrata* enzyme where arginine 244 plays multiple roles in tRNA nucleotidyltransferase depending on the position of the tRNA that requires nucleotide addition. The first incoming CTP would be recognized directly by Arg244 through Watson-Crick interactions (blocking ATP incorporation due to incompatible interactions) in order to have an ideal distance between the nucleotide phosphates and the 3' end of the tRNA. Both molecules would then be oriented by the two divalent metal ions. The new 3' end of the tRNA would then refold to facilitate the binding of the second CTP to the dynamic amino acid template (motif D, Li *et al.*, 2002). The longer tRNA could now form additional interactions with Arg244 and a β -turn on the opposite side of the active site (as suggested by Tomita *et al.*, 2006) to stabilize the 3' end of the tRNA. Both of these interactions allow limited access to the active site so the larger

ATP is discriminated against and the second CTP is added as in the *B. stearothermophilus* enzyme with Arg244 coordinating D201 of the (E/D)DxxR motif (Li *et al.*, 2002). After this second CTP is added, the tRNA 3' end refolds once again and induces a conformational change in the enzyme, further allowing Arg204 of motif D to rotate and use ATP as a substrate as the arginine can now form only two hydrogen bonds instead of three (Fig. 1-6). Overall, the results suggest that arginine 244 plays a role in binding and orienting the substrates (nucleotide triphosphates and tRNA), as well as excluding ATP from the active site prior to nucleotide addition to positions 74 and 75. Finally, it was suggested that mutational analysis of motif D may confirm that C74 addition can occur without the presence of these residues, whereas C75 and A76 addition requires them. Due to this, the role of Arg204 in motif D was put into question for this current study.

1.8 An alternate mechanism of substrate recognition by class II tRNA nucleotidyltransferases

Although the shift from CTP to ATP binding occurs through reorientation of the motif D amino acids, there is evidence that this reorganization is not restricted to the individual amino acids (Betat *et al.*, 2010). Moreover, the extensive movement of individual enzyme domains relative to each other is supported by various experiments (Tomita *et al.*, 2004; Kim *et al.*, 2009) confirming the existence of a flexible loop element (Betat *et al.*, 2010). Mutations/deletions in this flexible loop demonstrated its specific involvement in AMP incorporation as the incorporation of the first two CMP residues remained unaffected (Zhu *et al.*, 1986; Neuenfeldt *et al.*, 2008; Just *et al.*, 2008; Toh *et al.*, 2009; Betat *et al.*, 2010). In addition, a loop mutation in the *E. coli* enzyme resulted in an unchanged K_M for ATP binding compared to the native enzyme, indicating that

ATP binding is not directly affected by the mutation (McGann *et al.*, 1980). Loop exchange experiments also revealed that different loops are only functional within enzymes of the same phylogenetic origin, suggesting that the loop acts as a lever that pulls the amino acid template of motif D into the required position (Betat *et al.*, 2010). In the crystal structure of *T. maritima* tRNA nucleotidyltransferase (Toh *et al.*, 2009), a tyrosine residue located in this loop was identified as hydrophobically interacting with the first position of the amino acid triad EDxxR in motif D. It was suggested by Toh *et al.* (2009), that this interaction may influence the orientation of the arginine during the specificity switch of the amino acid template (Neuenfeldt *et al.*, 2008). In addition, changing the aspartate in the first position of the triad to alanine reduced only the AMP incorporation rate, and not the CMP incorporation rate (Toh *et al.*, 2009). This further supports that an interaction between tyrosine and glutamate aids in the specificity switch. Furthermore, Tyr108 is conserved in the *C. glabrata* enzyme as Tyr135 (Fig. 1-2), although it is not conserved in all of the class II enzymes. Overall, substrate recognition in class II enzymes is a complex three-dimensional mechanism which should be studied further.

1.9 Rationale

In the current study, the role of arginine 204 in the *Candida glabrata* tRNA nucleotidyltransferase is explored. This arginine residue lies within motif D and is conserved in all class II tRNA nucleotidyltransferases (Fig. 1-2). Arginine 204 is the third conserved amino acid of this motif, and it is said to be part of a dynamic amino acid template (Li *et al.*, 2002) which is involved in the nucleotide specificity shift from CTP to ATP in class II CCA adding enzymes (Section 1.5). To determine if the arginine residue

at position 204 was indeed of interest, the *Candida glabrata* *CCA1* gene was isolated through complementation in *Saccharomyces cerevisiae* (Hanic-Joyce and Joyce, 2002) and QuikChange™ (Stratagene) mutagenesis was used to change arginine 204 to alanine, glutamate, or glutamine alone or in combination with the conversion of arginine 244 to alanine. *In vivo* plasmid shuffling experiments indicated that each of these amino acid changes at position 204 resulted in cell death on FOA (Fig 1-9), indicating that Arg204 plays a vital role in the enzyme's structure and/or function.

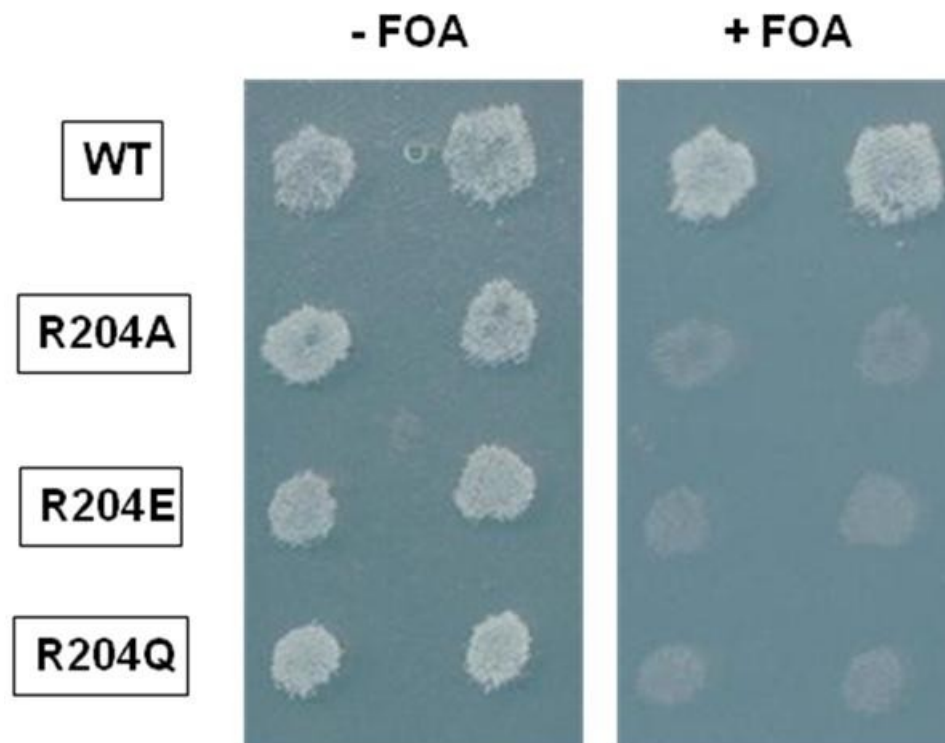


Fig. 1-9. Viability of *Candida glabrata* tRNA nucleotidyltransferase strains with substitutions at Arg204 (Dr. Pamela J. Hanic-Joyce, personal communication). A *C. glabrata* strain (GCP1-2) lacking its own *CCA1* gene and carrying the *Saccharomyces cerevisiae* *CCA1* gene on plasmid pRS316 was transformed with pRS313 (Sikorski and Hieter, 1989) derivatives bearing *C. glabrata* *CCA1* genes coding for either native or variant (R204A, R204E, and R204Q) tRNA nucleotidyltransferase enzymes. The transformed colonies were grown on synthetic complete medium lacking histidine and uracil (SC-His-Ura). The cells were then grown in complete medium (SC), patched on SC-His-Ura, and then replica plated to new plates (SC-His-Ura) containing 5-fluorourotic acid (FOA) and incubated at 30°C for 3 days.

In order to distinguish between these possibilities, the corresponding proteins were purified and explored by a combination of biophysical and biochemical approaches. The secondary and tertiary structures of the native and variant enzymes were studied by circular dichroism and fluorescence spectroscopy, respectively. Furthermore, the effects on enzyme activity were assessed using *in vitro* enzyme assays.

In addition to exploring the specific role of arginine 204, the same experiments were performed with double variants of Arg244-Arg204. These results may shed more light on the relationship between these two residues. Figure 1-10 shows a close-up of the predicted model, highlighting residues which are predicted to form polar contacts with Arg204 and Arg244.

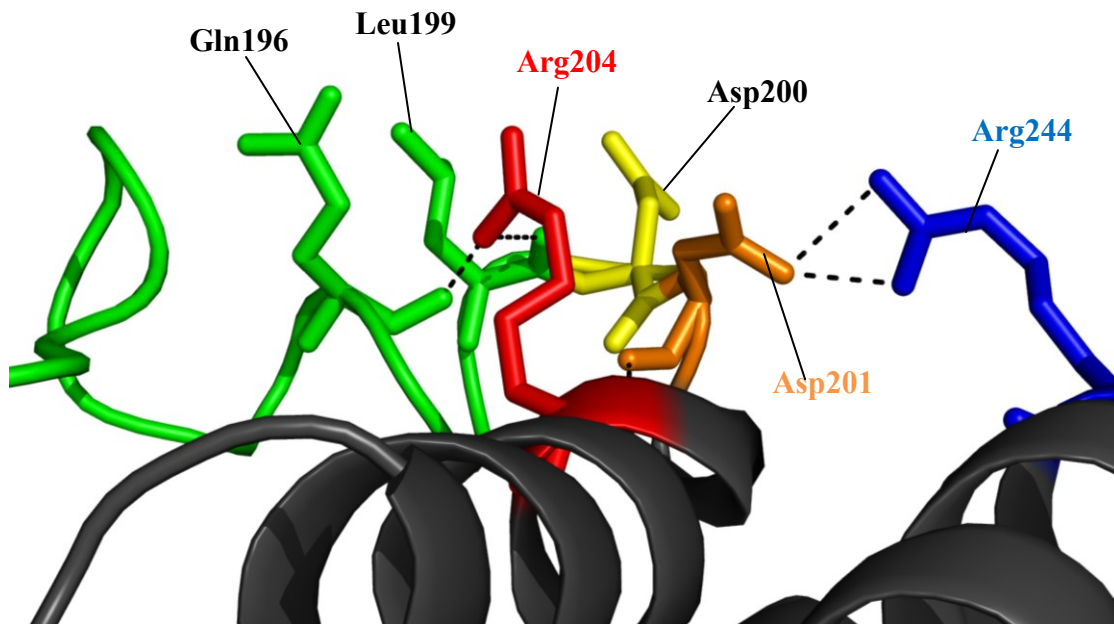


Fig. 1-10. Close up model of domain D of *C. glabrata* tRNA nucleotidyltransferase without a substrate bound. *C. glabrata* (CAG62257) tRNA nucleotidyltransferase. Only the D, D and R residues of the DDxxR motif of motif D are shown. The side chain of Arg204 is predicted to interact with the main chain carbonyls of Gln196 and Leu199. The side chain of Arg244 is predicted to interact with the side chain of Asp201. The loop stabilized by Arg204 and Arg244 is shown in green. Polar contacts were predicted and viewed with PyMol (see Fig. 1-4 for details).

The predicted polar contacts can be used as a rough model to help determine effects that amino acid substitutions may have on the enzyme's structure. According to Fig. 1-4 and Fig. 1-10, both arginines are predicted to be located at the ends of two adjacent helices. This positioning is important because this would enable both residues to play a possible structural and/or active site role. Since variants of arginine 244 do not demonstrate major changes in secondary structure (Arthur, 2009), arginine 204 variants are an excellent candidate to view structure effects, if any.

Of particular interest is the flexible loop region described in section 1.8 (Tomita *et al.*, 2004; Betat *et al.*, 2010). A major difference can be observed in this region when comparing the predicted *C. glabrata* enzyme model (Fig. 1-4) to all of the currently solved class II tRNA nucleotidyltransferase crystal structures (Fig. 1-3). The predicted model shows a β -sheet in place of the flexible loop which was only resolved in the *H. sapiens* enzyme. According to sequence alignments (Fig. 1-2), this region seems to be conserved in *S. cerevisiae*, *K. lactis*, *L. albus*, and *A. thaliana*. Notably, there is evidence that one of the conserved residues (tyrosine 135) may interact with the glutamic residue in motif D, and may influence the orientation of the arginine during the specificity switch from CTP to ATP. This information, together with biophysical studies, and nucleotide incorporation assays, can possibly provide further insights into the role of arginine 204.

2. Materials and Methods

2.1 Strains, Buffers, Growth Media, and Solutions

The *E. coli* strain BL21 (DE3) was purchased from Stratagene. Buffers and growth media that were used for this study are listed in Table 2-1. All chemicals, including their grade of purity, can be found in Table 2-2.

Table 2-1 Components for buffers, growth media, and solutions

Buffers, Growth Media, and Solutions	Components
Acrylamide solution – 30% (29:1) (Sambrook <i>et al.</i> , 1989)	29.2 g acrylamide, 0.8 g bis-acrylamide, to 100 mL in dH ₂ O
Acrylamide solution – 40% (37.5:1) (Bio-Rad Laboratories, 1995)	38.96 g acrylamide, 1.04 g bis-acrylamide, to 100 mL in dH ₂ O
Elution/cleavage buffer (modified from Arthur, 2009)	50 mM Tris, 140 mM NaCl, 15 mM glutathione, 2.5 mM CaCl ₂ , adjusted to pH 8.3 with HCl
Lysis buffer for protein purification (modified from Arthur, 2009)	PBS (pH 7.4), 1mM EDTA
PBS (1L) (Sambrook <i>et al.</i> , 1989)	8 g NaCl, 0.2 g KCl, 1.44 g Na ₂ HPO ₄ , 0.24 g KH ₂ PO ₄ , pH 7.4, other desired pH's were altered with HCl or NaOH
Peattie's loading buffer (Peattie, 1979)	10 M urea, 5 mM Tris-borate (pH 8.3), 0.1 mM EDTA, 0.05% xylene cyanol, 0.05% bromophenol blue
Polyacrylamide 7M urea denaturing sequencing gel – 12% (100 mL) (Bio-Rad Laboratories, 1995)	30 mL 40% acrylamide solution, 42 g urea, 20 mL 5X TBE, 100 μL 25% ammonium persulfate, 100 μL tetramethylethylenediamine (TEMED)

Polyacrylamide 7M urea denaturing sequencing gel – 20% (100 mL) (Bio-Rad Laboratories, 1995)	50 mL 40% acrylamide solution, 42 g urea, 20 mL 5X TBE, 100 µL 25% ammonium persulfate, 100 µL tetramethylethylenediamine (TEMED)
Sodium dodecyl sulfate polyacrylamide gel electrophoresis (SDS-PAGE) running buffer (5X) (modified from Sambrook <i>et al.</i> , 1989)	72 g/L glycine, 15 g/L Tris-HCl, 5 g/L SDS
SDS-PAGE sample loading buffer (5X) (modified from Walker, 2002)	300 mM Tris-HCl (pH 6.8), 10% w/v SDS, 50% v/v glycerol, 25% v/v β-mercaptoethanol, 0.25% w/v bromophenol blue
SDS-PAGE staining and destaining solutions: (Wong <i>et al.</i> , 2000) Staining solution A Staining solution B Destaining solution	25% isopropanol, 10% acetic acid, 0.05% Coomassie brilliant blue 10% isopropanol, 10% acetic acid, 0.005% Coomassie brilliant blue 10% isopropanol, 10% acetic acid
SDS-PAGE stacking gel (modified from Sambrook <i>et al.</i> , 1989)	1.3 mL 30% acrylamide solution, 6.1 mL dH ₂ O, 2.5 mL 0.5 M Tris-HCl (pH 6.8), 100 µL 10% SDS, 100 µL 10% Ammonium persulfate (APS), 10 µL TEMED
SDS-PAGE resolving gel (13%) (modified from Sambrook <i>et al.</i> , 1989)	4.3 mL 30% acrylamide solution, 3 mL dH ₂ O, 2.5 mL 1.5 M Tris-HCl (pH 8.8), 100 µL 10% SDS, 100 µL 10% APS, 10 µL TEMED
Sodium acetate (NaOAc, 3 M, pH 5.2) (modified from Sambrook <i>et al.</i> , 1989)	40.8 g NaOAc•3H ₂ O, approximately 12 mL acetic acid (glacial) to pH, fill to 100 mL with dH ₂ O
TBE (5X) (modified from Sambrook <i>et al.</i> , 1989)	30 g/L Tris, 15.5 g/L boric acid, 10 mL 0.5 M EDTA (pH 8) for every L of buffer desired.

YT (Sambrook <i>et al.</i> , 1989)	0.5% Yeast extract, 0.8% Tryptone, 0.5% NaCl
------------------------------------	--

Table 2-2 List of chemicals, restriction enzymes, and manufacturers

Supplier	Chemical
Bioshop	Acrylamide (Ultra pure grade)
	Agarose (Biotechnology grade)
	Ampicillin (Biotechnology grade)
	Ammonium persulfate (APS) (Electrophoresis grade)
	Bio-tryptone (Bacteriological grade)
	Bis-acrylamide (Bio Ultra pure grade)
	Boric acid (Biotechnology grade)
	Calcium chloride (Bacteriological grade)
	Coomassie brilliant blue R-250
	D-Lactose, monohydrate
	EDTA (Biotechnology grade)
	Glycine (Biotechnology grade)
	Potassium chloride
	Potassium phosphate monobasic (ACS grade)
	Sodium acetate, trihydrate
	Sodium phosphate dibasic heptahydrate (ACS grade)
	Sucrose (Ultra pure grade)
	Tetramethylethylenediamine (TEMED)
	Tris (Bio Ultra pure grade)
Urea (Bio Ultra pure grade)	
Yeast Extract powder	
Commercial Alcohols Inc.	Ethanol (99%)
EM Science	Magnesium chloride hexahydrate
Eppendorf	Perfectprep [®] Plasmid XL kit
Fermentas	Adenosine-5'-triphosphate (ATP)
	<i>BpiI</i> restriction enzyme
	Cytidine-5'-triphosphate (CTP)
	Guanosine-5'-triphosphate (GTP)
	Uridine-5'-triphosphate (UTP)
Fisher Scientific	Acetic acid, glacial (ACS grade)
	Glycerol (Enzyme grade)

	Isopropanol (ACS grade)
	Sodium chloride (Biological grade)
GE Healthcare	Glutathione Sepharose 4 Fast Flow
	Thrombin
Gold Biotechnology	Isopropyl β -D-1-thiogalactopyranoside (IPTG) (Molecular biology grade)
Integrated DNA Technologies	Nuclease-free water
MP Biomedicals	Sodium dodecyl sulfate (SDS) (Ultra pure grade)
NewEngland Biolabs	<i>FokI</i> restriction enzyme
Perkin Elmer	[α - 32 P] guanosine triphosphate (GTP) (10 μ Ci/ μ L, 3000 Ci/mmol)
Promega	<i>Bst</i> OI restriction enzyme
Sigma-Aldrich	Agar
	Nuclease-free dH ₂ O

2.2 Construction of expression system

2.2.1 Generation of products and ligation into pGEX-2T

The *Candida glabrata* *CCA1* gene (strain CBS138) had been cloned and sequenced previously (Hanic-Joyce and Joyce, 2002). This gene was inserted into a modified (Shan, 2005) pGEX-2T (GE Healthcare) expression plasmid between the *Bam*HI and *Sal*I sites by Paul Joyce. QuikChange™ (Stratagene) mutagenesis performed by Fadi Marzouk was used to change arginine 204 to alanine, glutamate, or glutamine alone or in combination with the conversion of arginine 244 to alanine in the *Candida glabrata* *CCA1* gene in the vector pGEX-2T.

2.3 Expression and purification of tRNA nucleotidyltransferase

2.3.1 Protein expression

A single colony of *E. coli* BL21(DE3) carrying a plasmid of interest was inoculated into 5 mL YT + 50 µg/mL ampicillin and grown overnight at 37°C with shaking at 237 rpm in a New Brunswick Scientific Innova 4330 Refrigerated Incubator Shaker. This culture was then equally divided between three flasks each containing 1.3 L of YT + 50 µg/mL ampicillin medium, returned to the shaker, and grown as described above until an OD₆₀₀ of 0.4-0.5 was achieved. Protein production was then induced by adding IPTG and D-lactose to final concentrations of 0.5 mM and 0.2% w/v, respectively. The cultures were then placed on the shaker at 18°C and 193 rpm for 16-24 hours.

2.3.2 Cell lysis

The cells were centrifuged for 15 minutes, at 4°C and 6 500 xg in a Beckman JA-10 rotor. The resulting pellets were frozen at -70°C for at least one hour and thawed on ice. The pellets were then resuspended in cold lysis buffer (Table 2-1) and passed through a French® Pressure cell press (ThermoSpectonic) three times at 1000 psi.

2.3.3 Glutathione Sepharose Fast Flow 4B chromatography (GE Healthcare)

Fresh resin (3 mL) was packed by gravity in a 1.5 cm x 10 cm Bio-Rad column. The column was rinsed with 10 bed volumes of 1X PBS buffer (pH 7.4). After each use, the resin was regenerated as recommended by the supplier (GE Healthcare) by washing with 3 mL of 25 mM reduced glutathione in water and then 3 mL each of 6 M guanidine-HCl, 25 mM reduced glutathione in water, and 70% ethanol. The resin was also rinsed

with 20 mL of 1X PBS (pH 7.4) between washes. The resin was stored in 20% ethanol when not being used.

2.3.4 Purification and thrombin cleavage of GST-tagged tRNA nucleotidyltransferase

Cell lysate was cleared by centrifugation twice for 40 minutes at 4°C and 40 000 xg in a Beckman JA-20 rotor. The cleared supernatant was cycled through the column with a Pharmacia LKB Pump P-1 peristaltic pump (overnight, 4°C, at a flow rate of 1 mL/min). Unbound protein was washed out with a minimum volume of 500 mL of PBS (pH7.4). The column was then filled with elution/cleavage buffer (Table 2-1) and 1.5 mL fractions were collected manually, using a rubber bulb. The fractions were analyzed by SDS-PAGE (section 2.3.5) and fractions containing GST-tRNA nucleotidyltransferase fusion protein were pooled and transferred to a 6-8 kDa Spectra/Por (Spectrum Laboratories) dialysis bag (50 mm wide, typically 0.5 cm dialysis tubing per mL of solution). Thrombin (GE Healthcare) was added (as recommended by the supplier, typically 1 mg/g protein) and dialysis was carried out at 4°C in 4 L of cold elution/cleavage buffer (Table 2-1) overnight. Protein cleavage was assessed by SDS-PAGE. If needed, thrombin was added again and the dialysis was repeated. Once the cleavage had reached a satisfactory level (>90%), the sample was transferred to a 50 kDa Spectra/Por dialysis bag (34 mm wide, typically 1 cm dialysis tubing per mL of solution) and dialyzed at 4°C overnight in 4L of cold PBS (pH 7.8). The dialysis buffer was replaced and the dialysis was then repeated for at least 4 hours. A regenerated Glutathione Sepharose fast flow column was equilibrated with a minimum of 300 mL of dialysis buffer and the cleaved sample was loaded and cycled manually (with a rubber bulb) through the column 3-5 times to remove any remaining GST. GST removal was

analyzed by SDS-PAGE. If the GST was not sufficiently removed the sample was placed in a fresh 50 kDa Spectra/Por dialysis bag and the dialysis repeated at 4°C overnight in 4L of cold PBS (pH 7.3). Once again, the samples were loaded and cycled through the column as described above. The level of GST removal was analyzed by SDS-PAGE once more. When the GST was sufficiently removed (>90%), glycerol was added to the sample to a final concentration of 10%. The solution was split into 300 µL and 50 µL fractions and stored at -70°C.

2.3.5 Sodium dodecyl sulfate polyacrylamide gel electrophoresis (SDS-PAGE)

The resolving gel (Table 2-1) was prepared and cast with a Pasteur pipette between two 4 cm by 10 cm glass plates separated by 4 mm spacers. Isopropanol (60%) was layered on top of the resolving gel for levelling purposes. Once the gel had polymerized, the isopropanol was removed and the stacking gel (Table 2-1) was added. The appropriate comb was inserted and the gel was left to polymerize for 30-60 minutes. After adding SDS-PAGE sample loading buffer (Table 2-1) to the samples, they were boiled for 5 minutes, cooled on ice, and loaded. Samples were allowed to separate for ~1 hour at 200 volts. Similar to a previously published procedure (Wong *et al.*, 2000), the gel was transferred to a vessel containing 50 mL of staining solution A (Table 2-1) and heated in a 700W microwave oven for 1.5 minutes (on high). The vessel was shaken on an orbital shaker at room temperature for about 5 minutes. The gel was then rinsed with dH₂O and 50 mL of staining solution B (Table 2-1) were added to the vessel with the microwave/shaking procedure repeated. The gel was rinsed again and 50 mL of destaining solution (Table 2-1) were added to the vessel along with two folded

Kimwipes. The microwave/shaking procedure was repeated and the gel was rinsed, framed with cellophane, and left to dry.

2.3.6 Determination of protein concentration

Protein sequences were analyzed using the ProtParam tool (Gasteiger *et al.*, 2006). This analysis resulted in a predicted $72\,435\text{ M}^{-1}\text{cm}^{-1}$ native extinction coefficient at 280 nm. The predicted molecular weight was also calculated to be $62\,022\text{ g mol}^{-1}$. The absorbance of 1 mL protein in 1X PBS pH 7.3 was then measured at 280 nm using a 1.0 cm quartz cell in a Varian Cary 100 Bio UV-Visible Spectrophotometer. This information was used in conjunction with the Beer-Lambert law ($A = \epsilon CL$, where A = absorbance, ϵ = molar extinction coefficient, C = concentration and L = path length) to determine the protein concentration of each protein sample. The concentrations determined were consistently 2.4 fold greater than those determined by a BCA™ Protein Assay Kit (MJS BioLynx). For consistency, the concentrations used for all experiments were calculated through the extinction coefficient method.

2.4 Biophysical characterization of tRNA nucleotidyltransferase

2.4.1 Secondary structure determination by circular dichroism

A Jasco-815 circular dichroism spectrophotometer along with the ‘Spectrum Measurement’ program (Jasco) was used. The instrument was set to scan over the region of 285 nm to 200 nm using a 0.5 cm cell. At standard sensitivity, a bandwidth of 1 nm was used, along with a response time of 0.25 seconds, data pitch of 0.2 nm, and a scanning speed of 20 nm/min. Data was accumulated five times at 20°C using a Pelletier water bath accessory while nitrogen was set to flow through the instrument at a constant

rate of 3 L/min. Aliquots of 1 mL at 1.4 μ M (0.1 mg/mL) of protein were used for the spectrum measurements. The data obtained were smoothed using the smoothing function in the Spectra Analysis (Jasco) program.

2.4.2 Temperature denaturation monitored by circular dichroism

The same instrument, accessory, flow rate, and cell (as used for the secondary structure determination) were used for thermal denaturation experiments. The program used was 'Variable Temperature'. Signal was monitored at 208 nm at standard sensitivity using a bandwidth of 1 nm, response time of 0.25 seconds, and a data pitch of 0.2°C. A temperature slope of 20°C/hour was used while the start and end temperatures were 25°C and 55°C. Aliquots of 1 mL at 1.4 μ M or 0.1 mg/mL of protein were used per measurement. The cell was sealed with parafilm to limit evaporation. The data obtained were smoothed as in section 2.2.1.

2.4.3 Tertiary structure determination by fluorescence spectroscopy

The instrument used was a Varian Cary Eclipse Fluorescence Spectrophotometer along with a Varian single cell Pelletier Cary accessory (water bath). The application "Scan" was used to obtain emission spectra at 20°C averaged over 10 scans between 300 nm to 400 nm with an excitation wavelength of 280 nm. Scan speed was set to medium (600 nm/min) with a 1.0 nm data sampling interval, 5 nm excitation and emission slit widths, and voltage was set to medium (600 volts). A 1.0 cm cell was used with aliquots of 1 mL at 1.4 μ M or 0.1 mg/mL of protein were used for the spectrum measurements. The data obtained were smoothed using the smoothing function in the "Scan" application above.

2.5 Enzyme activity assays

2.5.1 Agarose gel electrophoresis

Agarose was dissolved in TBE at the desired concentration (typically 0.5 g in 50 mL for a 1% gel). DNA loading buffer (6X, ZmTech Scientific) was added to each sample and the samples were then loaded onto a TBE submerged gel. Electrophoresis was carried out at 80 volts for approximately one hour. The separated bands were viewed on a FluorChem[®] FC2 ultraviolet light emitting apparatus (Alpha Innotech).

2.5.2 Large scale isolation of plasmids G73 and pmBSDCCA from *E. coli*

Plasmids G73 and pmBsDCCA were a generous gift from Dr. Alan Weiner (University of Washington). They were originally constructed by Cho *et al.* (2003) and Oh and Pace (1994), respectively. Each plasmid contained a *Bacillus subtilis* aspartate tRNA gene modified to produce specific 3'-ends after restriction digestion and *in vitro* transcription. For large scale plasmid isolation, 1 L of YT growth medium + 50 µg/mL ampicillin was inoculated with 5 mL of an overnight culture of *E. coli* XL2-Blue carrying the desired plasmid. The culture was grown overnight in a New Brunswick Scientific Innova 4330 Refrigerated Incubator Shaker (37°C, 237 rpm). Cells were collected by centrifugation for 15 minutes at 5 000 xg and 4°C. The pellet was then resuspended in 30 mL of cold Solution I in order to perform a large scale plasmid DNA extraction with a Perfectprep[®] Plasmid XL kit (Eppendorf). The kit was used as recommended by the supplier and the DNA was analysed using agarose gel electrophoresis (section 2.5.1) to confirm the identity (and purity) of the sample.

2.5.3 Preparation of template for *in vitro* run-off transcription

As summarized on Table 2-3, the digestion of G73 with *FokI* (NewEngland Biolabs) provides a template for run-off transcription which generates tRNA ending at G73 (tRNA-N), the discriminator base. Similarly, digestion of pmBsDCCA with different restriction enzymes provides templates for run-off transcription which generates tRNAs ending at C74 (tRNA-NC), C75 (tRNA-NCC), and A76 (tRNA-NCCA). The restriction enzymes used to generate the above transcripts are *FokI* (NewEngland Biolabs), *BpiI* (Fermentas), and *BstOI* (Promega), respectively. Approximately 35 µg of plasmid DNA was digested with either 12 units *FokI*, 40 units *BpiI*, or 40 units *BstOI* in a total volume of 100 µL for 3 hours. After the digestions, one-tenth volume (10 µL) of 3 M sodium acetate (pH 5.2, Table 2-1) was added to the samples of linearized DNA. Extractions were then performed by adding an equal volume of phenol, vortexing, and centrifuging for 5 minutes at 16 000 xg and 4°C. The aqueous phase was transferred to a new tube and the phenol extraction was repeated. An equal volume of ether was added and the tube was vortexed. Centrifugation was performed as with the phenol extractions and the ether layer was discarded. The ether extraction was repeated and any remaining ether in the sample after discarding was left to evaporate. Cold 99% ethanol (2.5 volumes) was added and the tube was vortexed before being incubated at -70°C for at least one hour. The plasmid DNA was pelleted by centrifugation for 30 minutes at 16 000 xg and 4°C. The pellet was washed with one volume of 80% ethanol and centrifuged for 5 minutes at 16 000 xg and 4°C. The ethanol was discarded and the plasmid DNA was dried under vacuum for 20 minutes. The pellet was resuspended in 10-20 µL of nuclease-free dH₂O (Sigma-Aldrich). DNA concentrations were determined by UV absorbance at 260 nm assuming an A₂₆₀ of 1 is equal to 50 µg of DNA (Sambrook *et al.* 1989).

Plasmid	Restriction enzyme	3' end	Total bases
G73	<i>FokI</i>	tRNA-N	73
pmBsDCCA	<i>FokI</i>	tRNA-NC	74
	<i>BpiI</i>	tRNA-NCC	75
	<i>BstOI</i>	tRNA-NCCA	76

Table 2-3. Construction of tRNAs with specific 3' ends. Plasmids, restriction enzymes, and 3' ends produced after *in vitro* run-off transcription. “N” represents the discriminator base (guanosine) at position 73 of *B. subtilis* Asp-tRNA^{GUC}.

2.5.4 Preparation of *in vitro* run-off transcribed tRNA with specific 3' ends

Each run-off transcription reaction contained 20 μ L 5X transcription buffer (Fermentas), 5 μ L of 10 mM ATP (Fermentas), 5 μ L 10 mM CTP (Fermentas), 5 μ L 10 mM UTP (Fermentas), 5 μ L 1 mM GTP (Fermentas), approximately 50 μ Ci (5-6 μ L depending on the extent of radioactive decay) [α -³²P] GTP (10 μ Ci/ μ L, 3000 Ci/mmol), 13 μ g of linearized DNA template (specific to the reaction), 60 units of T7 RNA polymerase (Fermentas), and nuclease-free water to 100 μ L. The reactions were incubated at 37°C for three hours and terminated by adding 200 μ L phenol, 5 μ L 0.5 mM EDTA, 75 μ L dH₂O, and 18 μ L 3 M sodium acetate (pH 5.2, Table 2-1). The samples were vortexed and centrifuged for 5 minutes at 16 000 xg and 4°C. The transcripts were precipitated with 2.5 volumes of cold 99% ethanol and incubated at -70°C for at least one hour. The precipitated tRNA was pelleted by centrifugation for 30 minutes at 16 000 xg and 4°C. The supernatant was removed and the pellets were dried under vacuum for 20 minutes. The pellets were resuspended in 10 μ L nuclease-free water and 10 μ L Peattie's loading buffer (Table 2-1). The samples were incubated at 70°C for 10 minutes, centrifuged for 30 seconds at 16 000 xg and 4°C, and loaded onto a 4 cm by 10 cm 20% polyacrylamide/7M urea denaturing gel (section 2.5.5). Electrophoresis was carried out

for 2-3 hours at 200 volts. The gel was removed from the apparatus; its surface was covered with cellophane plastic wrap and X-ray film (Super RX Fujifilm) for 30-60 minutes of autoradiography. The developed film was aligned with the gel in order to excise the desired bands. The excised bands were transferred to individual 1.5 mL microfuge tubes and 400 μ L of phenol was added to each tube. The gel slices were crushed with a sterile spatula until only small pieces could be seen in the phenol. An aqueous phase for the purified transcripts to diffuse into was made by adding 27 μ L 7.5 M NH_4OAc , 4 μ L 1 M $\text{Mg}(\text{OAc})_2$, 8 μ L 50 mM EDTA, and 361 μ L nuclease-free water. The tubes were rotated overnight (16-24 hours) on a rotisserie at 4°C. The samples were centrifuged for 5 minutes at 16 000 xg and 4°C and the supernatant was collected from above the phenol phase and transferred to a new microfuge tube. Cold 99% ethanol (2.5 volumes) was added to the collected aqueous phase and the samples were incubated at -70°C for at least one hour. The precipitated tRNA was pelleted by centrifugation for 30 minutes at 16 000 xg and 4°C. The supernatant was removed and the pellet was resuspended in 50 μ L of nuclease-free water by vortexing. The transcripts were stored at -70°C.

2.5.5 Urea denaturing polyacrylamide sequencing gels

See Table 2-1 for the components of 100 mL of 12% or 20% polyacrylamide/7M urea denaturing sequencing gels. First, a seal was needed at the base of the electrophoresis apparatus. A plug was formed with 50 mL 30% acrylamide (Table 2-1), 50 mL dH_2O , 200 μ L 25% APS, and 200 μ L TEMED. For a 38 cm by 50 cm sequencing apparatus, 150 mL of gel solution (some excess) was essential for proper casting. The solution (without APS and TEMED) was slightly heated under hot water in order to

dissolve the urea completely. The solution was then degassed by vacuum suction (in a side-arm flask) while being cooled on ice (prevented polymerization during the casting process) for 30 minutes. APS and TEMED were then added to flask (sealed at the arm with Parafilm) and inverted about 10 times. The 150 mL solution was funnelled into an upright Bio-Rad apparatus by using a 150 mL syringe (without needle and plunger) and plastic tubing with a spout (provided with the Bio-Rad apparatus). While filling, the outer glass plate was tapped with the flat end of a flint spark lighter in order to remove any air bubbles and force them out of solution. A 32-well 0.4 mm plastic comb was inserted at the top of the glass plates and the apparatus was placed horizontally (levelled) onto an absorbent paper covered bench (this was done slowly in order to prevent air bubbles from forming) for polymerization of the gel. Polymerization was typically complete 1-3 hours after casting of the gel; however, the gel usually was left on the workbench overnight to ensure full polymerization. Once the gel was fully polymerized, the comb was removed and the gel was transferred to the rest of the electrophoresis apparatus and submerged in TBE buffer (2 litres). Electrophoresis was performed for 30-60 minutes at 1950 volts prior to loading. Each well was individually rinsed with TBE buffer using a syringe (with needle) prior to loading the samples. Electrophoresis of the samples was then carried out at 1950 volts for 5-6 hours.

2.5.6 Standard activity assays with various [α - 32 P] GTP transcribed tRNA

Gel-purified labelled transcripts were diluted 2-fold and 10-fold to determine the minimum amount of transcript required to be detected by Phosphor imaging. Standard enzyme assay conditions were modified from Cudny *et al.* (1978) as in Arthur (2009). The reactions for this study were carried out in a total volume of 10 μ L. Each standard

assay reaction mix contained 100 mM glycine buffer (pH 9), 10 mM MgCl₂, 1 mM ATP, 0.4 mM CTP, approximately 1 μL of the resulting [α -³²P] GTP transcribed tRNA after gel extraction, and approximately 100 ng of protein. The amount of radioactive template used for each reaction was estimated to be approximately 0.5 μg as Shi *et al.* (1998b) typically obtained approximately 30 μg of RNA during run-off transcription (under similar conditions) and Arthur (2009) estimates 70% radioactive GTP incorporation during run-off transcription and a 90% recovery from gel extraction (under similar conditions). This amount of template was the minimal amount for detection using the Typhoon™ TRIO Variable Mode Imager (GE Healthcare). The sequence of tRNA^{Asp} from *Bacillus subtilis* was obtained (GenBank accession number: K00637, Region: 6531 – 6607, see Fig. 1-1) and a DNA/RNA Base Composition Calculator (Current Protocols, DNA/RNA Base Composition Calculator, <http://www.currentprotocols.com/tools/dnarna-base-composition-calculator>) was used to calculate a molecular weight of approximately 24 500 - 25 500 g/mol (with and without the 3'-end CCA sequence). From this, a molar concentration of approximately 2 μM (0.5 μg / (1 mol/25 000 g)*10 μL) of tRNA template (concentration limiting) can be calculated as the final concentration of tRNA template in a single reaction (10 μL). Each standard reaction was carried out for 2 minutes at room temperature and was terminated by adding one volume (10 μL) of Peattie's loading buffer. The tubes were then incubated for 10 minutes at 70°C, and the samples were centrifuged for 30 seconds at 16 000 xg and 4°C before being loaded onto a 12% denaturing sequencing gel. Alternatively, the assays were incubated for 10 minutes at 70°C and stored at -70°C until loaded onto a gel (after another 10 minute 70°C incubation and 30 second centrifugation). Other reaction conditions were tested (*e.g.*, 1

mM ATP or 0.4 mM CTP alone) with all other components remaining constant. The various tRNA templates used for each group of assays were tRNA-N, tRNA-NC, and tRNA-NCC (preparation described in sections 2.5.3 and 2.5.4). A Geiger counter was used to detect the section of the gel with the highest number of counts per minute (indicating the position of the run-off transcripts). That section of the gel was transferred to a pick-up film and the gel was exposed to a Storage Phosphor screen (GE Healthcare) at room temperature for 16-24 hours. The screen was then developed by using a Typhoon™ TRIO Variable Mode Imager (GE Healthcare), visualized with ImageQuant (Molecular Dynamics) software, and analyzed with ImageQuant TL (GE Healthcare) software.

2.5.7 Time course assays with the various tRNA substrates

For each assay the standard assay mixture was multiplied to a final volume of 80 μ L containing 100 mM glycine buffer (pH 9), 10 mM $MgCl_2$, 1 mM ATP, 0.4 mM CTP, and 800 ng of enzyme. Aliquots of 10 μ L of this were transferred to a microfuge tube containing 10 μ L Peattie's loading buffer (Table 2-1) to terminate the reaction at times 2, 4, 10, 15, 30, 60, and 120 minutes. The samples were then loaded onto a 12% Polyacrylamide 7 M Urea denaturing gel and treated as described previously in sections 2.5.5 and 2.5.6. These assays were also performed in the absence of ATP, as well as in the absence of CTP. Other modified time course assays (times: 30, 120 minutes) were performed with no ATP and CTP, but in the presence of either 0.4 mM GTP or 0.4 mM UTP. The various tRNA templates used for each group of assays were tRNA-N, tRNA-NC, and tRNA-NCC.

3. Results

Position 204 in *Candida glabrata* tRNA nucleotidyltransferase is an arginine residue that is conserved in multiple tRNA nucleotidyltransferases (Fig. 1-2). Previous experiments in other organisms suggest a role for this amino acid in nucleotide specificity and incorporation efficiency (Li *et al.*, 2002; Lizano *et al.*, 2008). Plasmid shuffling experiments (Fig. 1-9) demonstrate that select amino acid substitutions of Arg204 result in cell death. This study was carried out to assign a role to this conserved arginine residue by analyzing, by biophysical and biochemical methods, native and variant forms of tRNA nucleotidyltransferase.

3.1 Expression and purification of native and variant enzymes

Native and variant (R204, R204A, R204E, R204Q, R244A-R204E, and R244A-R204Q) tRNA nucleotidyltransferase proteins were expressed and their purity determined by SDS-PAGE. All of the proteins were isolated at the same level of purity (Fig. 3-1). An example purification of the alanine variant is shown on Figures 3-2 and 3-3. The predicted size of the GST fused protein was approximately 90 kDa (see lane 2 in Fig. 3-2, Panel B). Each native or variant tRNA nucleotidyltransferase protein alone was approximately 60 kDa (see lane 3 in Fig. 3-2, Panel B). After thrombin cleavage, free GST (~26 kDa) was left in solution. Primary dialysis in a 6-8 kDa bag reduced the level of glutathione in the elution/cleavage buffer (see Table 2-1). Secondary dialysis in 50 kDa pore size dialysis tubing allowed the removal of thrombin, as well as a further reduction in glutathione concentration.

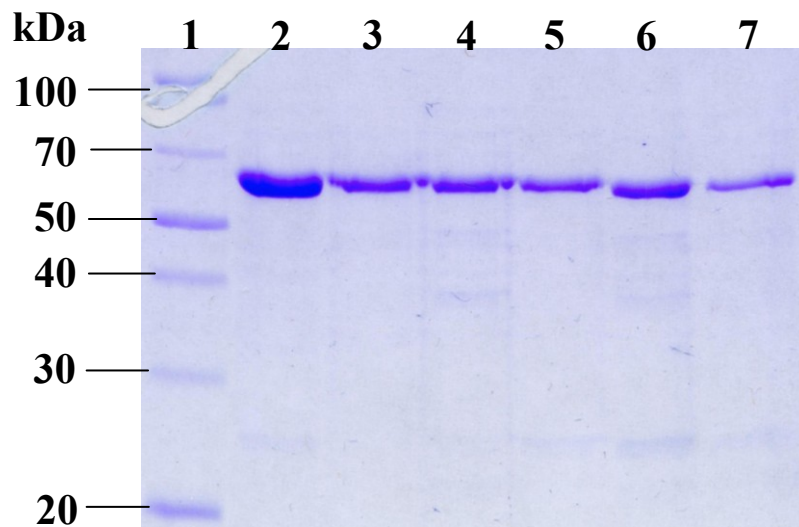


Fig. 3-1. Coomassie blue-stained SDS-PAGE of purified native and variant nucleotidyltransferases. Lane 1: molecular weight markers (PageRuler™ Unstained Broad Range Protein Ladder, #SM1881); lane 2: native enzyme (Arg204); lane 3: alanine variant (R204A); lane 4: glutamate variant (R204E); lane 5: glutamine variant (R204Q); lane 6: R244A-R204E variant; lane 7: R244A-R204Q variant. The same volume of purified protein was loaded into each lane (16 μ L). The sizes of the molecular weight markers (kDa) are shown to the left of the gel.

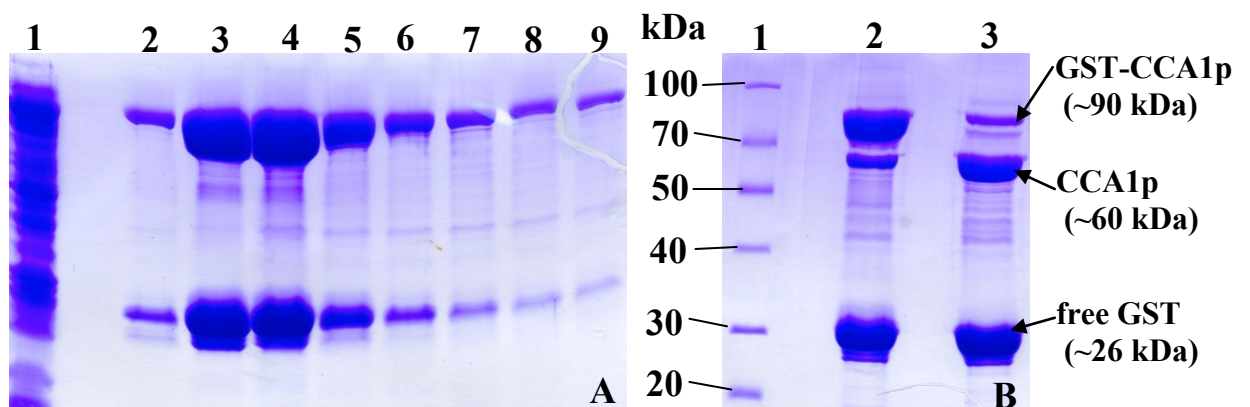


Fig. 3-2. Coomassie blue-stained SDS-PAGE representing the stepwise purification of the alanine variant of tRNA nucleotidyltransferase. **Panel A:** lane 1: crude cell lysate; lanes 2-9: fractions 1, 3, 5, 7, 9, 11, 13, and 15 after GST-column elution with 15 mM glutathione; **Panel B:** lane 1: molecular weight markers (PageRuler™ Unstained Broad Range Protein Ladder, #SM1881); lane 2: thrombin cleavage of pooled fractions (after 15 minutes); lane 3: thrombin cleavage of pooled fractions (overnight). The sizes of the molecular weight markers (kDa) are shown to the left of panel B.

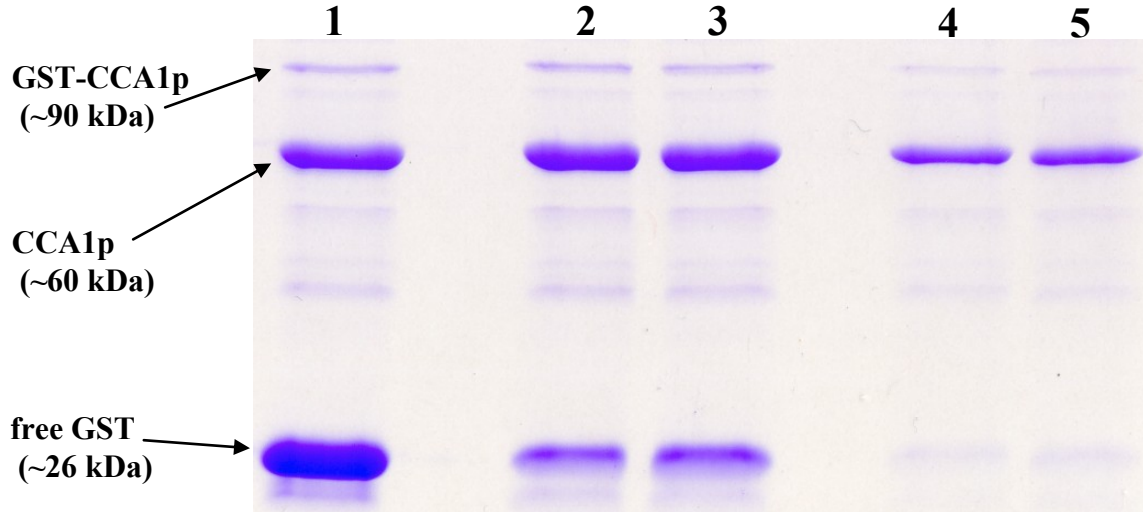


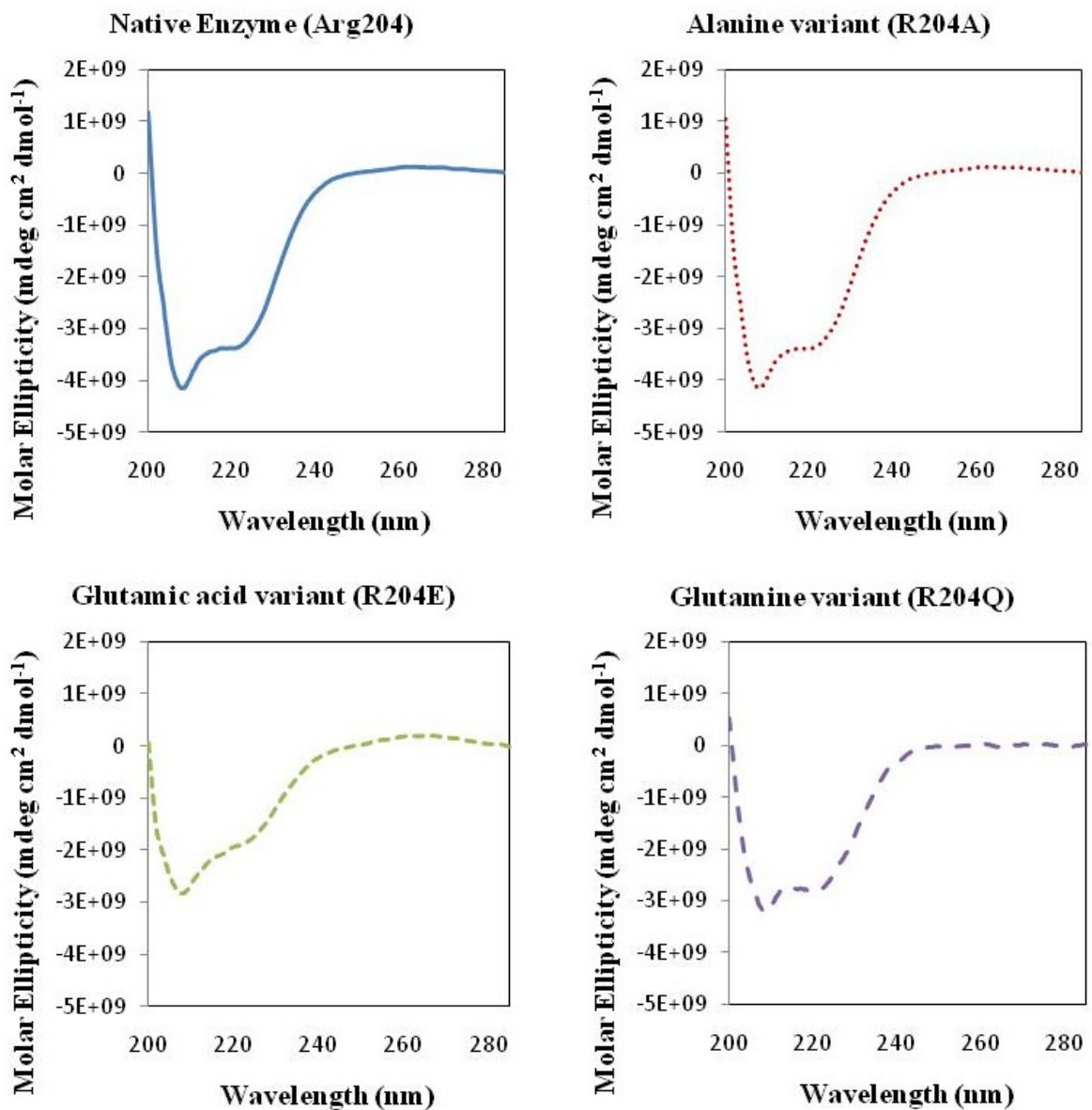
Fig. 3-3. SDS-PAGE (Coomassie blue stained) representing the stepwise removal of free GST after thrombin cleavage. Lane 1: GST eluate after thrombin cleavage and dialysis in a 50 kDa dialysis bag; lane 2: after cycling through the GST column 3 times; lane 3: after cycling through the GST column 5 times; lane 4: after cycling again through a regenerated GST column 3 times; lane 5: after cycling again through a regenerated GST column 5 times. Sizes of the bands of interest and their molecular weights (kDa) are shown the left of the gel.

The 26 kDa GST tag should dialyze out of solution; however, this was not observed (see lane 1 in Fig. 3-2). This may be explained by GST forming a dimer, as observed in GST crystallized from *Schistosoma japonicum* (Lim *et al.*, 1994). In order to remove GST, the solution was passed through a regenerated glutathione resin five times (see lane 3 in Fig. 3-2, the column was regenerated and the sample (after another dialysis to adjust for a final pH of 7.3) was cycled through the resin another five times. At this point only minimal amounts of free GST remained (see lane 5 in Fig. 3-2). None of the R204 variants showed any major differences in expression levels (data not shown) compared to the native enzyme. In contrast, the variant proteins were not recovered as efficiently during the purification process (Fig 3-1).

3.2 Biophysical characterization of tRNA nucleotidyltransferase

3.2.1 Secondary structure determination by circular dichroism

An assessment of the effects of altering arginine 204 on the secondary structure of the protein was determined by circular dichroism. The protein samples were scanned in the far-UV region from 285 nm to 200 nm. Figure 3-4 shows native and variant enzyme spectra separately, while Figure 3-5 shows the overlaid spectra.



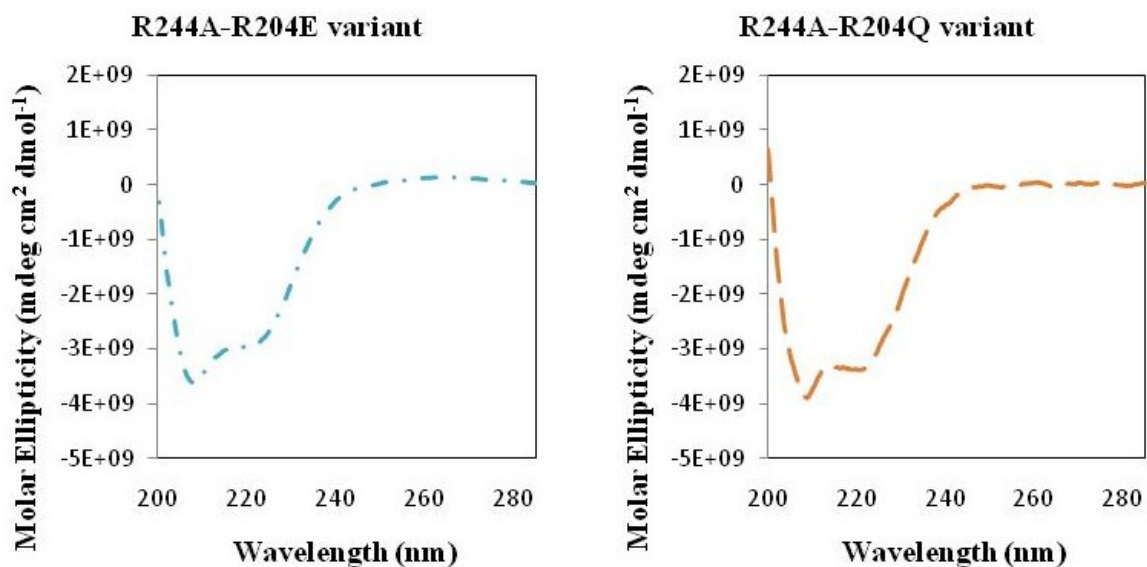


Fig. 3-4. Far-UV CD spectra of native & variant tRNA nucleotidyltransferases. Spectra were generated between 285 nm and 200 nm using a 0.2 cm quartz cell with 600 μ L of protein (0.1 mg/mL) at 20°C.

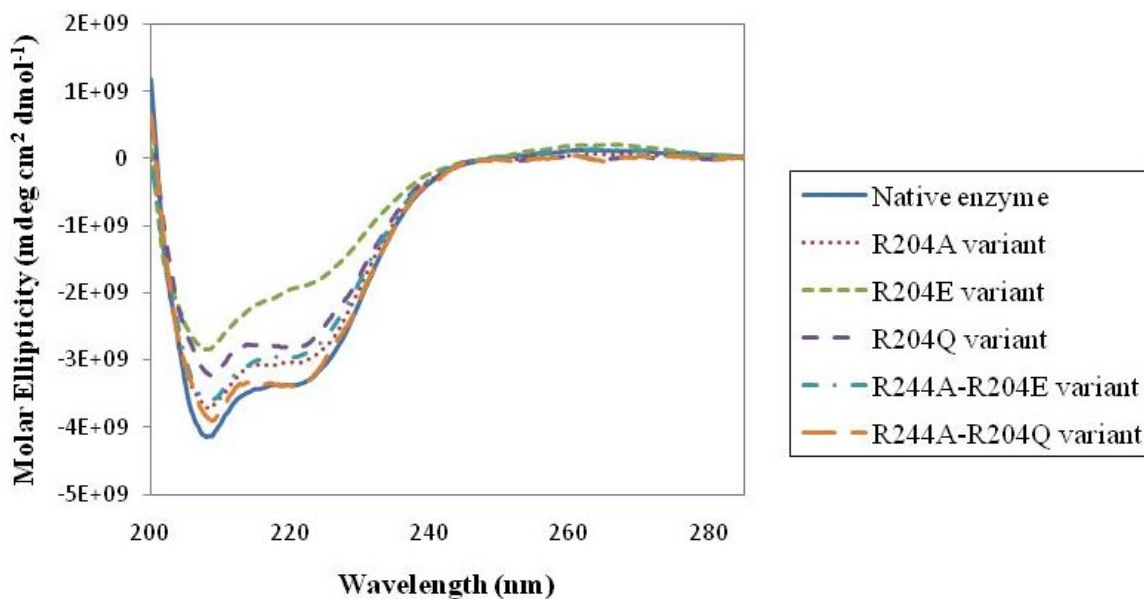


Fig. 3-5. Overlaid Far-UV CD spectra of native & variant tRNA nucleotidyltransferases. (see Fig. 3-4 for details)

All proteins show minima at 208 nm and 222 nm characteristic of an alpha-helical secondary structure (consistent with reported crystal structures Li *et al.*, 2002; Augustin *et al.*, 2003; Tomita *et al.*, 2004; Toh *et al.*, 2009). The most dramatic change in any spectrum was seen with the R204E variant which had much reduced minima at both 208

nm and 222 nm, suggesting a perturbation of alpha-helical structure. Interestingly, this perturbation was restored somewhat in the R244A-R204E variant.

3.2.2 Thermal denaturation of native and variant enzymes monitored by circular dichroism (CD) spectroscopy

Temperature denaturation studies monitored by CD spectroscopy between 20°C and 60°C (Fig. 3-6) were performed in order to assess the stability of the native and variant enzymes. Estimated melting temperatures are summarized in Table 3-1. A melting temperature (T_m) of approximately 42.9°C for the wild-type enzyme is in reasonable agreement with a value of 38.4°C determined previously (Arthur, 2009). The 4.5°C difference in melting temperature may be explained by small changes in the experimental procedures (*e.g.*, protein purification protocol, cell path length, etc.). The R204E and R204Q variants showed a similar and small (1.6°C) increase in T_m while the R204A variant showed a slightly larger shift in T_m (2.8°C). The R244A-R204Q and R244A-R204E variants both showed the largest increase in T_m (4.4°C). Interestingly, Arthur (2009) had shown a similar increase in T_m over the native enzyme of about 4.2°C for the single R244A variant. Each of the single and double variants studied here showed T_m changes in the range seen previously by Arthur (2009) for R244 variants. All melting temperatures were manually estimated by the mid-point values of the ellipticity between the native and denatured states. Signal variations at the beginning of the measurement may represent slight differences at the start of the unfolding process. Unstable signal at the end of the curves may be due to aggregation from denaturation, although no visible precipitate was observed. After cooling the protein samples to room temperature, the spectra obtained were similar to those of the warmed samples (data not shown). This

suggests that thermal denaturing is irreversible. Finally, with the exception of the R204E variant, all of the thermal denaturation curves show a general cooperative two-state unfolding transition for the proteins. This suggests that an intermediate species may exist for the R204E variant, consistent with the loss in helicity observed in the CD data (Figures 3-4 and 3-5). This intermediate results in a loss of sigmoidicity, representing a different unfolding profile for the intermediate structure.

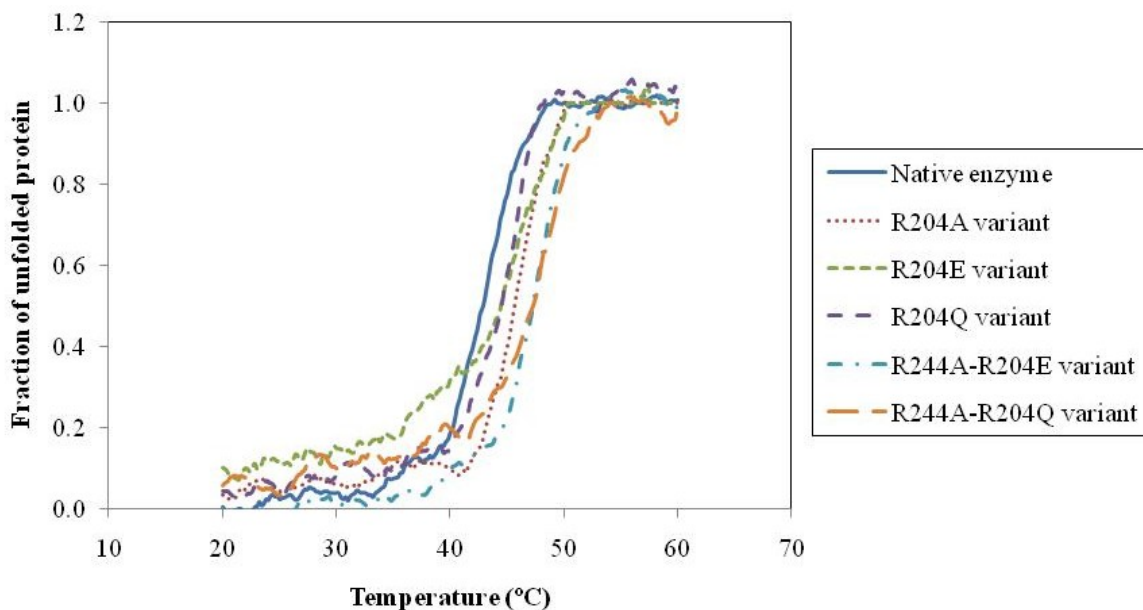


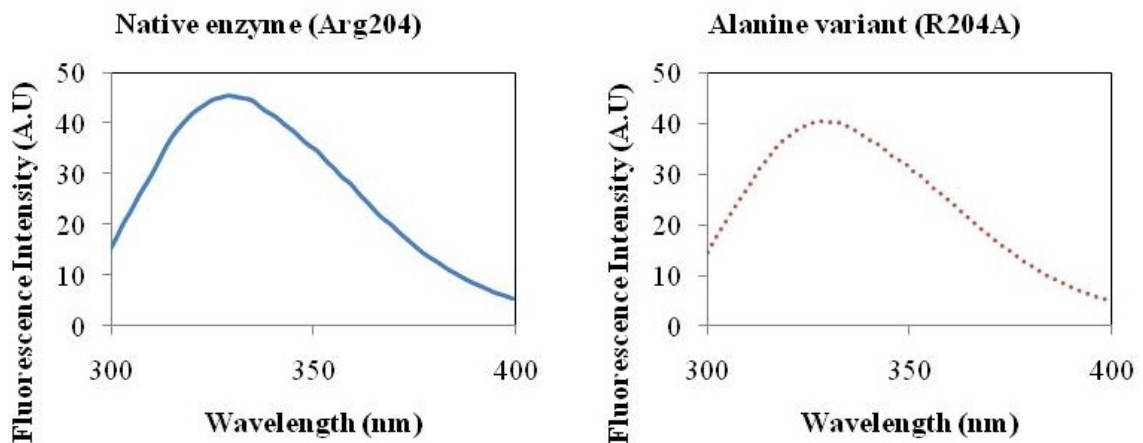
Fig. 3-6. Temperature denaturation of native & variant enzymes monitored by circular dichroism spectroscopy. Signal intensity at 208 nm was monitored between 20°C and 60°C. The spectra were generated using a 0.2 cm quartz cell with 600 μ L of protein (0.1 mg/mL).

Type of enzyme	Approximate T_m (°C)	ΔT_m compared to native enzyme (°C)
Native enzyme (R204)	42.9	0
Alanine variant (R204A)	45.7	+ 2.8
Glutamic acid variant (R204E)	44.5	+ 1.6
Glutamine variant (R204Q)	44.5	+ 1.6
R244A-R204E variant	47.3	+ 4.4
R244A-R204Q variant	47.3	+ 4.4

Table 3-1. Melting temperature (T_m) analysis of native and variant enzymes.

3.2.3 Tertiary structure characterization by fluorescence spectroscopy

An evaluation of the effects of various amino acid changes on the tertiary structure of the protein was carried out by fluorescence spectroscopy. This technique is used to determine any environmental shifts that aromatic residues in the protein may go through. Excitation at a specific wavelength results in aromatic residues (phenylalanine, tyrosine, and tryptophan) emitting light at longer wavelengths. Although all three of these aromatic residues absorb and emit light, Trp fluorescence dominates a spectrum because free Trp has similar emission intensity as free Tyr and Phe at higher concentrations (Creighton, 1989). The intensity and wavelength of any emission depends on the polarity of the environment surrounding these residues (aromatics) and also their proximity to one another. The native and variant proteins were all excited at 280 nm and generated the spectra shown separately in Figure 3-7 and overlaid in Figure 3-8. The native enzyme demonstrated a similar shift (330 nm) as reported previously for the *C. glabrata* enzyme (Arthur, 2009), however, the intensity reported is not directly comparable due to differences in concentrations used in the two sets of experiments.



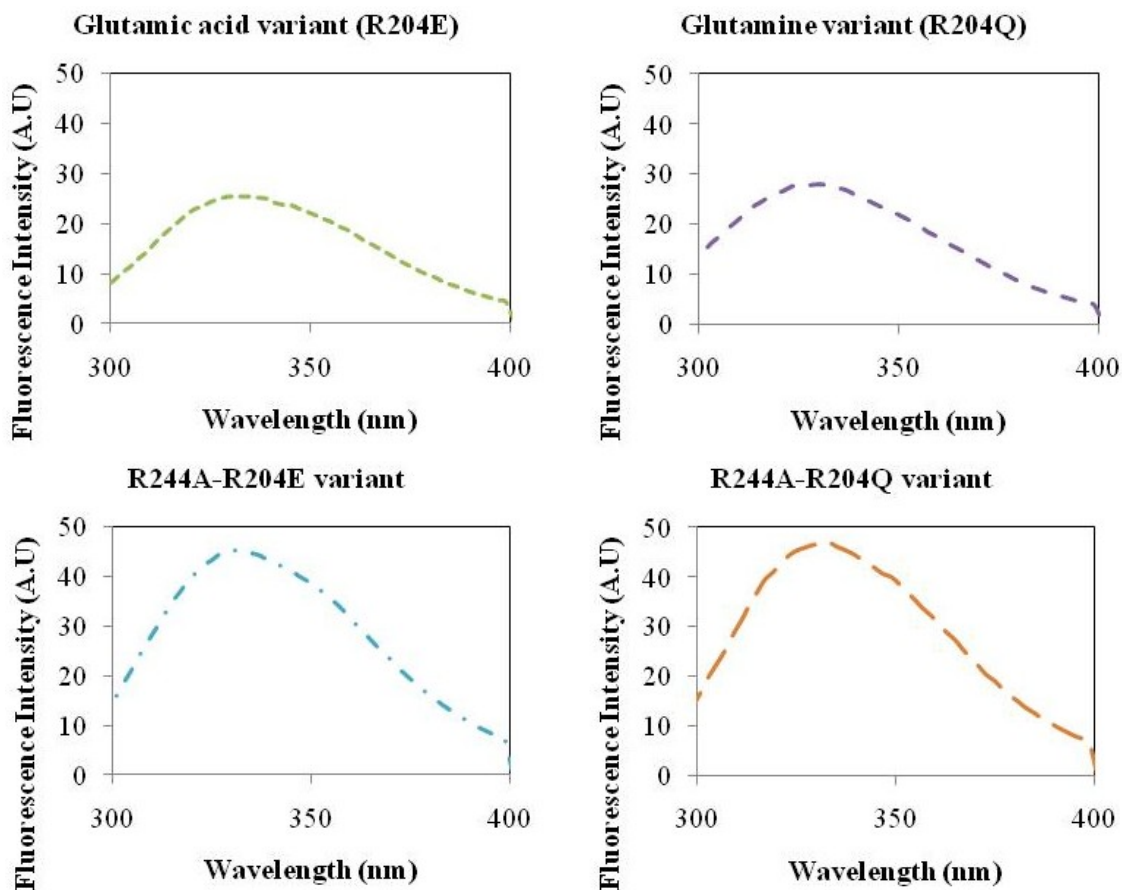


Fig. 3-7. Emission spectra of native & variant tRNA nucleotidyltransferases.

All proteins were excited with 280 nm light. Emission between 300 nm and 400 nm was observed in a 1.0 cm quartz fluorescence cell. All proteins were fixed to a concentration of 1.4 μM (0.1 mg/mL) of protein. A 1.0 mL volume at 20°C was used for each reading.

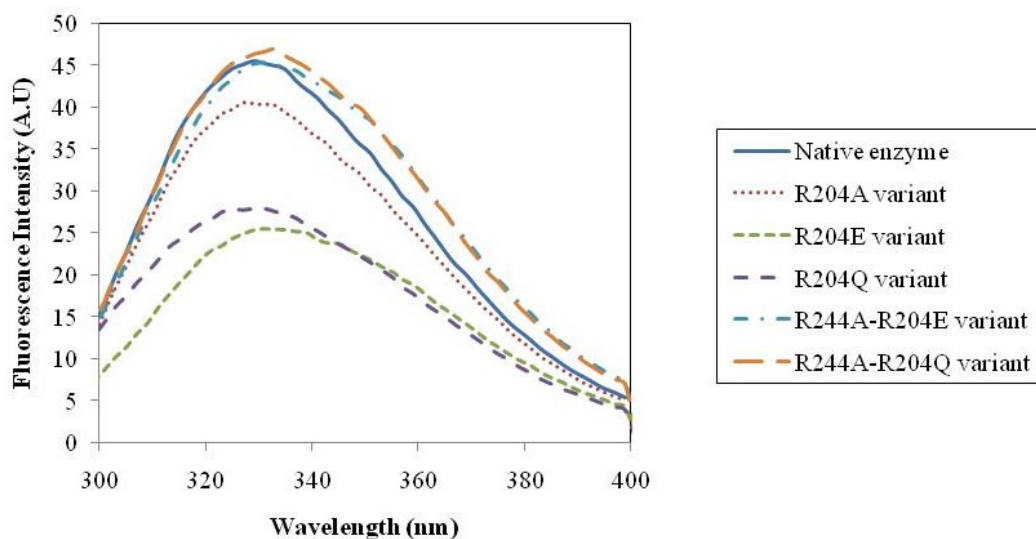


Fig. 3-8. Overlaid spectra of native & variant tRNA nucleotidyltransferases (see Fig. 3-7 for details).

Type of enzyme	Wavelength maximum (nm)	Fluorescence intensity maximum (A.U)
Native (R204)	329	45.4
Alanine variant (R204A)	328	40.6
Glutamic acid variant (R204E)	331	25.4
Glutamine variant (R204Q)	330	27.8
R244A-R204E variant	331	45.4
R244A-R204Q variant	331	46.6

Table 3-2. Peak wavelength and intensity of all studied tRNA nucleotidyltransferases.

As summarized in Table 3-2, the glutamic acid variant (R204E) along with the double variants (R244A-R204E, R244A-R204Q) show the greatest peak shifts to higher wavelength as compared to the native enzyme (red shift). Overall, the red shifts observed are not large, suggesting that aromatic residues in these proteins are in an environment of similar polarity to the native enzyme. Moreover, the R204E and R204Q variants show a significant decrease in fluorescence intensity (quenching) that is recovered in the R244A-R204E and R244A-R204Q variants. Arthur (2009) observed a 1 nm blue shift and no peak intensity effect for the R244A variant, suggesting that the observed quenching effect for the R204E and R204Q variants may be due to the pulling of Arg244 onto Asp201 (Fig. 1-10). Quenching may be observed when the environment of the aromatic residues is disrupted, causing energy transfer to other residues (now closer in proximity). These quenching data along with the slight red shift observed for both of these variants (R204E, R204Q) suggest a more drastic change in tertiary structure compared to the other variants and that the R244A substitution seems to relieve this change (or strain).

3.3. Enzyme assays

3.3.1 Run-off transcription assays

3.3.1.1 Restriction enzyme digests of G73 and pmBsDCCA plasmids

In order to characterize the effects of the changes at position 204 on the addition of ATP and/or CTP, plasmids G73 and pmBsDCCA were linearized for the production by *in vitro* run-off transcription of specific tRNA substrates with differing 3'-ends. The tRNA products produced are indicated in Table 2-3. Agarose gel electrophoresis was used to ensure the complete digestion of the plasmids (Fig. 3-9). The expected fragment sizes following digestion are listed in Table 3-3. Although some partial digestion can be observed for the *FokI* lanes (2 and 3), this was not a problem during run-off transcription as the amount of undigested product was minimal (Fig. 3-9).

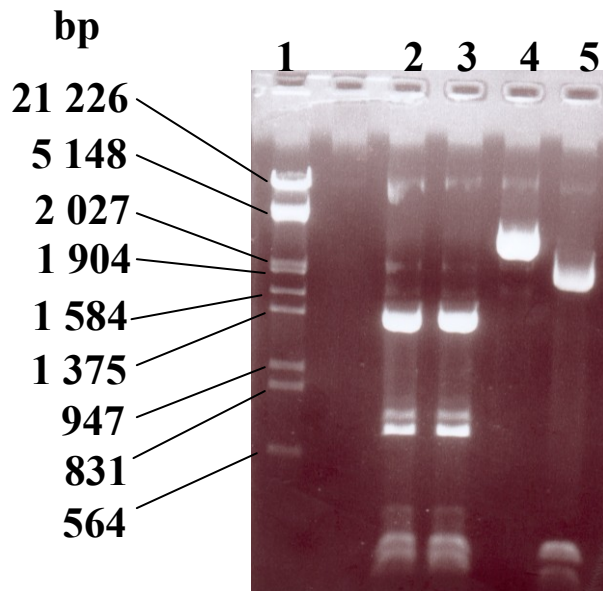


Fig. 3-9. Agarose gel of digested G73 and pmBsDCCA plasmids. Lane 1: *EcoRI* and *HindIII* digested lambda DNA ladder (Fermentas); lane 2: G73 digested with *FokI*; lanes 3-5: pmBsDCCA digested with *FokI*, *BpiI*, and *BstOI*, respectively. DNA ladder band sizes (bp) are shown to the left of the gel.

Plasmid	Restriction enzyme	Approximate fragment sizes (bp)
G73	<i>FokI</i>	1331, 643, 287, 244, 181
pmBsDCCA	<i>FokI</i>	1331, 643, 287, 244, 181
	<i>BpiI</i>	2686
	<i>BstOI</i>	2071, 288, 191, 123, 13

Table 3-3. Fragment sizes (in base pairs) after digestion of G73 and pmBsDCCA plasmids.

3.3.1.2 Run-off transcription

Radiolabelled [α -³²P] GTP was used for the *in vitro* transcription assay. The resulting transcripts were separated on a 20% polyacrylamide 7 M urea denaturing sequencing gel, visualized by autoradiography, and excised (Fig. 3-10).

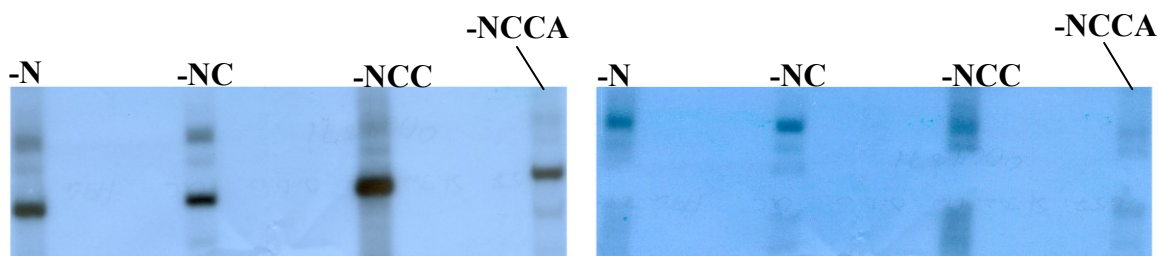


Fig. 3-10. Autoradiogram of run-off transcription products separated on a 20% polyacrylamide 7 M urea denaturing sequencing gel. Left: before band excision; right: after band excision.

3.3.1.3 Standard and modified tRNA nucleotidyltransferase assays

3.3.1.3.1 Assays with the tRNA-N substrate (native and single variant enzymes)

After run-off transcription, the radiolabeled transcript was used under standard conditions with the native Arg204 protein and its single variants. In many cases the products of run-off transcription showed a second band corresponding in size to N+1 as compared to the expected product (see Fig. 3-11, Template, for example). The N+1 band represented in some cases up to approximately 20% of the product (Table 3-4) and may represent either 3' or 5' end heterogeneity. Pleiss *et al.* (1998) reported that consecutive

guanosine nucleotides at the 5' end of the tRNA to be transcribed could lead to 5' end heterogeneity. As illustrated in Figure 1-1, *B. subtilis* tRNA^{ASP} begins with the sequence GGU (GenBank accession number: K00637, Region: 6531 – 6607) and Pleiss *et al.* (1998) showed that a transcript beginning with three Gs could have up to 13% 5' end heterogeneity. In contrast, Milligan and Uhlenbeck (1989) and Schurer *et al.* (2002) reported 3' end heterogeneity resulting from run-off transcription. Regardless of the source of this heterogeneity, an un-extended template was included in the analysis of each enzyme assay and the results obtained with any variant enzyme were always compared to the results obtained with the native enzyme to highlight any differences. Overall, the native enzyme in this study demonstrates the ability to fully extend all templates when supplied with both ATP and CTP (lane 3, Figures 3-11 to 3-13). In addition, the native enzyme also shows a decreased extension efficiency when supplied with ATP alone (lane 4, Figures 3-11 to 3-13) or with CTP alone (lane 5, Figures 3-11 to 3-13). Given that it has been shown previously (Lizano *et al.*, 2008) that tRNA nucleotidyltransferase will abort extension after misincorporation these data showing extension of all products suggest that the heterogeneity present in this study is due to 3' extended products containing an additional CMP for the tRNA-N and -NC templates. If CMP is indeed the extra nucleotide, then this would imply that heterogeneity observed for the tRNA-NCC template would be due to the generation of a small amount of tRNA-NCCC. This species is not a problem during subsequent analysis as it will not be further extended and can be subtracted (if necessary) from the final tRNA-NCCA-sized product observed in any reaction. Finally, this heterogeneity also is observed sometimes in the tRNA-NCCA template (1 and 15, Figures 3-11 to 3-13). As none of the species are

extended to a size greater than that of the tRNA-NCCA product, this supports 3' and not 5' heterogeneity as 5' heterogeneity would allow for products containing more than 76 nucleotides to be generated. In conclusion, although the heterogeneity of the starting template may make analysis slightly more difficult, it does not affect the goal of this study in analyzing nucleotide incorporation differences resulting from the amino acid substitutions as the template prior to modification by tRNA nucleotidyltransferase is included in each assay for the purposes of comparison.

When supplied with both ATP and CTP, the native enzyme efficiently generates a product suggesting that the template has been extended from position 73, the discriminator base (tRNA-N), to position 76 (tRNA-NCCA) (Fig. 3-11). When the native enzyme was supplied with only ATP, three bands were observed, with the most intense band corresponding in size to extension to position 75 (tRNA-NCC) (Table 3-4). This suggests that ATP may be misincorporated at positions 74 (corresponding to tRNA-NC) and 75, blocking further extension although the possibility that incorporation of CMP at positions 74 and 75 is simply less efficient cannot be excluded. Misincorporation of AMP under *in vitro* conditions has previously been seen with other tRNA nucleotidyltransferases (Deutscher, 1983), including the *C. glabrata* enzyme (Arthur, 2009). In addition, when Arthur (2009) used a less heterogeneous (percentages unreported) starting material he saw only 3.6% of the template extended to a size corresponding to the incorporation of two AMPs. Based on this, the band corresponding to insertion to position 75 may be the result of the addition of one AMP to the heterogeneous portion of the initial template. When only CTP was supplied to the native enzyme, it showed the ability to add CMPs all the way to position 76. Misincorporation

of CMP at position 76 has also been observed *in vitro* for the *Candida* enzyme (Arthur, 2009), and for the *E. coli* and rabbit liver tRNA nucleotidyltransferases (Deutscher, 1973a; Deutscher, 1973b; Hou, 2000; Seth et al., 2002).

When the alanine variant (R204A) is supplied with both ATP and CTP approximately 13.7% of the product shows apparent extension to position 76, while approximately 33.3% of the product corresponds in size to extension to position 75 (tRNA-NCC). The fact that some of the starting template (approximately 21.5%) had a size corresponding to extension to position 74 suggests that the substrate was either not extended efficiently, or that the templates corresponding in size to products extended to positions 75 and 76 were extended by two nucleotides. Similarly, when this variant was supplied with CTP or ATP alone, inefficient addition of up to two nucleotides is observed at 29.7% and 16.3% of product, respectively. Once again, these apparent increases in incorporation may be less due to the heterogeneity of the initial template. Finally, the other variants (R204E and R204Q) showed no significant extension of the template under any of the conditions tested. Overall, since the primary transcript (tRNA-N) is never extended efficiently to tRNA-NCCA by any of the variant enzymes, this could explain the *in vivo* observation of cell death as incomplete extension would lead to a lack of aminoacylation and the inability to carry out protein synthesis. Taken as a whole, these results imply that the arginine residue at position 204 plays a vital role in CMP incorporation to tRNA-N, as all of the variants demonstrate a reduced ability to add the first nucleotide. In order to clarify arginine 204's role at this position, experiments with tRNA substrates having longer 3' ends (tRNA-NC and tRNA-NCC) are required.

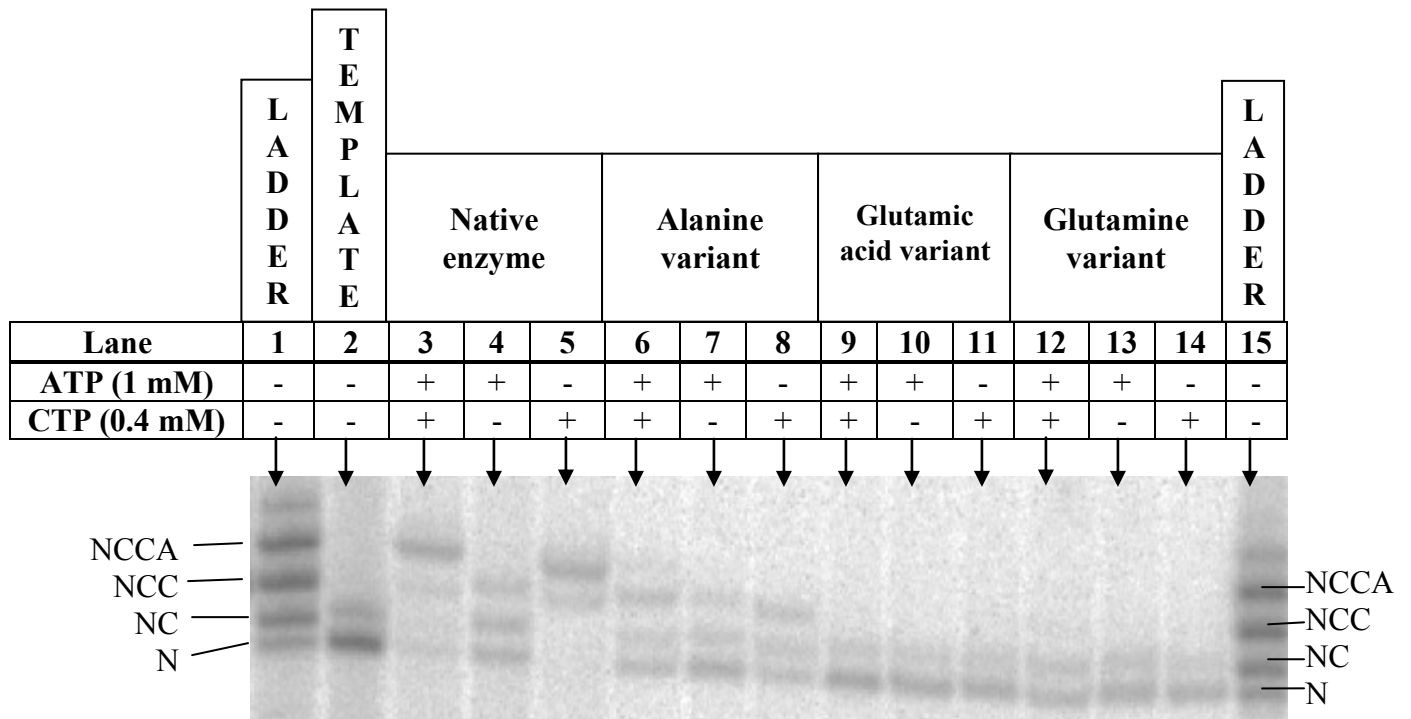


Fig. 3-11. Denaturing polyacrylamide gel showing assays under standard conditions using substrate tRNA-N (native and single variants). Control lane: tRNA-N without enzyme. Double variant results can be seen in Fig. 3-14.

	Template	Native enzyme			Alanine variant		
		ATP + CTP	ATP	CTP	ATP + CTP	ATP	CTP
NCCA	-	65.1	-	69.5	13.7	-	-
NCC	-	16.7	23.3	30.5	33.3	16.3	29.7
NC	21.5	6.6	37.3	-	18.5	24.4	31.2
N	78.5	11.6	39.4	-	34.5	59.3	39.1

	Glutamic acid variant			Glutamine variant		
	ATP + CTP	ATP	CTP	ATP + CTP	ATP	CTP
NCCA	-	-	-	-	-	-
NCC	-	-	-	-	-	-
NC	22.6	24.2	28.2	38.3	34.0	28.3
N	77.4	75.8	71.8	61.7	66.0	71.7

Table 3-4. Percentages of products obtained using tRNA-N as the substrate for standard assays (native and single variants). The percentage of each product from a single lane is shown for the native and variant enzymes. Double variant results can be seen in Table 3-7. The percentages were calculated by densitometry using ImageQuant TL (GE Healthcare).

3.3.1.3.2 Assays with the tRNA-NC substrate (native and single variant enzymes)

To further address the role (if any) that R204 plays for incorporation at positions 75 and 76 the native and variant enzymes were tested with the tRNA-NC substrate (Fig. 3-12 and Table 3-5). Again, the template lane shows some heterogeneity within the starting material as described previously. When supplied with both ATP and CTP the native enzyme (Arg204) efficiently extended the tRNA substrate to a size corresponding to extension to position 76. Under the same conditions, the alanine and glutamine variants were less efficient in completely extending tRNA-NC to a size corresponding to position 76 (only 24.3% and 19.3% of the final product, respectively). However, given that 16% of the initial template already has a size corresponding to tRNA-NC+1 (Template, Table 3-5), this suggests that complete extension may actually be much less with both variants showing a limited ability to add two NTPs, or with misincorporation causing the enzyme to abort further extension. Further experiments (*i.e.*, time course assays) will be required in order to distinguish between these possibilities. Moreover, as with the tRNA-N template, the glutamate variant could not add nucleotides at any measurable level. Overall, all of the variant enzymes demonstrated reduced incorporation efficiency in adding one nucleotide to the tRNA-NC template. This further suggests that Arg204 is vital for nucleotide incorporation to both tRNA-N (above) and tRNA-NC. Experiments with the tRNA-NCC substrate will enable us to determine whether Arg204 is important for AMP addition to tRNA-NCC as well.

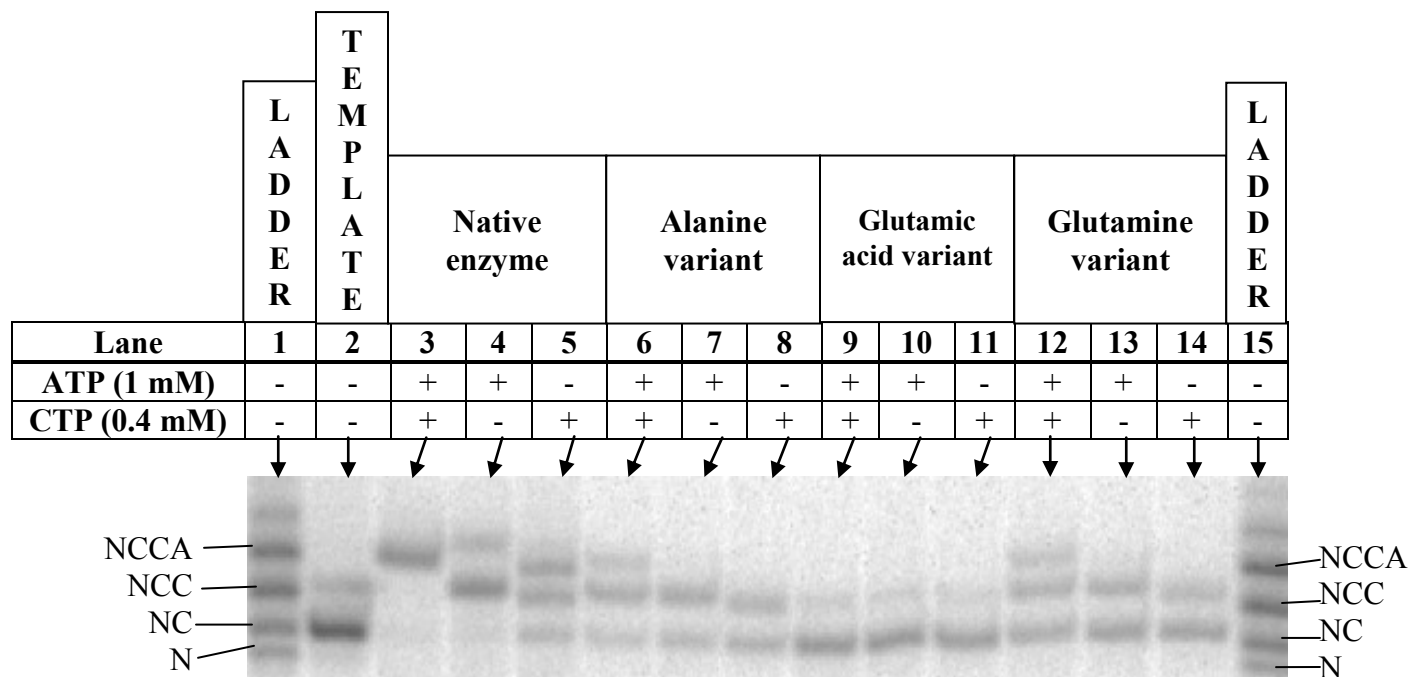


Fig. 3-12. Denaturing polyacrylamide gel showing assays under standard conditions using substrate tRNA-NC (native and single variants). Template lane: tRNA-NC without enzyme. Double variant results can be seen in Fig. 3-15.

	Template	Native enzyme			Alanine variant		
		ATP + CTP	ATP	CTP	ATP + CTP	ATP	CTP
NCCA	-	90.0	24.2	40.9	24.3	-	-
NCC	16.0	-	68.0	39.0	52.9	62.5	45.5
NC	84.0	10.0	7.8	20.1	22.8	37.5	54.5

	Glutamic acid variant			Glutamine variant		
	ATP + CTP	ATP	CTP	ATP + CTP	ATP	CTP
NCCA	-	-	-	19.3	-	-
NCC	13.3	13.5	14.0	35.6	42.6	33.5
NC	86.7	86.5	86.0	45.1	57.4	66.5

Table 3-5. Percentages of products obtained using tRNA-NC as the substrate for standard assays (native and single variants). The percentage of each product from a single lane is shown for the native and variant enzymes. Double variant results can be seen in Table 3-8. The percentages were calculated by densitometry using ImageQuant TL (GE Healthcare).

3.3.1.3.3 Assays with the tRNA-NCC substrate (native and single variant enzymes)

Finally, the activities of the native and variant enzymes were tested with the tRNA-NCC substrate (Fig. 3-13 and Table 3-6). Once more, the template lane shows heterogeneity of the starting material. As previously seen with the other templates, the native enzyme extended the tRNA substrate almost completely (approximately 86.3% of product) to a size corresponding to extension to position 76 when supplied with both ATP and CTP. Under the same conditions, the alanine variant demonstrated a similar result (approximately 84.6% of the product corresponding to the size of tRNA-NCCA). The glutamine variant also showed similar results with 90.8% of the product corresponding to the size of tRNA-NCCA. In contrast, the glutamate variant did not show any product corresponding to complete extension. When supplied with either CTP or ATP alone (Table 3-6), the variant enzymes show an increased selectivity for incorporation at this position as compared to the native enzyme (*i.e.*, they show a reduced incorporation of CMP and incorporate AMP as efficiently as the native enzyme).

Based on the experiments performed with the various templates to this point we cannot define a specific role for R204. It is possible that in each case removing R204 simply allows for an increase in incorporation of AMP (or a decrease in incorporation of CMP) into the template (leading to more misincorporation at positions 74 and 75 and subsequent premature termination of extension), and an increase in incorporation of AMP at position 76. Moreover, we cannot exclude the possibility that we are simply reducing the efficiency of incorporation (most dramatically to tRNA-N and tRNA-NC, and less so to tRNA-NCC). To address these two possibilities we will monitor the reaction over a

longer period of time, in order to see whether the variant enzymes demonstrate significantly more extension with time.

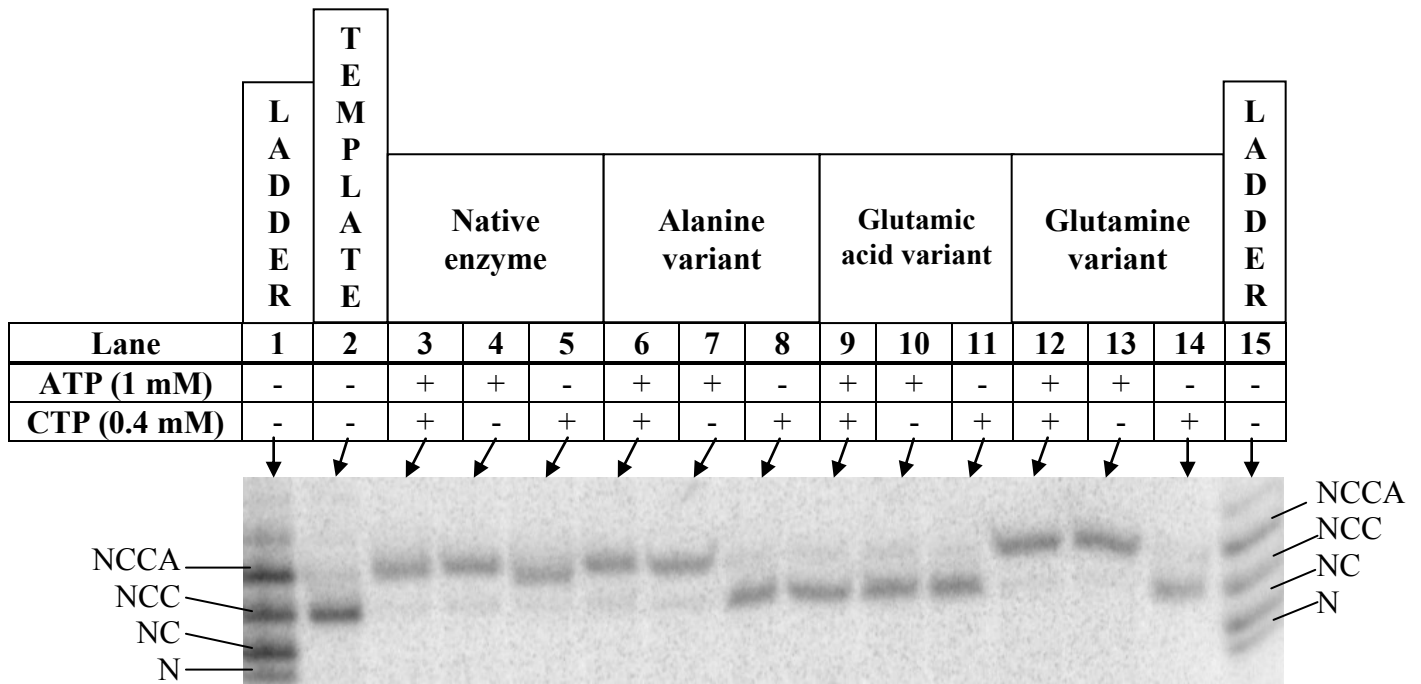


Fig. 3-13. Denaturing polyacrylamide gel showing assays under standard conditions using substrate tRNA-NCC (native and single variants). Template lane: tRNA-NCC without enzyme. Double variant results can be seen in Fig. 3-16.

	Template	Native enzyme			Alanine variant		
		ATP + CTP	ATP	CTP	ATP + CTP	ATP	CTP
NCCA	16.4	86.3	86.8	85.8	84.6	85.2	22.4
NCC	83.6	13.7	13.2	14.2	15.4	14.8	77.6

	Glutamic acid variant			Glutamine variant		
	ATP + CTP	ATP	CTP	ATP + CTP	ATP	CTP
NCCA	16.4	17.2	14.5	90.8	91.8	22.4
NCC	83.6	82.8	85.5	9.2	8.2	77.6

Table 3-6. Percentages of products obtained using tRNA-NCC as the substrate for standard assays (native and single variants). The percentage of each product from a single lane is shown for the native and variant enzymes. Double variant results can be seen in Table 3-9. The percentages were calculated by densitometry using ImageQuant TL (GE Healthcare).

3.3.1.3.4 Double variant enzyme assays (with tRNA-N, -NC, and -NCC substrates)

Previous experiments by Arthur (2009) have shown that changing arginine 244 in the *C. glabrata* enzyme to Ala, Lys, or Met resulted in cell death. Specific nucleotide incorporation assays determined that these substitutions resulted in a loss of nucleotide addition at position 74, a reduction of specificity at position 75, and an increase in specificity at position 76. Knowing the effects of the R244A substitution, we chose to test this variant in combination with the variants described previously. When supplied with ATP, CTP or both nucleotide triphosphates the double variants (R244A-R204E and R244A-R204Q) were unable to extend any of the templates to an appreciable degree (Figures 3-14, 3-15, and 3-16). The R244A-R204Q variant demonstrated minimal activity when adding a single nucleotide to the tRNA-NCC template when supplied with both nucleotides, or with ATP alone (Fig. 3-16).

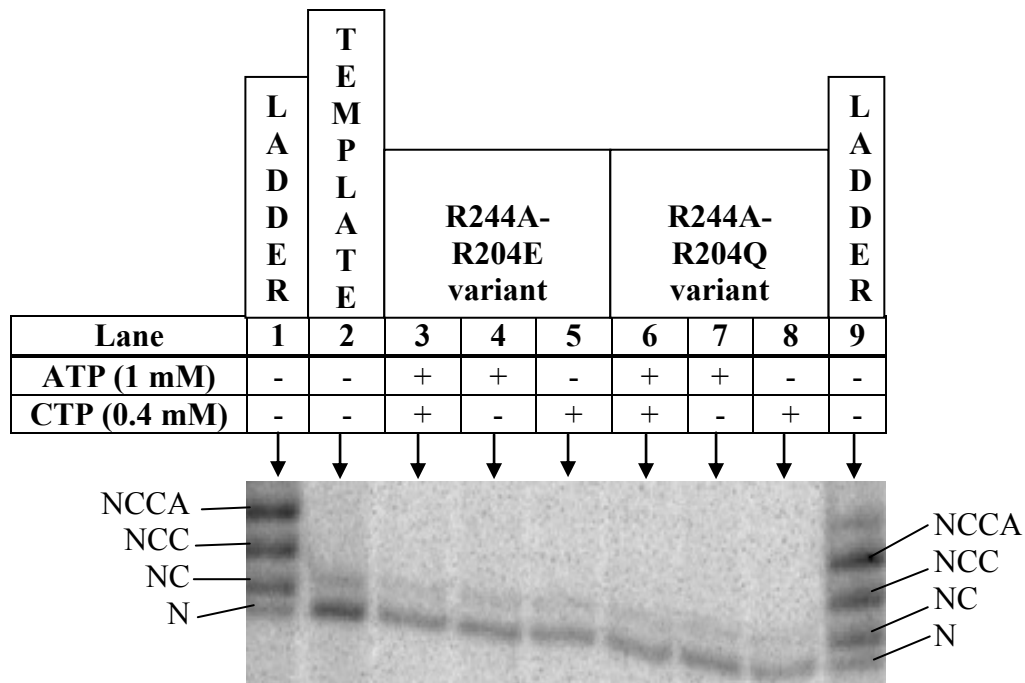


Fig. 3-14. Denaturing polyacrylamide gel showing assays under standard conditions using substrate tRNA-N (double variants). Template lane: tRNA-N without enzyme.

	Template	R244A-R204E variant			R244A-R204Q variant		
		ATP + CTP	ATP	CTP	ATP + CTP	ATP	CTP
NCCA	-	-	-	-	-	-	-
NCC	-	-	-	-	-	-	-
NC	21.0	19.9	20.1	20.9	25.1	22.5	25.1
N	79.0	80.1	79.9	79.1	74.9	77.5	74.9

Table 3-7. Percentages of products obtained using tRNA-N as the substrate for standard assays (double variants). The percentage of each product from a single lane is shown for the double variant enzymes. The percentages were calculated by densitometry using ImageQuant TL (GE Healthcare).

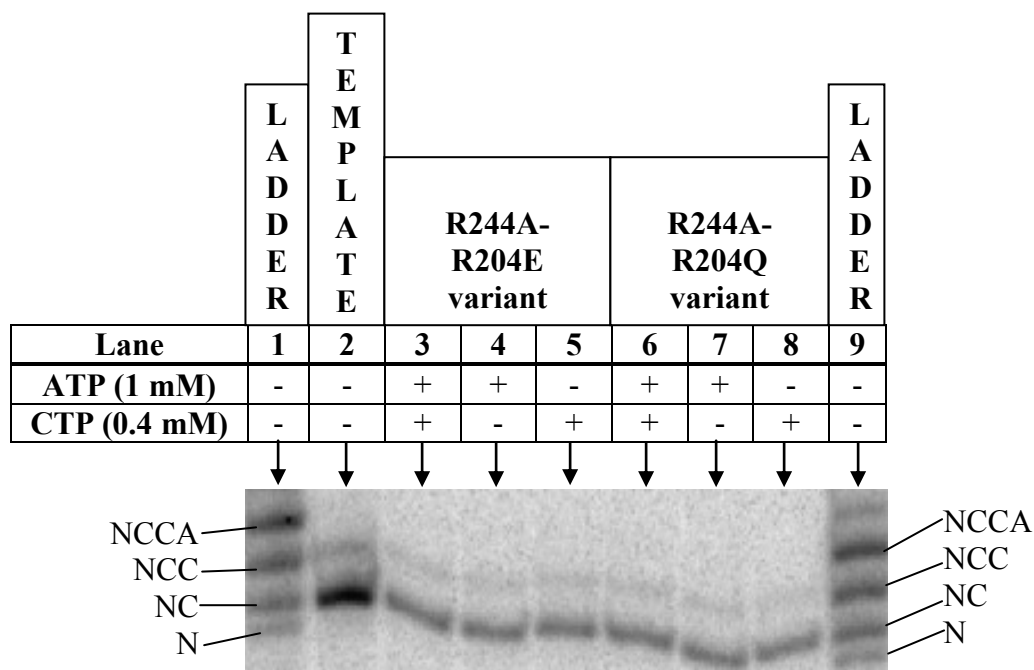


Fig. 3-15. Denaturing polyacrylamide gel showing assays under standard conditions using substrate tRNA-NC (double variants). Template lane: tRNA-NC without enzyme.

	Template	R244A-R204E variant			R244A-R204Q variant		
		ATP + CTP	ATP	CTP	ATP + CTP	ATP	CTP
NCCA	-	-	-	-	-	-	-
NCC	12.9	18.4	12.0	13.1	13.3	12.5	12.6
NC	87.1	81.6	88.0	86.9	86.7	87.5	87.4

Table 3-8. Percentages of products obtained using tRNA-NC as the substrate for standard assays (double variants). The percentage of each product from a single lane is shown for the double variant enzymes. The percentages were calculated by densitometry using ImageQuant TL (GE Healthcare).

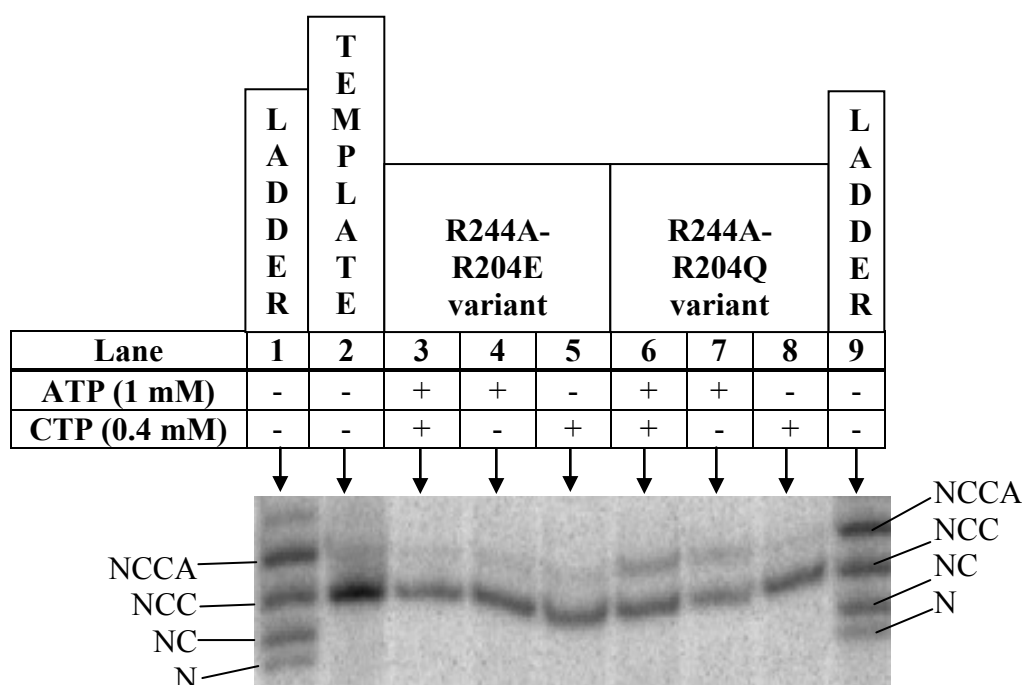


Fig. 3-16. Denaturing polyacrylamide gel showing assays under standard conditions using substrate tRNA-NCC (double variants). Template lane: tRNA-NCC without enzyme.

	Template	R244A-R204E variant			R244A-R204Q variant		
		ATP + CTP	ATP	CTP	ATP + CTP	ATP	CTP
NCCA	14.9	12.9	13.6	15.1	29.0	28.5	15.3
NCC	85.1	87.1	86.4	84.9	71.0	71.5	84.7

Table 3-9. Percentages of products obtained using tRNA-NCC as the substrate for standard assays (double variants). The percentage of each product from a single lane is shown for the native and variant enzymes. The percentages were calculated by densitometry using ImageQuant TL (GE Healthcare).

3.3.1.4 Time-course assays under standard conditions with tRNA nucleotidyltransferase

Since the possibility remained that the standard assay conditions did not allow for full extension of the initial template (*i.e.*, the enzyme could extend the molecules fully but did so less efficiently), time course assays were performed to see if a longer reaction time (up to two hours) would result in further extension. The native enzyme, along with all five variant enzymes were incubated with both NTPs and the appropriate transcript: tRNA-N (Fig. 3-17 to Fig. 3-22), tRNA-NC (Fig. 3-23 to Fig. 3-28), or tRNA-NCC (Fig. 3-29 to Fig. 3-34). During the course of the reaction aliquots were removed at 2, 4, 10, 15, 30, 60, and 120 minutes and transferred to Peattie's loading buffer to terminate the reaction. As seen under standard assay conditions all reactions with the native enzyme had extended the template to a size corresponding to complete extension to position 76 within two minutes. Percentages of the resulting products are summarized from Table 3-10 to Table 3-27.

3.3.1.4.1 Assays with the tRNA-N substrate

When beginning from tRNA-N, none of the variants were able to fully generate a product corresponding in size to extension to position 76. By the 15 minute time point the alanine variant showed product corresponding to extension to at least position 75 with some extension corresponding to a product extended to position 76 even after only 2 minutes (approximately 20% of products), consistent with the results of the standard assays. Moreover, at the two hour time point, product corresponding in size to position 76 was only represented about 34.4% of the total template, suggesting that extension was essentially complete after two minutes and that the inability to extend further after this point represents a loss of specificity and increased misincorporation at position 75. This

results in the blocking of additional incorporation as opposed to a simple reduction in processivity (*i.e.*, a reduced rate of incorporation). In contrast, the glutamine variant demonstrated product corresponding in size to extension to position 75 starting at the 10 minute mark with the generation of a larger product after 30 minutes. At later time points, more of the terminal product is evident suggesting (in this case) that processivity is affected and addition can continue through the course of the reaction. By the final time points, most of the lower molecular weight species have shifted to a higher molecular weight. The glutamic acid variant demonstrated products corresponding in size to extension to positions 75 and 76 only after 60 minutes and only minimal extension occurred after the reaction was sampled at 120 minutes. This is in good agreement with what was seen in the glutamine variant and suggests that incorporation rather than specificity is more dramatically altered in this variant (although a role in loss of specificity cannot be completely excluded at this point). Assays containing both double variant proteins (R244A-R204E and R244A-R204Q) did not show appreciable extension even after 120 minutes (Tables 3-14 and 3-15).

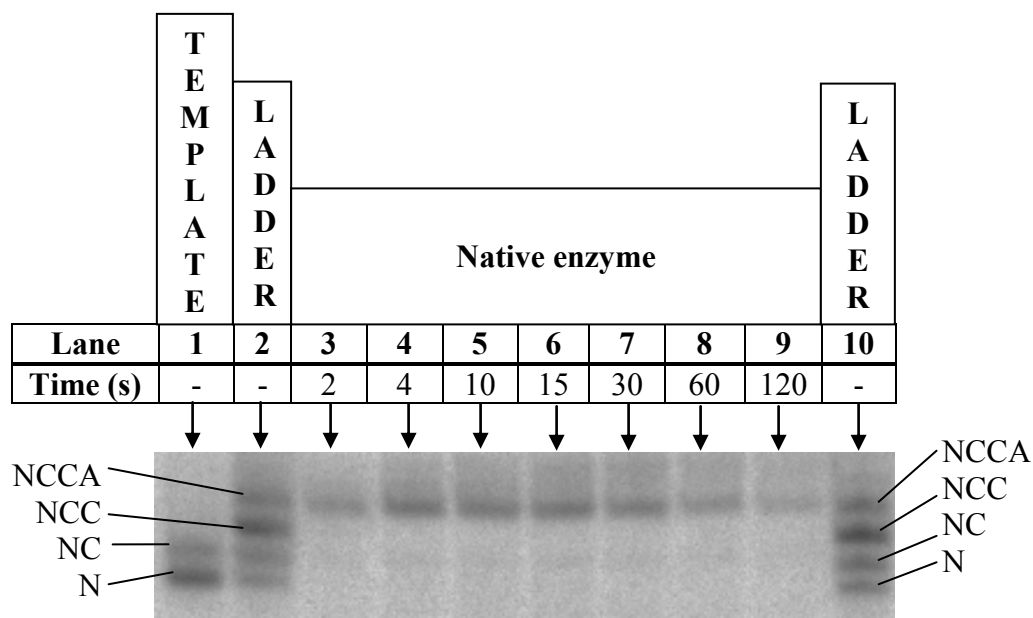


Fig. 3-17. Denaturing polyacrylamide gel showing a time-course assay under standard conditions using substrate tRNA-N (Arg204). Template lane: tRNA-N without enzyme.

	Template	Native enzyme						
		Length of reaction (min)						
		2	4	10	15	30	60	120
NCCA	-	100.0	100.0	100.0	100.0	100.0	100.0	100.0
NCC	-	-	-	-	-	-	-	-
NC	24.6	-	-	-	-	-	-	-
N	75.4	-	-	-	-	-	-	-

Table 3-10. Percentage of resulting tRNAs from a time-course assay with tRNA-N under standard conditions (Arg204). The percentage of each product formed after 2, 4, 10, 15, 30, 60, and 120 minutes were calculated by densitometry ImageQuant TL (GE Healthcare).

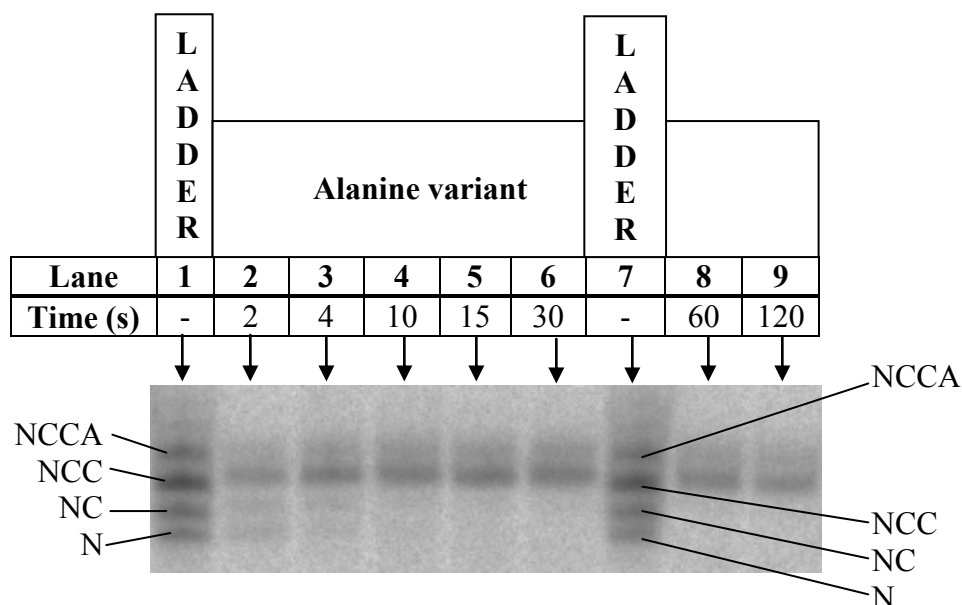


Fig. 3-18. Denaturing polyacrylamide gel showing a time-course assay under standard conditions using substrate tRNA-N (R204A). Template lane: see template in Fig. 3-17.

		Alanine variant						
		Length of reaction (min)						
	Template	2	4	10	15	30	60	120
NCCA	-	20.2	23.8	29.9	30.5	32.6	32.6	34.4
NCC	-	49.2	59.9	62.4	69.5	67.4	67.4	65.7
NC	24.6	16.9	10.5	7.7	-	-	-	-
N	75.4	13.7	5.8	-	-	-	-	-

Table 3-11. Percentage of resulting tRNAs from a time-course assay with tRNA-N under standard conditions (R204A). The percentage of each product formed after 2, 4, 10, 15, 30, 60, and 120 minutes were calculated by densitometry using ImageQuant TL (GE Healthcare).

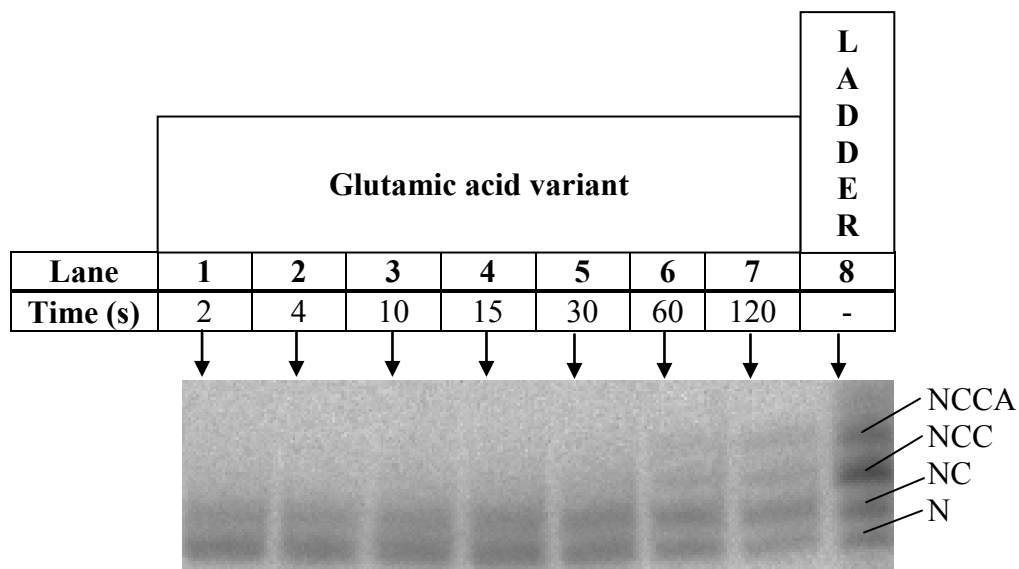


Fig. 3-19. Denaturing polyacrylamide gel showing a time-course assay under standard conditions using substrate tRNA-N (R204E). Template lane: see template in Fig. 3-17.

		Glutamic acid variant						
		Length of reaction (min)						
	Template	2	4	10	15	30	60	120
NCCA	-	-	-	-	-	-	6.2	12.0
NCC	-	-	-	-	-	-	15.7	18.5
NC	24.6	33.5	36.7	37.0	41.0	45.3	41.0	42.4
N	75.4	66.5	63.3	63.0	59.0	54.7	37.1	27.1

Table 3-12. Percentage of resulting tRNAs from a time-course assay with tRNA-N under standard conditions (R204E). The percentage of each product formed after 2, 4, 10, 15, 30, 60, and 120 minutes were calculated by densitometry using ImageQuant TL (GE Healthcare).

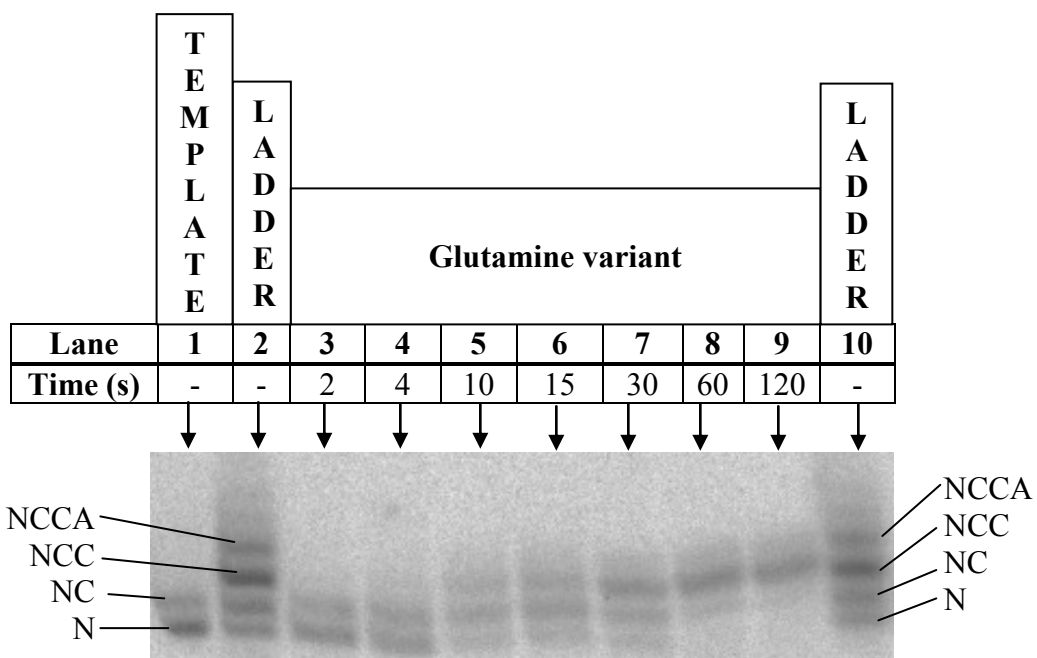


Fig. 3-20. Denaturing polyacrylamide gel showing a time-course assay under standard conditions using substrate tRNA-N (R204Q). Template lane: tRNA-N without enzyme.

		Glutamine variant						
		Length of reaction (min)						
	Template	2	4	10	15	30	60	120
NCCA	-	-	-	-	-	12.5	17.1	20.5
NCC	-	-	-	32.7	34.0	45.8	65.9	67.6
NC	21.2	36.1	43.9	45.1	45.9	28.0	17.0	11.9
N	79.8	63.9	56.1	22.2	20.1	13.7	-	-

Table 3-13. Percentage of resulting tRNAs from a time-course assay with tRNA-N under standard conditions (R204Q). The percentage of each product formed after 2, 4, 10, 15, 30, 60, and 120 minutes were calculated by densitometry using ImageQuant TL (GE Healthcare).

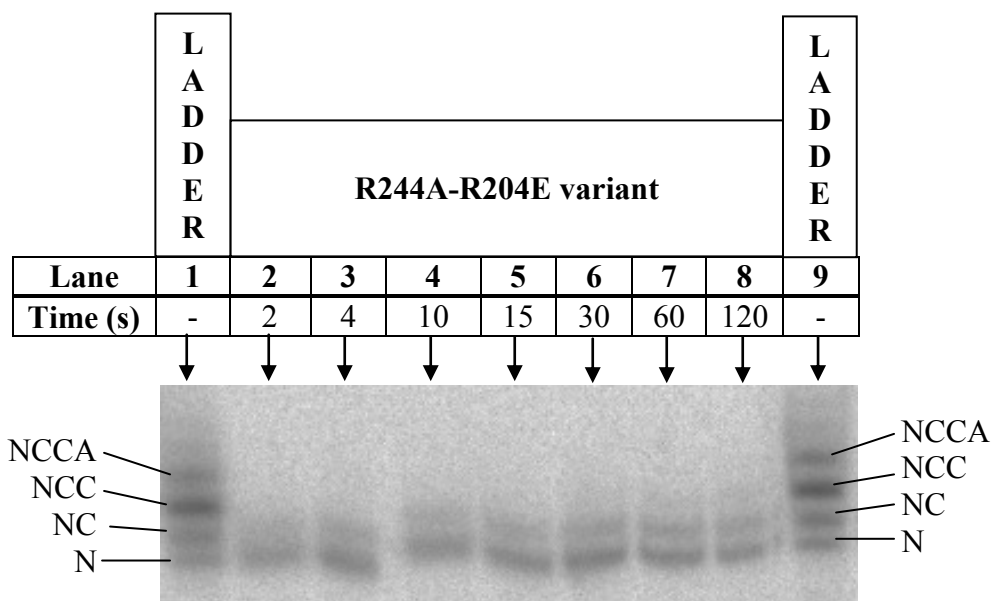


Fig. 3-21. Denaturing polyacrylamide gel showing a time-course assay under standard conditions using substrate tRNA-N (R244A-R204E). Template lane: see template in Fig. 3-20.

		R244A-R204E variant						
		Length of reaction (min)						
	Template	2	4	10	15	30	60	120
NCCA	-	-	-	-	-	-	-	-
NCC	-	-	-	-	-	-	-	-
NC	21.2	29.0	30.0	30.2	30.9	31.2	31.7	32.2
N	79.8	71.0	70.0	69.8	69.1	68.8	68.3	67.8

Table 3-14. Percentage of resulting tRNAs from a time-course assay with tRNA-N under standard conditions (R244A-R204E). The percentage of each product formed after 2, 4, 10, 15, 30, 60, and 120 minutes were calculated by densitometry using ImageQuant TL (GE Healthcare).

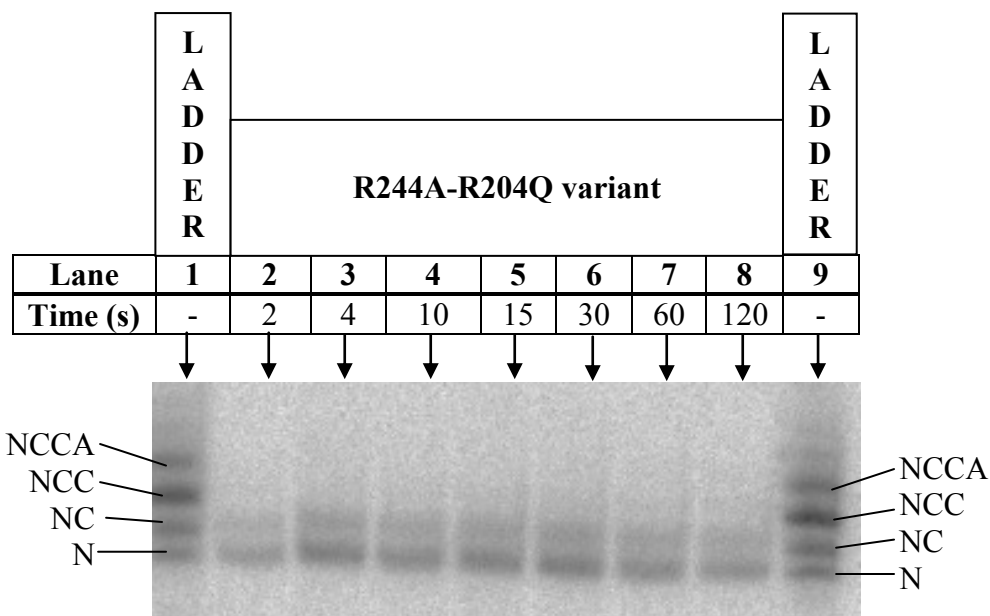


Fig. 3-22. Denaturing polyacrylamide gel showing a time-course assay under standard conditions using substrate tRNA-N (R244A-R204Q). Template lane: see template in Fig. 3-20.

		R244A-R204Q variant						
		Length of reaction (min)						
	Template	2	4	10	15	30	60	120
NCCA	-	-	-	-	-	-	-	-
NCC	-	-	-	-	-	-	-	-
NC	21.2	27.7	30.4	31.3	31.7	32.8	35.5	36.0
N	79.8	72.3	69.6	68.7	68.3	67.2	64.5	64.0

Table 3-15. Percentage of resulting tRNAs from a time-course assay with tRNA-N under standard conditions (R244A-R204Q). The percentage of each product formed after 2, 4, 10, 15, 30, 60, and 120 minutes were calculated by densitometry using ImageQuant TL (GE Healthcare).

3.3.1.4.2 Assays with the tRNA-NC substrate

When tRNA-NC was used as the starting template, none of the variants were able to fully extend 100% of the template to a product corresponding in size to tRNA-NCCA (position 76) after two hours. The alanine variant showed full extension of 62% of the template to products corresponding in size to at least position 75 within 2 minutes, but was unable to further extend more than 38% of the product to a size corresponding to position 76 after 120 minutes. Similarly, the glutamine variant was able to extend 44% of the template to a product corresponding in size to position 76 after two hours, but only showed product extended to a size corresponding to at least position 75 after 60 minutes. Once more, the glutamic acid variant showed the least activity of the single variant enzymes. This variant only showed some addition after 10 minutes and left 31.0% of the tRNA-NC substrate unextended after two hours. Finally, reactions with the double variants once again only showed minimal extension (see Figures 3-27 and 3-28 along with corresponding Tables) although the R244A-R204Q variant was able to generate a small amount (17% of total) of product corresponding to extension of the template to position 76 after two hours. Overall, while the alanine variant did not show decreased incorporation efficiency for nucleotide addition to tRNA-N and tRNA-NC, all of the other variants showed reduced incorporation at these positions.

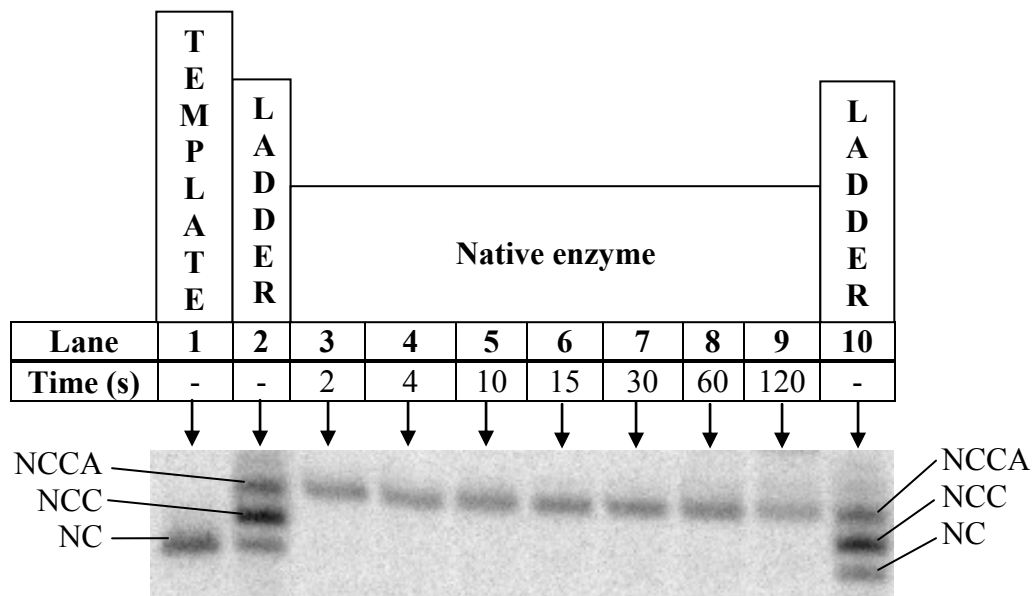


Fig. 3-23. Denaturing polyacrylamide gel showing a time-course assay under standard conditions using substrate tRNA-NC (Arg204). Template lane: tRNA-NC without enzyme.

		Native enzyme						
		Length of reaction (min)						
	Template	2	4	10	15	30	60	120
NCCA	-	100.0	100.0	100.0	100.0	100.0	100.0	100.0
NCC	-	-	-	-	-	-	-	-
NC	100.0	-	-	-	-	-	-	-

Table 3-16. Percentage of resulting tRNAs from a time-course assay with tRNA-NC under standard conditions (Arg204). The percentages of each product formed after 2, 4, 10, 15, 30, 60, and 120 minutes were calculated by densitometry using ImageQuant TL (GE Healthcare).

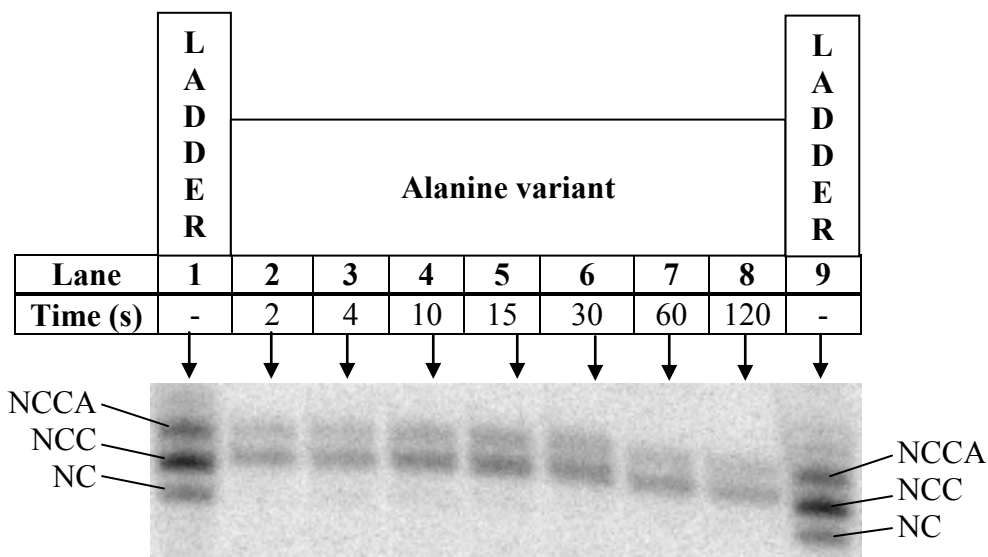


Fig. 3-24. Denaturing polyacrylamide gel showing a time-course assay under standard conditions using substrate tRNA-NC (R204A). Template lane: see template in Fig. 3-23.

		Alanine variant						
		Length of reaction (min)						
	Template	2	4	10	15	30	60	120
NCCA	-	38.0	37.8	36.6	36.5	39.0	37.2	38.0
NCC	-	62.0	62.2	63.4	63.5	61.0	62.8	62.0
NC	100.0	-	-	-	-	-	-	-

Table 3-17. Percentage of resulting tRNAs from a time-course assay with tRNA-NC under standard conditions (R204A). The percentages of each product formed after 2, 4, 10, 15, 30, 60, and 120 minutes were calculated by densitometry using ImageQuant TL (GE Healthcare).

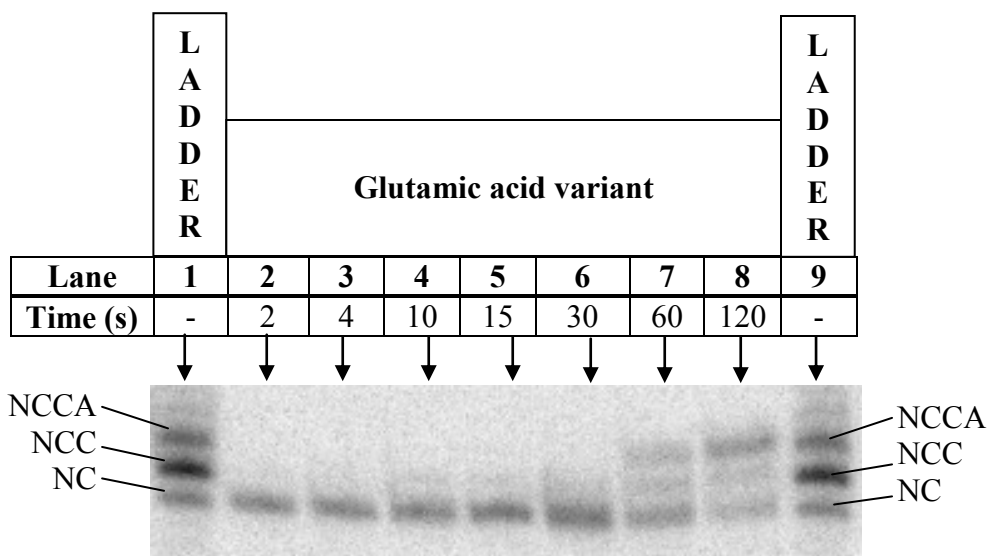


Fig. 3-25. Denaturing polyacrylamide gel showing a time-course assay under standard conditions using substrate tRNA-NC (R204E). Template lane: see template in Fig. 3-23.

		Glutamic acid variant						
		Length of reaction (min)						
	Template	2	4	10	15	30	60	120
NCCA	-	-	-	-	-	-	27.0	45.2
NCC	-	-	-	13.4	16.8	20.4	24.9	23.9
NC	100.0	100.0	100.0	86.6	83.2	79.6	48.1	31.0

Table 3-18. Percentage of resulting tRNAs from a time-course assay with tRNA-NC under standard conditions (R204E). The percentages of each product formed after 2, 4, 10, 15, 30, 60, and 120 minutes were calculated by densitometry using ImageQuant TL (GE Healthcare).

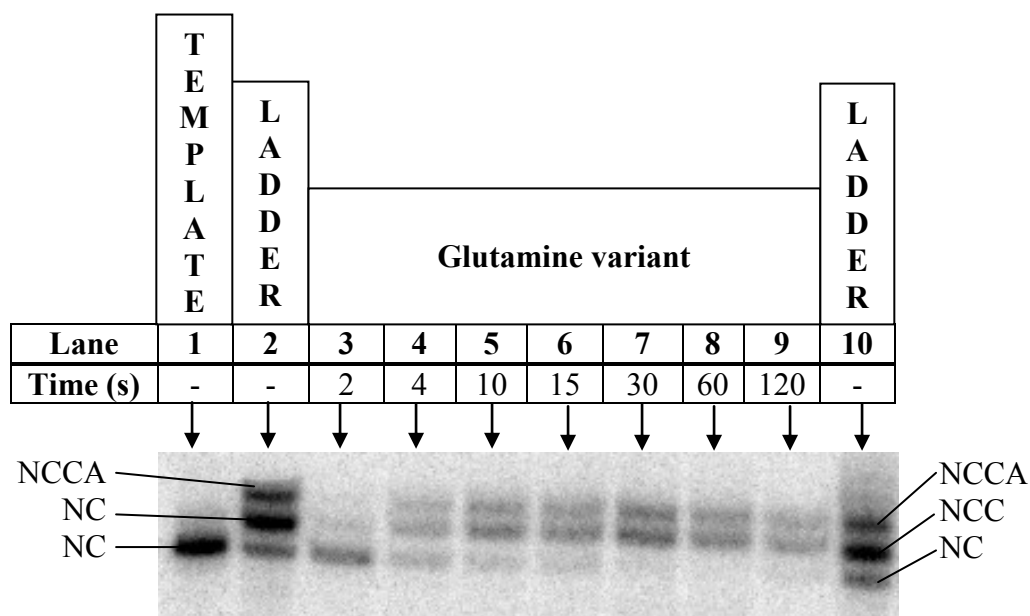


Fig. 3-26. Denaturing polyacrylamide gel showing a time-course assay under standard conditions using substrate tRNA-NC (R204Q). Template lane: tRNA-NC without enzyme.

		Glutamine variant						
		Length of reaction (min)						
	Template	2	4	10	15	30	60	120
NCCA	-	-	29.2	29.7	36.0	37.5	45.2	44.0
NCC	-	21.4	42.5	43.3	51.4	51.1	54.8	56.0
NC	100.0	78.6	28.3	27.0	12.6	11.4	-	-

Table 3-19. Percentage of resulting tRNAs from a time-course assay with tRNA-NC under standard conditions (R204Q). The percentages of each product formed after 2, 4, 10, 15, 30, 60, and 120 minutes were calculated by densitometry using ImageQuant TL (GE Healthcare).

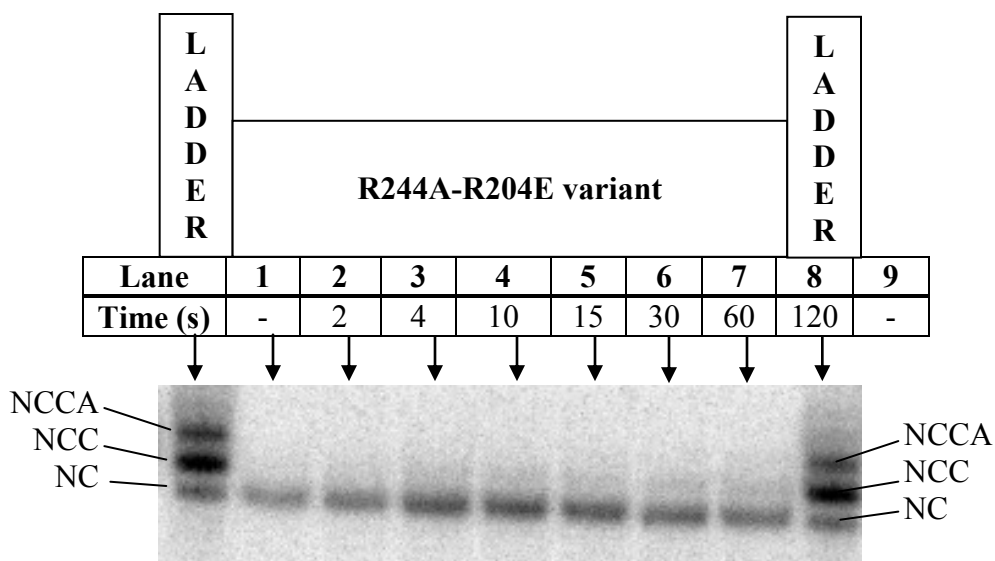


Fig. 3-27. Denaturing polyacrylamide gel showing a time-course assay under standard conditions using substrate tRNA-NC (R244A-R204E). Template lane: see template in Fig. 3-26.

		R244A-R204E variant						
		Length of reaction (min)						
	Template	2	4	10	15	30	60	120
NCCA	-	-	-	-	-	-	-	-
NCC	-	6.7	10.8	14.1	15.2	16.7	17.3	23.8
NC	100.0	93.3	89.2	85.9	84.8	83.3	82.7	76.2

Table 3-20. Percentage of resulting tRNAs from a time-course assay with tRNA-NC under standard conditions (R244A-R204E). The percentages of each product formed after 2, 4, 10, 15, 30, 60, and 120 minutes were calculated by densitometry using ImageQuant TL (GE Healthcare).

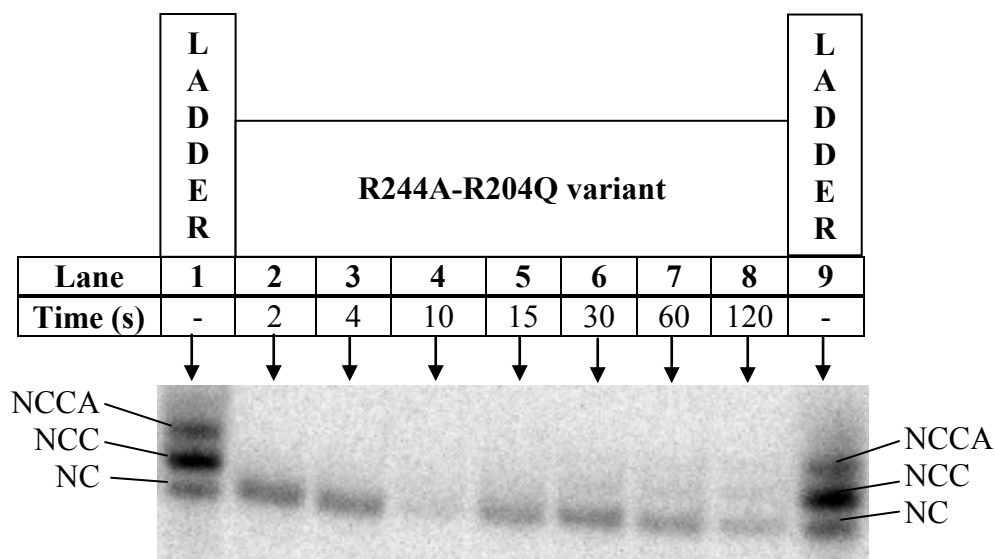


Fig. 3-28. Denaturing polyacrylamide gel showing a time-course assay under standard conditions using substrate tRNA-NC (R244A-R204Q). Template lane: see template in Fig. 3-26.

		R244A-R204Q variant						
		Length of reaction (min)						
	Template	2	4	10	15	30	60	120
NCCA	-	-	-	Sample lost	-	9.5	13.2	17.0
NCC	-	13.8	14.8		25.9	19.5	21.7	28.3
NC	100.0	86.2	85.2		74.1	71.0	65.1	54.8

Table 3-21. Percentage of resulting tRNAs from a time-course assay with tRNA-NC under standard conditions (R244A-R204Q). The percentages of each product formed after 2, 4, 10, 15, 30, 60, and 120 minutes were calculated by densitometry using ImageQuant TL (GE Healthcare).

3.3.1.4.3 Assays with the tRNA-NCC substrate

When the reaction was initiated using tRNA-NCC as the substrate in the presence of both ATP and CTP, all of the enzymes except the R244A-R204E variant were able to generate a product corresponding in size to extension to position 76. While both the alanine and glutamine variants showed full extension after only two minutes, the glutamic acid variant showed partial extension by the four minute mark, with no further extension beyond this time-point. The R244A-R204Q variant showed 70-76% extension by the 30 minute mark. Taking into account the heterogeneity of the starting template, the R204E variant only really extended approximately 20% of the tRNA-NCC template, while the R244A-R204Q variant extended approximately 58%. The decreased incorporation results observed here are consistent with standard two minute assays, for the double variants (Figures 3-16 and 3-17), as well as the glutamate variant (Fig. 3-13). In addition, when considering the alanine and glutamine variant time course data using the tRNA-N substrate (Figures 3-18 and 3-20, respectively) along with the tRNA-NC data (Figure 3-24 and 3-26, respectively); the build-up of a band corresponding to tRNA-NCC is observed. Considering the variant enzymes (R204A and R204Q) worked flawlessly during addition to position 76 (Figures 3-30 and 3-32, respectively), this build-up suggests that a common element (*i.e.*, misincorporation) is causing a decrease in incorporation at the terminal position for these assays. Overall, Arg204 may be involved primarily in nucleotide addition efficiency to tRNA-N, but in both efficiency and specificity to tRNA-NC and tRNA-NCC.

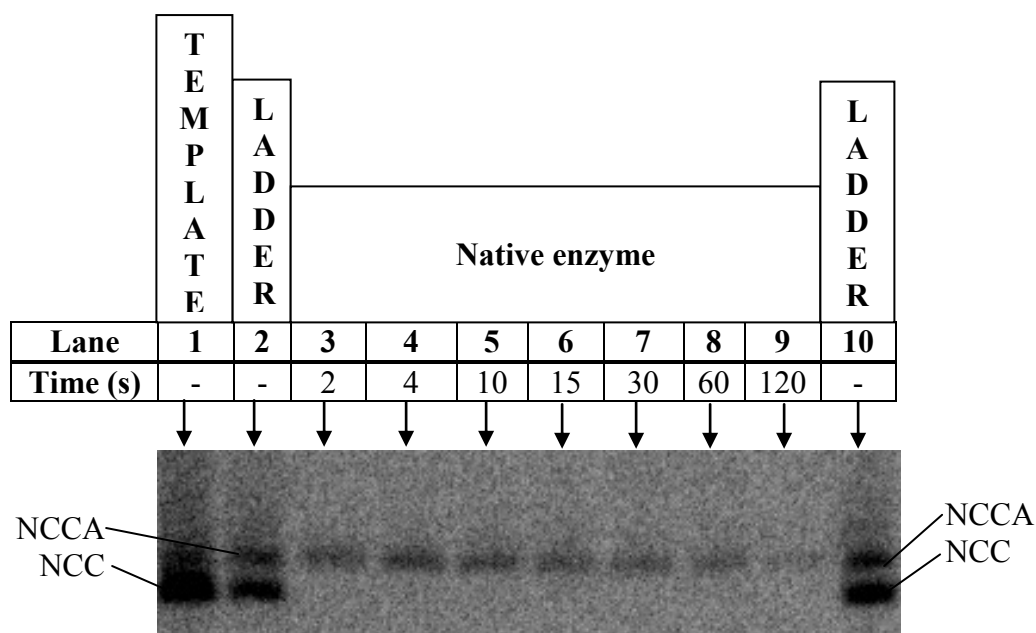


Fig. 3-29. Denaturing polyacrylamide gel showing a time-course assay under standard conditions using substrate tRNA-NCC (Arg204). Template lane: tRNA-NCC without enzyme.

		Native enzyme						
		Length of reaction (min)						
	Template	2	4	10	15	30	60	120
NCCA	27.7	100.0	100.0	100	100.0	100.0	100.0	100.0
NCC	72.3	-	-	-	-	-	-	-

Table 3-22. Percentage of resulting tRNAs from a time-course assay with tRNA-NCC under standard conditions (Arg204). The percentages of each product formed after 2, 4, 10, 15, 30, 60, and 120 minutes were calculated by densitometry using ImageQuant TL (GE Healthcare).

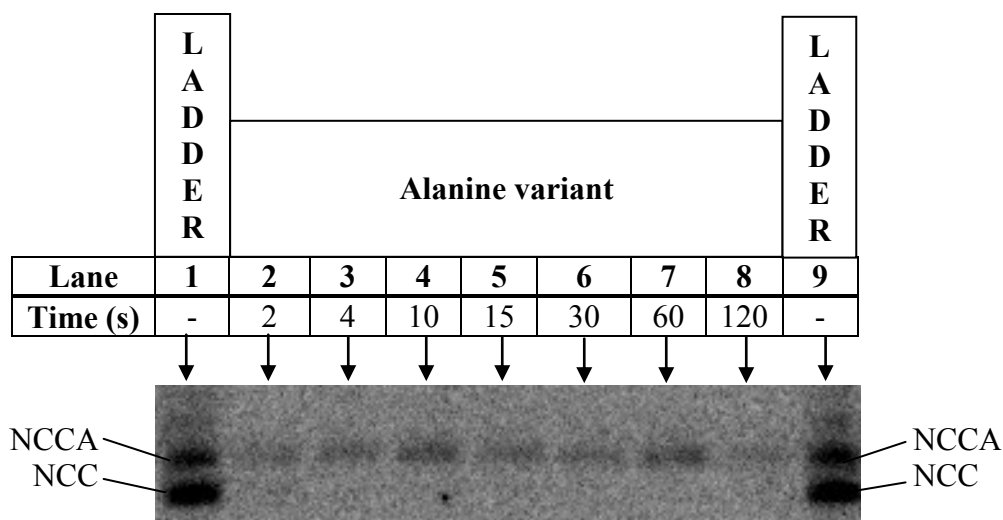


Fig. 3-30. Denaturing polyacrylamide gel showing a time-course assay under standard conditions using substrate tRNA-NCC (R204A). Template lane: see template in Fig. 3-29.

		Alanine variant						
		Length of reaction (min)						
	Template	2	4	10	15	30	60	120
NCCA	27.7	100.0	100.0	100.0	100.0	100.0	100.0	100.0
NCC	72.3	-	-	-	-	-	-	-

Table 3-23. Percentage of resulting tRNAs from a time-course assay with tRNA-NCC under standard conditions (R204A). The percentages of each product formed after 2, 4, 10, 15, 30, 60, and 120 minutes were calculated by densitometry using ImageQuant TL (GE Healthcare).

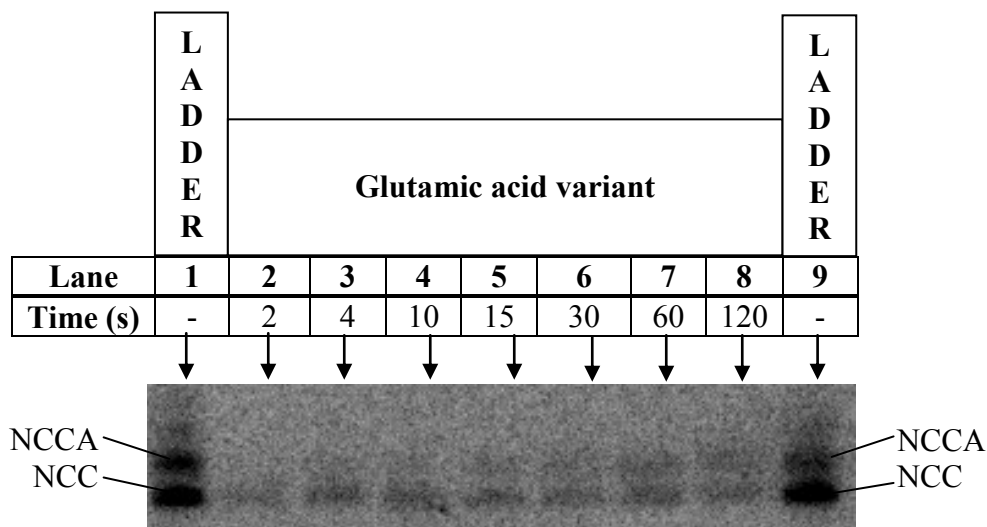


Fig. 3-31. Denaturing polyacrylamide gel showing a time-course assay under standard conditions using substrate tRNA-NCC (R204E). Template lane: see template in Fig. 3-29.

		Glutamic acid variant						
		Length of reaction (min)						
	Template	2	4	10	15	30	60	120
NCCA	27.7	27.7	42.3	42.5	45.6	47.4	47.7	47.8
NCC	72.3	72.3	57.7	57.5	54.4	52.6	52.3	52.2

Table 3-24. Percentage of resulting tRNAs from a time-course assay with tRNA-NCC under standard conditions (R204E). The percentages of each product formed after 2, 4, 10, 15, 30, 60, and 120 minutes were calculated by densitometry using ImageQuant TL (GE Healthcare).

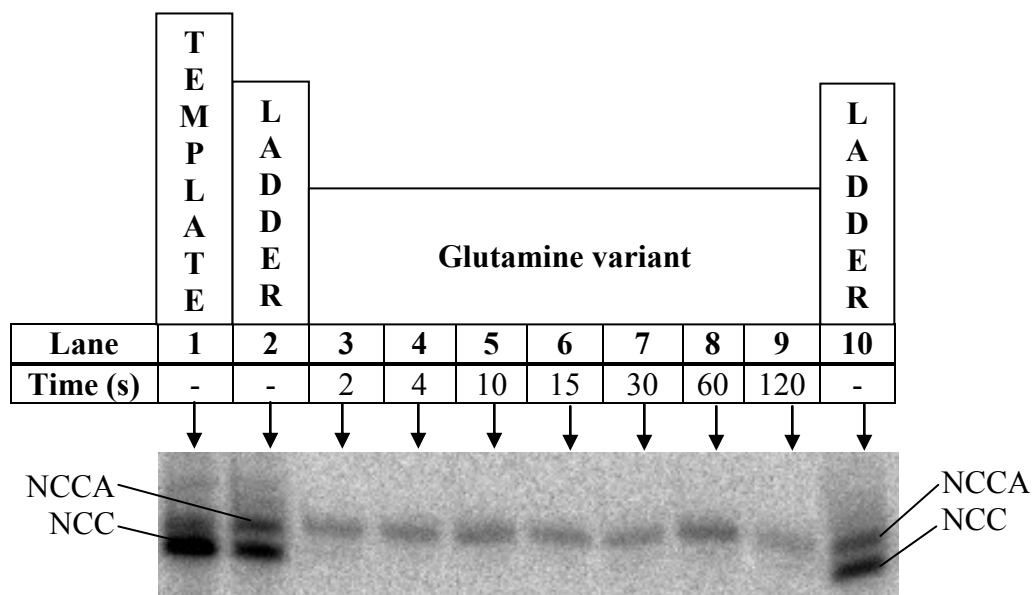


Fig. 3-32. Denaturing polyacrylamide gel showing a time-course assay under standard conditions using substrate tRNA-NCC (R204Q). Template lane: tRNA-NCC without enzyme.

		Glutamine variant						
		Length of reaction (min)						
	Template	2	4	10	15	30	60	120
NCCA	17.9	100.0	100.0	100	100.0	100.0	100.0	100.0
NCC	82.1	-	-	-	-	-	-	-

Table 3-25. Percentage of resulting tRNAs from a time-course assay with tRNA-NCC under standard conditions (R204Q). The percentages of each product formed after 2, 4, 10, 15, 30, 60, and 120 minutes were calculated by densitometry using ImageQuant TL (GE Healthcare).

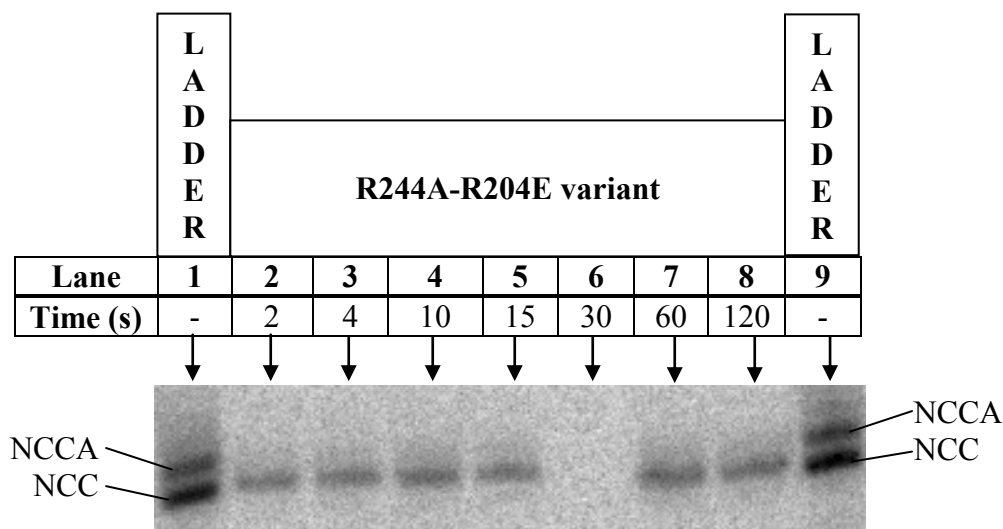


Fig. 3-33. Denaturing polyacrylamide gel showing a time-course assay under standard conditions using substrate tRNA-NCC (R244A-R204E). Template lane: see template in Fig. 3-32.

		R244A-R204E variant						
		Length of reaction (min)						
	Template	2	4	10	15	30	60	120
NCCA	17.9	17.6	17.6	17.8	17.9	Sample	18.1	18.3
NCC	82.1	82.4	82.4	82.2	82.1		Lost	81.9

Table 3-26. Percentage of resulting tRNAs from a time-course assay with tRNA-NCC under standard conditions (R244A-R204E). The percentages of each product formed after 2, 4, 10, 15, 30, 60, and 120 minutes were calculated by densitometry using ImageQuant TL (GE Healthcare).



Fig. 3-34. Denaturing polyacrylamide gel showing a time-course assay under standard conditions using substrate tRNA-NCC (R244A-R204Q). Template lane: see template in Fig. 3-32.

		R244A-R204Q variant						
		Length of reaction (min)						
	Template	2	4	10	15	30	60	120
NCCA	17.9	38.7	52.3	61.8	65.4	71.8	74.3	75.8
NCC	82.1	61.3	47.7	38.2	34.6	28.2	25.7	21.5

Table 3-27. Percentage of resulting tRNAs from a time-course assay with tRNA-NCC under standard conditions (R244A-R204Q). The percentages of each product formed after 2, 4, 10, 15, 30, 60, and 120 minutes were calculated by densitometry using ImageQuant TL (GE Healthcare).

3.3.1.4.4 Assays with the tRNA-NCCA substrate

A time-course assay using tRNA-NCCA as the starting template was carried out to check for extension beyond position 76 *in vitro* (Fig. 3-35). None of the proteins was able to extend the tRNA beyond position 76 after 60 or 120 minutes.

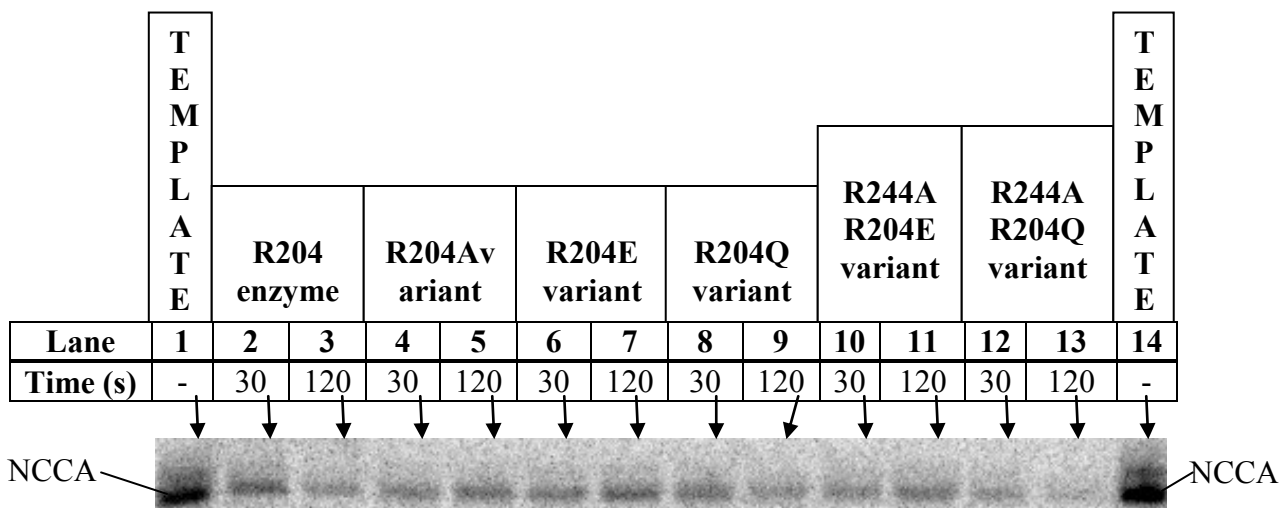


Fig. 3-35. Denaturing polyacrylamide gel showing time-course assays under standard conditions using substrate tRNA-NCC. Template lane: tRNA-NCCA without enzyme.

3.3.1.5 Time-course assays of tRNA nucleotidyltransferases using the tRNA-NCC template as a substrate with ATP alone

To further address the different specificities of the variant enzymes for ATP and CTP, each template was incubated in the presence of ATP alone (Fig. 3-36 to Fig. 3-41). After two minutes, the native enzyme and the glutamine variant were both able to extend the tRNA-NCC template to a size corresponding to extension to position 76. The alanine variant took four minutes to reach 100% extension (see Table 3-28 to Table 3-33 for all percentages), while the glutamic acid variant was only able to extend 47.1% of the template after two hours. Moreover, one of the double variants (R244A-R204Q) showed

87.4% extension after 120 minutes while the other (R244A-R204E) showed a complete inability to extend this template.

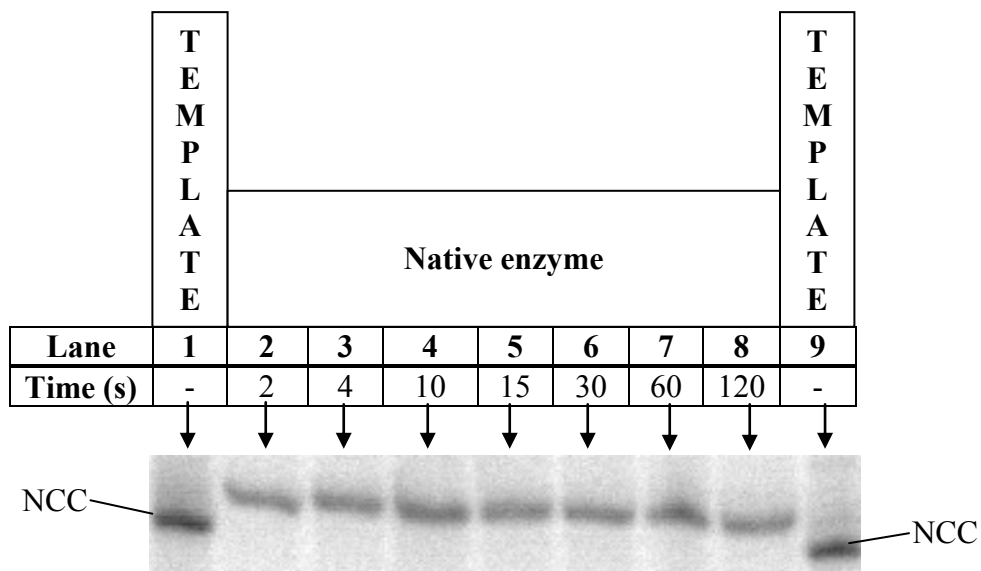


Fig. 3-36. Denaturing polyacrylamide gel showing a time-course assay in the absence of CTP using substrate tRNA-NCC (Arg204). Template lanes: tRNA-NCC without enzyme.

		Native enzyme						
		Length of reaction (min)						
	Template	2	4	10	15	30	60	120
NCCA	-	100.0	100.0	100	100.0	100.0	100.0	100.0
NCC	100.0	-	-	-	-	-	-	-

Table 3-28. Percentage of resulting tRNAs from a time-course assay with tRNA-NCC in the absence of CTP (Arg204). The percentages of each product formed after 2, 4, 10, 15, 30, 60, and 120 minutes were calculated by densitometry using ImageQuant TL (GE Healthcare).

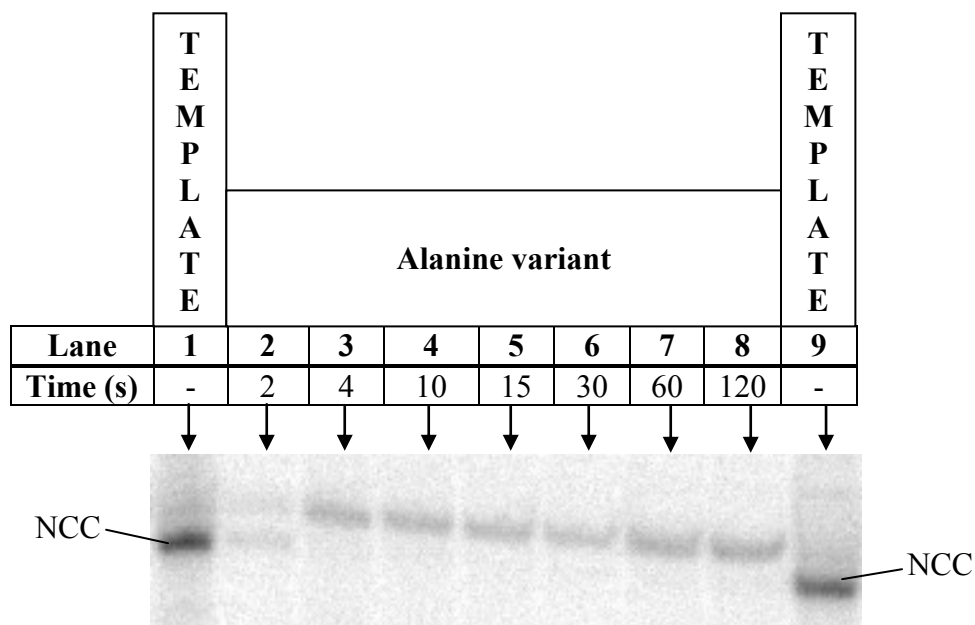


Fig. 3-37. Denaturing polyacrylamide gel showing a time-course assay in the absence of CTP using substrate tRNA-NCC (R204A). Template lanes: tRNA-NCC without enzyme.

		Alanine variant						
		Length of reaction (min)						
	Template	2	4	10	15	30	60	120
NCCA	-	46.2	100.0	100.0	100.0	100.0	100.0	100.0
NCC	100.0	53.8	-	-	-	-	-	-

Table 3-29. Percentage of resulting tRNAs from a time-course assay with tRNA-NCC in the absence of CTP (R204A). The percentages of each product formed after 2, 4, 10, 15, 30, 60, and 120 minutes were calculated by densitometry using ImageQuant TL (GE Healthcare).

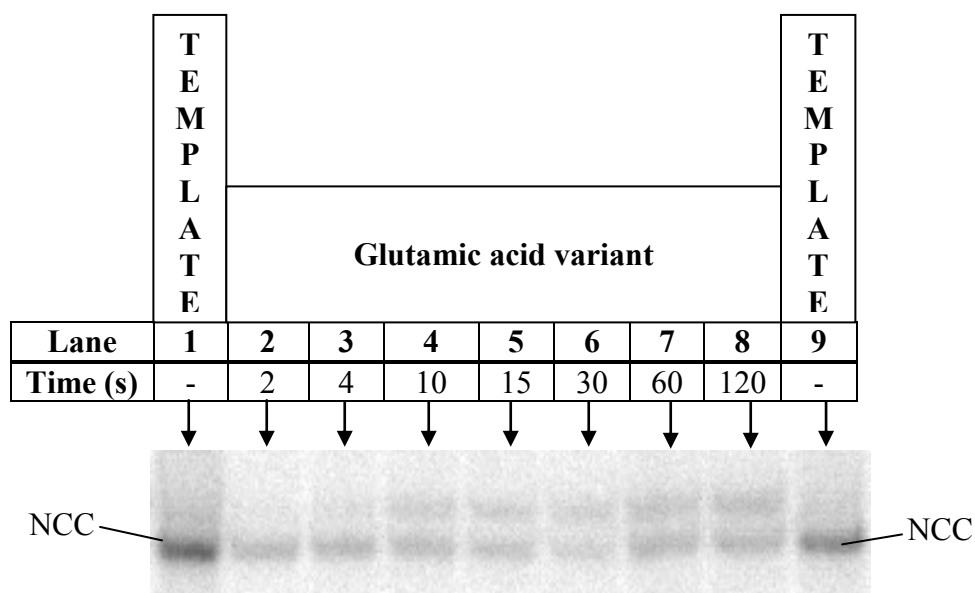


Fig. 3-38. Denaturing polyacrylamide gel showing a time-course assay in the absence of CTP using substrate tRNA-NCC (R204E). Template lanes: tRNA-NCC without enzyme.

		Glutamic acid variant						
		Length of reaction (min)						
	Template	2	4	10	15	30	60	120
NCCA	-	19.2	24.8	36.9	42.5	43.6	45.7	47.1
NCC	100.0	80.8	75.2	63.1	57.5	56.4	54.3	52.9

Table 3-30. Percentage of resulting tRNAs from a time-course assay with tRNA-NCC in the absence of CTP (R204E). The percentages of each product formed after 2, 4, 10, 15, 30, 60, and 120 minutes were calculated by densitometry using ImageQuant TL (GE Healthcare).

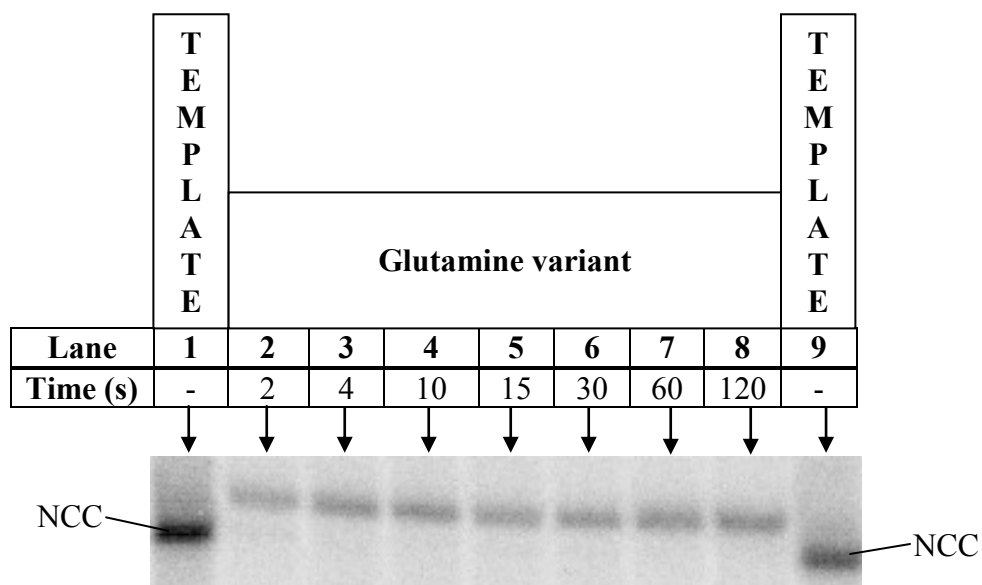


Fig. 3-39. Denaturing polyacrylamide gel showing a time-course assay in the absence of CTP using substrate tRNA-NCC (R204Q). Template lanes: tRNA-NCC without enzyme.

		Glutamine variant						
		Length of reaction (min)						
	Template	2	4	10	15	30	60	120
NCCA	-	100.0	100.0	100	100.0	100.0	100.0	100.0
NCC	100.0	-	-	-	-	-	-	-

Table 3-31. Percentage of resulting tRNAs from a time-course assay with tRNA-NCC in the absence of CTP (R204Q). The percentages of each product formed after 2, 4, 10, 15, 30, 60, and 120 minutes were calculated by densitometry using ImageQuant TL (GE Healthcare).

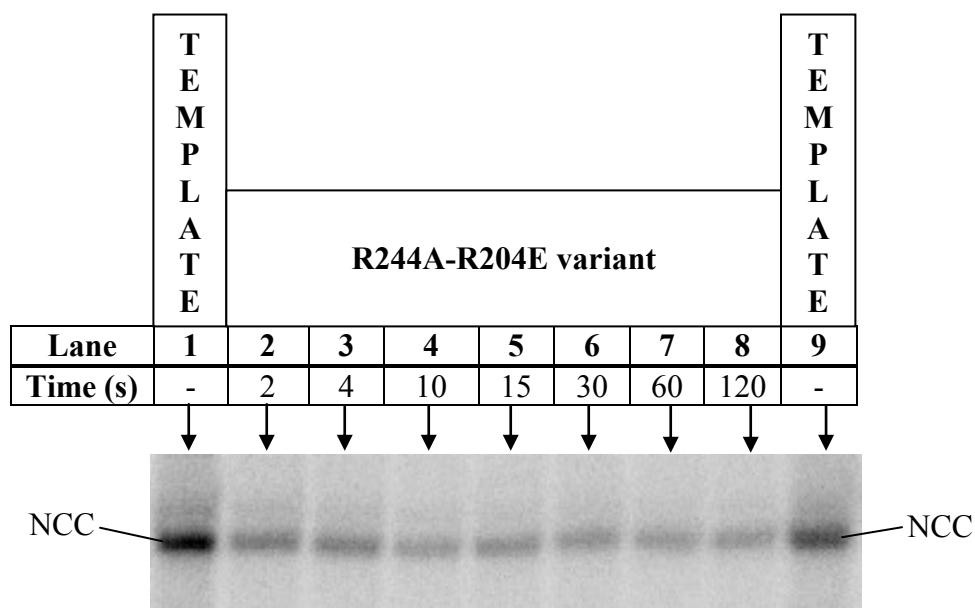


Fig. 3-40. Denaturing polyacrylamide gel showing a time-course assay in the absence of CTP using substrate tRNA-NCC (R244A-R204E). Template lanes: tRNA-NCC without enzyme.

		R244A-R204E variant						
		Length of reaction (min)						
	Template	2	4	10	15	30	60	120
NCCA	-	-	-	-	-	-	-	-
NCC	100.0	100.0	100.0	100.0	100.0	100.0	100.0	100.0

Table 3-32. Percentage of resulting tRNAs from a time-course assay with tRNA-NCC in the absence of CTP (R244A-R204E). The percentages of each product formed after 2, 4, 10, 15, 30, 60, and 120 minutes were calculated by densitometry using ImageQuant TL (GE Healthcare).

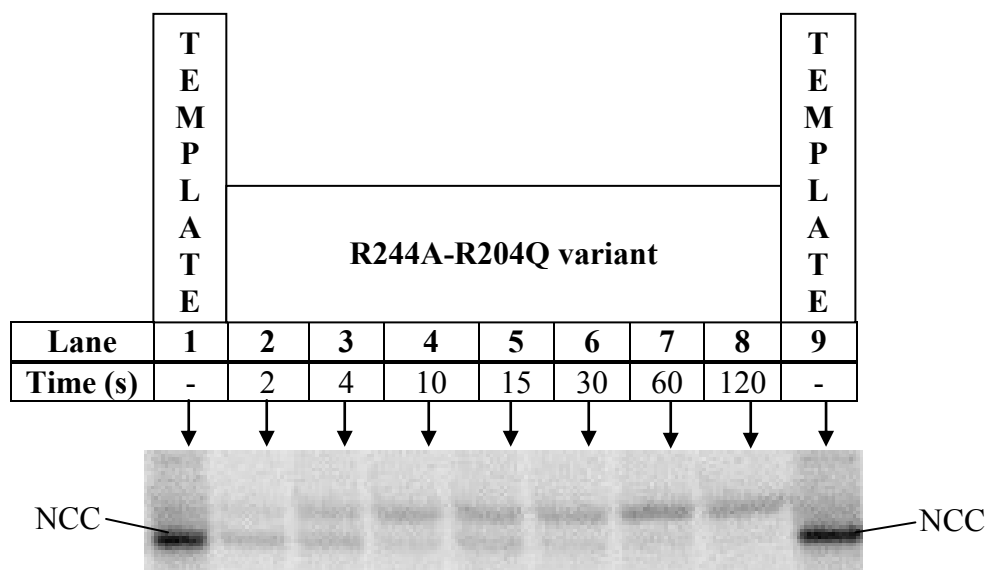


Fig. 3-41. Denaturing polyacrylamide gel showing a time-course assay in the absence of CTP using substrate tRNA-NCC (R244A-R204Q). Template lanes: tRNA-NCC without enzyme.

		R244A-R204Q variant						
		Length of reaction (min)						
	Template	2	4	10	15	30	60	120
NCCA	-	29.5	50.3	76.6	77.8	82.0	83.7	87.4
NCC	100.0	70.5	49.7	23.4	22.2	18.0	16.3	12.6

Table 3-33. Percentage of resulting tRNAs from a time-course assay with tRNA-NCC in the absence of CTP (R244A-R204Q). The percentages of each product formed after 2, 4, 10, 15, 30, 60, and 120 minutes were calculated by densitometry using ImageQuant TL (GE Healthcare).

3.3.1.6 Time-course assays of tRNA nucleotidyltransferases using the tRNA-NCC template as a substrate with CTP alone

Time-course assays were repeated in the presence of CTP alone to determine whether the variant enzymes were able to add CTP to position 76 (Fig. 3-42 to Fig. 3-47). Only the native enzyme was able to fully extend the entire starting template to a size corresponding to tRNA-CCC after two minutes. In fact, given an extended period of time (30 minutes), the native enzyme demonstrates the ability to extend to tRNA-NCCCC (lanes 6-8), possibly mimicking poly(C) polymerase activity as previously observed in rabbit liver tRNA nucleotidyltransferase (Deutscher 1972a; Deutscher, 1973b). The only other variant to show any activity with CTP was R204A. Extension was observed starting at the 2 minute mark (21.5% of product extended), and after 120 minutes showed 47.4% of product extended. All other enzymes showed no activity.

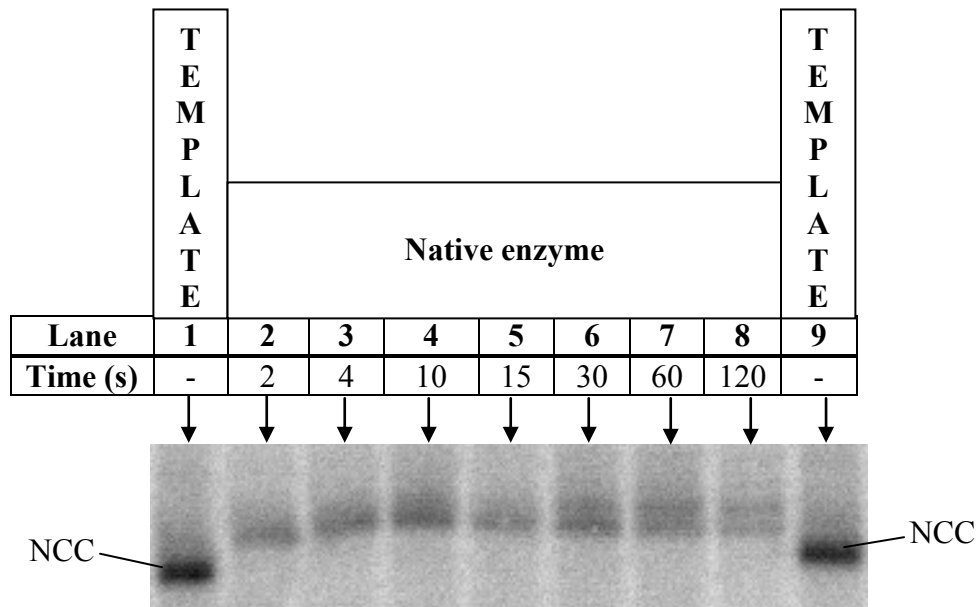


Fig. 3-42. Denaturing polyacrylamide gel showing a time-course assay in the absence of ATP using substrate tRNA-NCC (Arg204). Template lanes: tRNA-NCC without enzyme.

		Native enzyme						
		Length of reaction (min)						
	Template	2	4	10	15	30	60	120
NCCCC	-	-	-	-	-	39.6	50.8	54.3
NCCC	-	100.0	100.0	100.0	100.0	60.4	49.2	45.7
NCC	100.0	-	-	-	-	-	-	-

Table 3-34. Percentage of resulting tRNAs from a time-course assay with tRNA-NCC in the absence of ATP (Arg204). The percentages of each product formed after 2, 4, 10, 15, 30, 60, and 120 minutes were calculated by densitometry using ImageQuant TL (GE Healthcare).

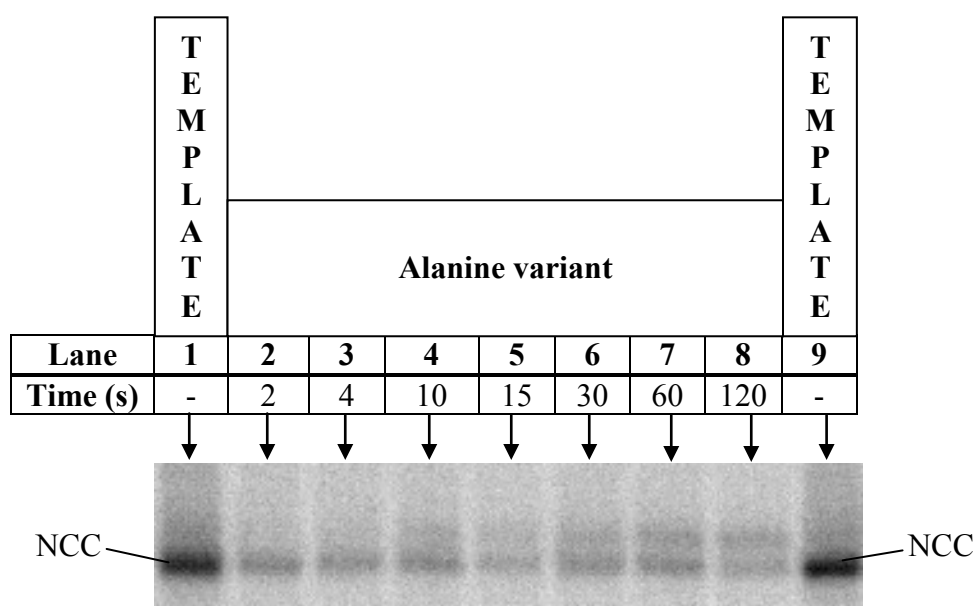


Fig. 3-43. Denaturing polyacrylamide gel showing a time-course assay in the absence of ATP using substrate tRNA-NCC (R204A). Template lanes: tRNA-NCC without enzyme.

		Alanine variant						
		Length of reaction (min)						
	Template	2	4	10	15	30	60	120
NCCC	-	21.5	26.3	32.0	36.4	38.2	41.2	47.4
NCC	100.0	78.5	73.7	68.0	63.6	61.8	58.8	52.6

Table 3-35. Percentage of resulting tRNAs from a time-course assay with tRNA-NCC in the absence of ATP (R204A). The percentages of each product formed after 2, 4, 10, 15, 30, 60, and 120 minutes were calculated by densitometry using ImageQuant TL (GE Healthcare).

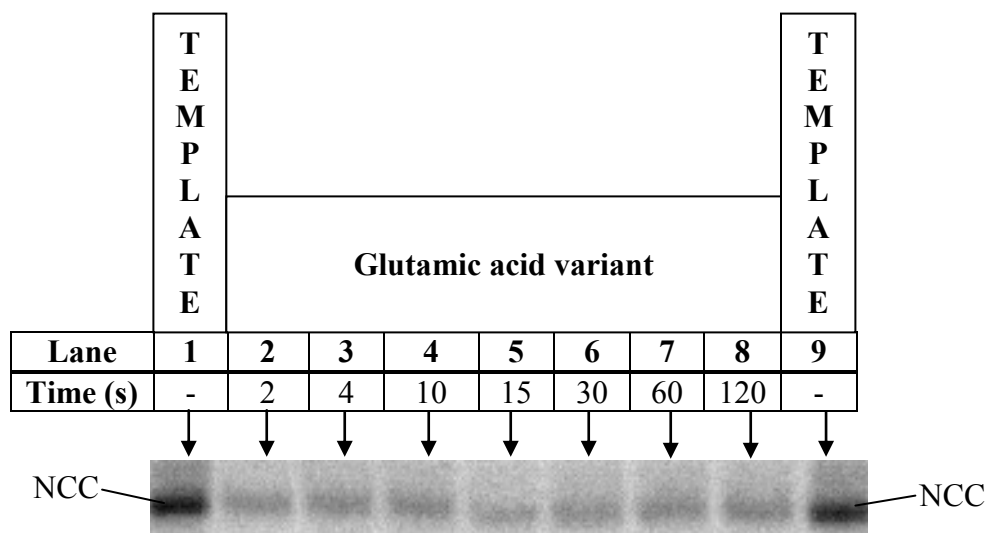


Fig. 3-44. Denaturing polyacrylamide gel showing a time-course assay in the absence of ATP using substrate tRNA-NCC (R204E). Template lanes: tRNA-NCC without enzyme.

		Glutamic acid variant						
		Length of reaction (min)						
	Template	2	4	10	15	30	60	120
NCCC	-	-	-	-	-	-	-	-
NCC	100.0	100.0	100.0	100.0	100.0	100.0	100.0	100.0

Table 3-36. Percentage of resulting tRNAs from a time-course assay with tRNA-NCC in the absence of ATP (R204E). The percentages of each product formed after 2, 4, 10, 15, 30, 60, and 120 minutes were calculated by densitometry using ImageQuant TL (GE Healthcare).

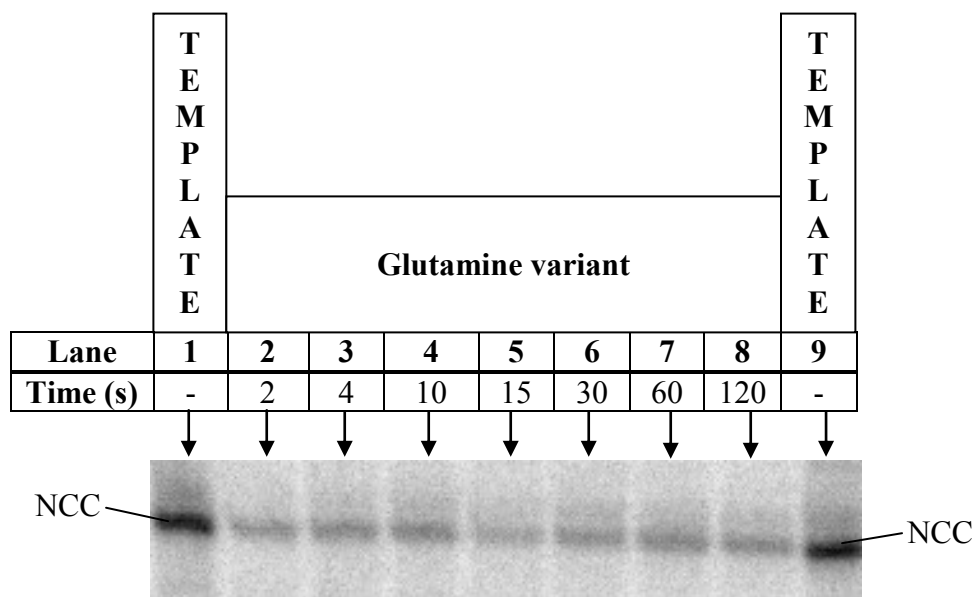


Fig. 3-45. Denaturing polyacrylamide gel showing a time-course assay in the absence of ATP using substrate tRNA-NCC (R204Q). Template lanes: tRNA-NCC without enzyme.

		Glutamine variant						
		Length of reaction (min)						
	Template	2	4	10	15	30	60	120
NCCC	-	-	-	-	-	-	-	-
NCC	100.0	100.0	100.0	100.0	100.0	100.0	100.0	100.0

Table 3-37. Percentage of resulting tRNAs from a time-course assay with tRNA-NCC in the absence of ATP (R204Q). The percentages of each product formed after 2, 4, 10, 15, 30, 60, and 120 minutes were calculated by densitometry using ImageQuant TL (GE Healthcare).

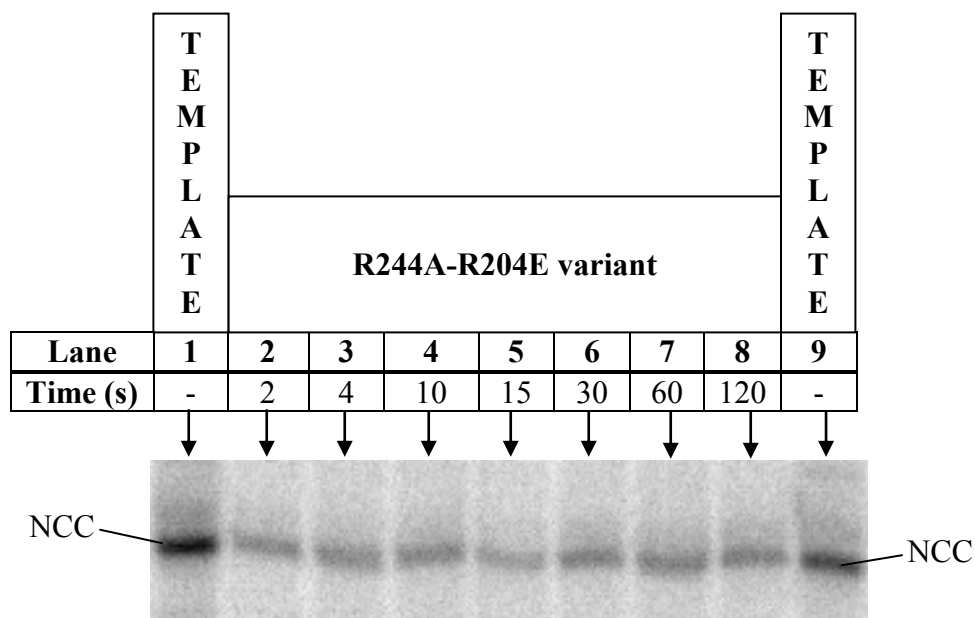


Fig. 3-46. Denaturing polyacrylamide gel showing a time-course assay in the absence of ATP using substrate tRNA-NCC (R244A-R204E). Template lanes: tRNA-NCC without enzyme.

		R244A-R204E variant						
		Length of reaction (min)						
	Template	2	4	10	15	30	60	120
NCCC	-	-	-	-	-	-	-	-
NCC	100.0	100.0	100.0	100.0	100.0	100.0	100.0	100.0

Table 3-38. Percentage of resulting tRNAs from a time-course assay with tRNA-NCC in the absence of ATP (R244A-R204E). The percentages of each product formed after 2, 4, 10, 15, 30, 60, and 120 minutes were calculated by densitometry using ImageQuant TL (GE Healthcare).

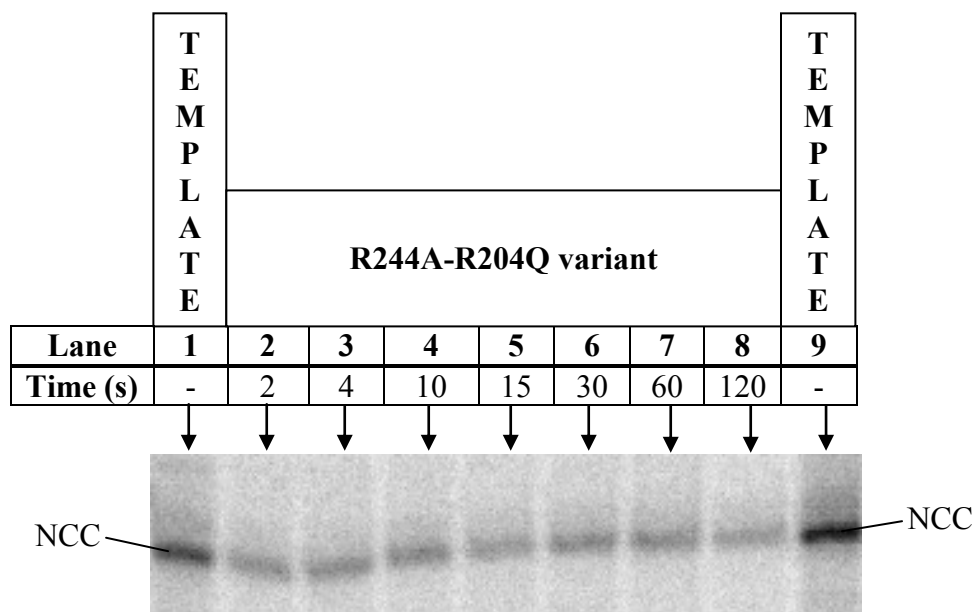


Fig. 3-47. Denaturing polyacrylamide gel showing a time-course assay in the absence of ATP using substrate tRNA-NCC (R244A-R204Q). Template lanes: tRNA-NCC without enzyme.

		R244A-R204Q variant						
		Length of reaction (min)						
	Template	2	4	10	15	30	60	120
NCCC	-	-	-	-	-	-	-	-
NCC	100.0	100.0	100.0	100.0	100.0	100.0	100.0	100.0

Table 3-39. Percentage of resulting tRNAs from a time-course assay with tRNA-NCC in the absence of ATP (R244A-R204Q). The percentages of each product formed after 2, 4, 10, 15, 30, 60, and 120 minutes were calculated by densitometry ImageQuant TL (GE Healthcare).

3.3.1.7 Modified assays of tRNA nucleotidyltransferase supplied with GTP or UTP alone

To see if the variant enzymes had an altered ability to incorporate other nucleotides, enzyme assays were carried out in the presence of either GTP or UTP alone. The reactions were analyzed at the 30 minute mark with a concentration of 0.4 mM GTP or UTP being used for each assay. Higher concentrations of GTP or UTP were used (1 mM and 10 mM) but these assays did not show any difference in nucleotide incorporation as compared to 0.4 mM NTP (data not shown).

3.3.1.7.1 Supplied with GTP alone

Assays in the presence of GTP alone using the tRNA-N, tRNA-NC, and tRNA-NCC templates can be observed in Figures 3-48 to 3-50 and Tables 3-40 to 3-42. None of the enzymes were able to incorporate GMP to the tRNA-N substrate. In contrast, the native enzyme was able to incorporate up to two GMPs when supplied with the tRNA-NC substrate (43.6% of product extended by one GMP and 36.8% of product extended by two GMPs). Of the variants, only the alanine variant showed activity with the tRNA-NC substrate, incorporating one GMP to generate (43.9% of product). Finally, both the native enzyme and alanine variant were able to extend the tRNA-NCC substrate by one GMP to 49.6% of product and 68.3% of product, respectively. None of the other variants demonstrated any measurable activity with any of the substrates.

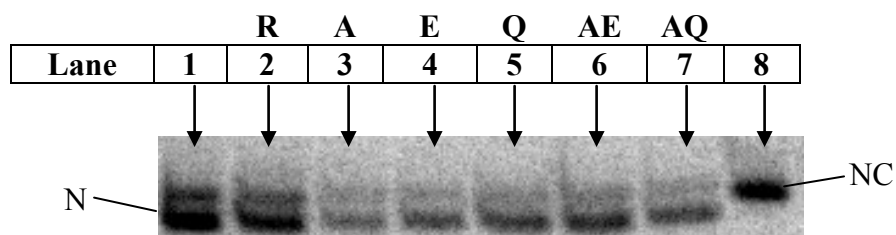


Fig. 3-48. Denaturing polyacrylamide gel of 30 minute assays using substrate tRNA-N with only GTP present. Lane 1: tRNA-N without enzyme; lane 2: native enzyme; lane 3: alanine variant; lane 4: glutamic acid variant; lane 5: glutamine variant; lane 6: R244A-R204E variant; lane 7: R244A-R204Q variant; lane 8: tRNA-NC without enzyme.

	Template	Enzymes					
		R204	R204A	R204E	R204Q	R244A-R204E	R244A-R204Q
NGGG	-	-	-	-	-	-	-
NGG	-	-	-	-	-	-	-
NG	32.8	37.0	35.0	31.0	29.4	31.4	28.4
N	67.2	63.0	65.0	69.0	70.6	68.6	71.6

Table 3-40. Percentage of resulting tRNAs from a 30 minute assay starting with tRNA-N and only GTP present. The percentages of each product formed were calculated by densitometry ImageQuant TL (GE Healthcare).

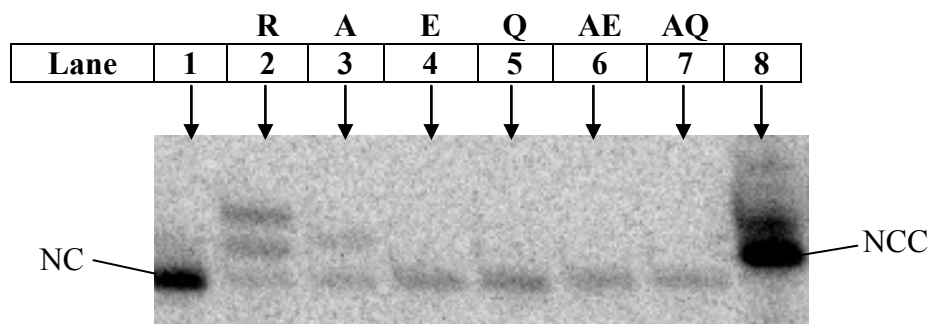


Fig. 3-49. Denaturing polyacrylamide gel of 30 minute assays using substrate tRNA-NC with only GTP present. Lane 1: tRNA-NC without enzyme; lane 2: native enzyme; lane 3: alanine variant; lane 4: glutamic acid variant; lane 5: glutamine variant; lane 6: R244A-R204E variant; lane 7: R244A-R204Q variant; lane 8: tRNA-NCC without enzyme.

	Template	Enzymes					
		R204	R204A	R204E	R204Q	R244A-R204E	R244A-R204Q
NCGG	-	43.6	-	-	-	-	-
NCG	-	36.8	43.9	-	-	-	-
NC	100.0	19.6	56.1	100.0	100.0	100.0	100.0

Table 3-41. Percentage of resulting tRNAs from a 30 minute assay starting with tRNA-NC and only GTP present. The percentages of each product formed were calculated by densitometry ImageQuant TL (GE Healthcare).

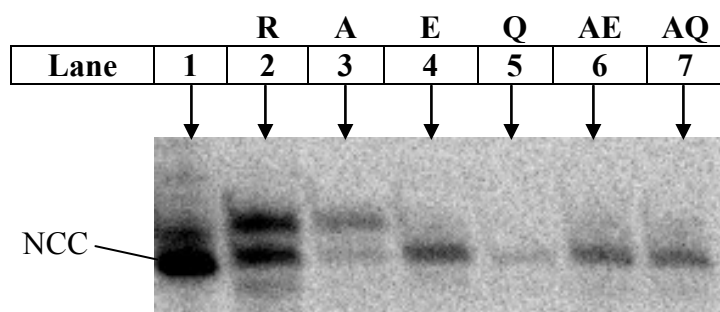


Fig. 3-50. Denaturing polyacrylamide gel of 30 minute assays using substrate tRNA-NCC with only GTP present. Lane 1: tRNA-NCC without enzyme; lane 2: native enzyme; lane 3: alanine variant; lane 4: glutamic acid variant; lane 5: glutamine variant; lane 6: R244A-R204E variant; lane 7: R244A-R204Q variant.

	Template	Enzymes					
		R204	R204A	R204E	R204Q	R244A-R204E	R244A-R204Q
NCCG	19.0	49.6	68.3	13.8	15.5	18.0	13.1
NCC	81.0	50.4	31.7	86.2	84.5	82.0	86.9

Table 3-42. Percentage of resulting tRNAs from a 30 minute assay starting with tRNA-NCC and only GTP present. The percentages of each product formed were calculated by densitometry ImageQuant TL (GE Healthcare).

3.3.1.7.2 Supplied with UTP alone

In addition to GTP alone, assays in the presence of UTP alone were also performed in order to determine whether the native and variant enzymes can accept UTP as a substrate *in vitro*. Figures 3-51 to 3-53 and Tables 3-43 to 4-45 demonstrate the products obtained from assays with tRNA-N, tRNA-NC, and tRNA-NCC substrates. The native enzyme, alanine variant, and glutamine variant were the only enzymes which showed any measurable activity. Due to the heterogeneity of the tRNA-N substrate (lane 1 in Fig. 3-41; Table 3-43), it was not clear whether the native enzyme added one or two UMPs (lane 2 in Fig. 3-41; Table 3-43). Still with the tRNA-N substrate, the alanine variant added one UMP (corresponding to 41.4% of product) while the glutamine variant also add one UMP (corresponding to 62.0% of the product). Moreover, all three enzymes (Arg204, R204A, and R204Q) added one UMP to the tRNA-NC substrate. The native enzyme demonstrated a product corresponding to 72.8% of the extended product, while the alanine and glutamine variants showed products corresponding to 71.5% and 60.5% of extended product, respectively. Finally, extension of the tRNA-NCC substrate resulted in products corresponding to approximately 80% of product extended by one UMP for the native enzyme and alanine variant, while the glutamine variant showed a band corresponding to 55.9% of the same product.

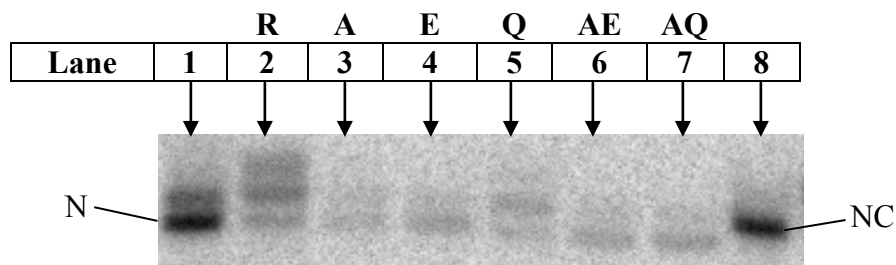


Fig. 3-51. Denaturing polyacrylamide gel of 30 minute assays using substrate tRNA-N with only UTP present. Lane 1: tRNA-N without enzyme; lane 2: native enzyme; lane 3: alanine variant; lane 4: glutamic acid variant; lane 5: glutamine variant; lane 6: R244A-R204E variant; lane 7: R244A-R204Q variant; lane 8: tRNA-NC without enzyme.

	Template	Enzymes					
		R204	R204A	R204E	R204Q	R244A-R204E	R244A-R204Q
NUUU	-	-	-	-	-	-	-
NUU	-	30.0	-	-	-	-	-
NU	29.1	45.2	41.4	29.2	62.0	28.6	29.1
N	70.9	24.8	58.6	70.8	38.0	71.4	70.9

Table 3-43. Percentage of resulting tRNAs from a 30 minute assay starting with tRNA-N and only UTP present. The percentages of each product formed were calculated by densitometry ImageQuant TL (GE Healthcare).

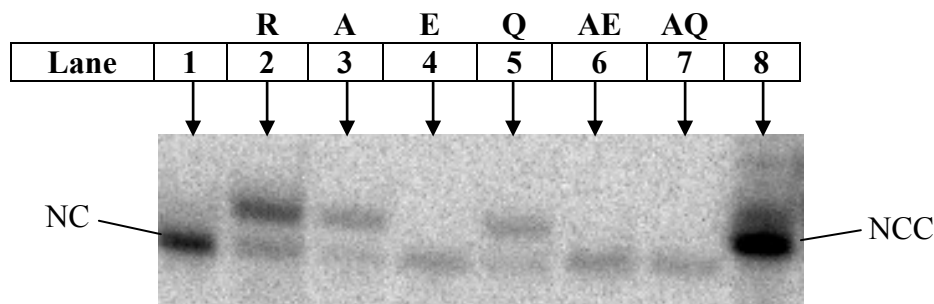


Fig. 3-52. Denaturing polyacrylamide gel of 30 minute assays using substrate tRNA-NC with only UTP present. Lane 1: tRNA-NC without enzyme; lane 2: native enzyme; lane 3: alanine variant; lane 4: glutamic acid variant; lane 5: glutamine variant; lane 6: R244A-R204E variant; lane 7: R244A-R204Q variant; lane 8: tRNA-NCC without enzyme.

	Template	Enzymes					
		R204	R204A	R204E	R204Q	R244A-R204E	R244A-R204Q
NCCU	-	-	-	-	-	-	-
NCU	-	72.8	71.5	-	60.7	-	-
NC	100.0	27.2	28.5	100.0	39.3	100.0	100.0

Table 3-44. Percentage of resulting tRNAs from a 30 minute assay starting with tRNA-NC and only UTP present. The percentages of each product formed were calculated by densitometry ImageQuant TL (GE Healthcare).

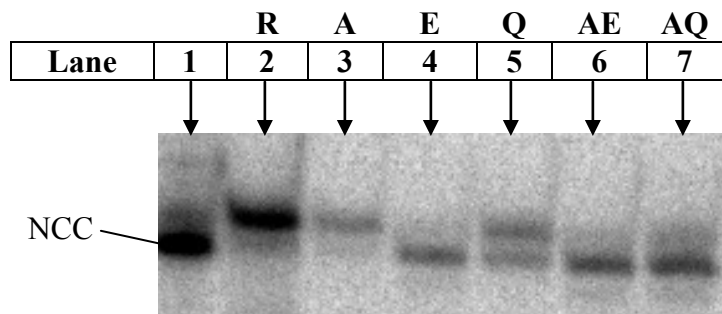


Fig. 3-53. Denaturing polyacrylamide gel of 30 minute assays using substrate tRNA-NCC with only UTP present. Lane 1: tRNA-NCC without enzyme; lane 2: native enzyme; lane 3: alanine variant; lane 4: glutamic acid variant; lane 5: glutamine variant; lane 6: R244A-R204E variant; lane 7: R244A-R204Q variant.

	Template	Enzymes					
		R204	R204A	R204E	R204Q	R244A-R204E	R244A-R204Q
NCCU	18.4	82.6	80.4	16.4	55.9	17.1	26.0
NCC	81.6	17.4	23.5	83.6	44.1	82.9	74.0

Table 3-45. Percentage of resulting tRNAs from a 30 minute assay starting with tRNA-NCC and only UTP present. The percentages of each product formed were calculated by densitometry ImageQuant TL (GE Healthcare).

4. Discussion

4.1 Role of arginine 204 in *Candida glabrata* tRNA nucleotidyltransferase

The studies described here were carried out to identify the role of arginine 204 in *C. glabrata* tRNA nucleotidyltransferase. The fact that this amino acid is conserved in tRNA nucleotidyltransferases across a broad range of species extending from eubacteria to multi-cellular eukaryotes (Fig. 1-2) suggests that it is important. The importance of this residue is supported by the *in vivo* experiments shown here (Fig. 1-9) and through previous *in vitro* experiments on other tRNA nucleotidyltransferases (Li *et al.*, 2002; Cho *et al.*, 2007; Lizano *et al.*, 2008). Available crystal structures (Li *et al.*, 2002; Augustin *et al.*, 2003; Tomita *et al.*, 2004; Toh *et al.*, 2009) and various other experiments, have suggested roles for this arginine residue. Arginine 204 is proposed to form Watson–Crick-like hydrogen bonds with the incoming nucleotides allowing for specific binding of CTP and ATP (Li *et al.*, 2002), while discriminating against UTP and GTP (Yue *et al.*, 1996; Shi *et al.*, 1998a; Betat *et al.*, 2010). When the corresponding arginine was changed to alanine in the *B. stearrowthermophilus* enzyme a dramatic loss of specificity (added one CMP, GMP, AMP, or UMP nucleotide) with tRNA-N and tRNA-NC substrates was observed (Cho *et al.*, 2007). These observations were further supported by kinetic analyses which demonstrated that this arginine ensures nucleotide specificity, and does not improve the kinetics of nucleotide incorporation (Cho *et al.*, 2007). In contrast, replacing the arginine residue by alanine in the *E. coli* and *H. sapiens* enzymes (Lizano *et al.*, 2008) demonstrated a reduced level of nucleotide incorporation with all three tRNA substrates (the *H. sapiens* enzyme was less affected in AMP incorporation), as well as decreased specificity with the tRNA-N substrate. Furthermore, arginine 204 is also proposed to undergo a binding pocket reorganizational specificity shift from CTP to ATP (Li *et al.*, 2002).

This reorientation is of the highly conserved EDxxR motif which would reposition the involved amino acids (the glutamate and arginine residues rotate together while enlarging the binding pocket for the larger adenine base) in such a way that ATP is now the preferred substrate (Fig. 1-6). There is also evidence that the glutamate and arginine residues may act through a flexible loop region to allow for extensive movement of individual enzyme domains relative to each other during the specificity shift, as a co-crystal of *Aquifex aeolicus* bound to tRNA-CC readily dissolved upon soaking with ATP (Tomita *et al.*, 2004; Betat *et al.*, 2010). Taken together, the exact role of arginine 204 may be quite complex. Considering the dynamic nature of the EDxxR motif, arginine 204 may assume different roles depending on the position of the nucleotide to be added to the 3' end of the tRNA. The studies described here were designed to clarify the role of arginine 204 in *C. glabrata* in nucleotide addition efficiency, specificity, or both at all three tRNA 3' end positions. In addition to this, the structural significance of this conserved arginine residue was also examined.

4.2 Arginine 204 is required for cell viability

The *Candida glabrata* *CCA1* gene was isolated through complementation in *Saccharomyces cerevisiae* (Hanic-Joyce and Joyce, 2002). QuikChange™ (Stratagene) mutagenesis was used to substitute arginine 204 with alanine, glutamate, or glutamine. *In vivo* plasmid shuffling studies demonstrated that any of these substitutions caused cell death (Fig. 1-9), suggesting an important role for this arginine residue in enzyme structure and/or function. The importance of this amino acid is supported by its conservation throughout evolution in multiple species ranging from bacteria, yeast, plants, and humans (Fig. 1-2), among others. In addition, arginine 204 is suggested to be involved in both nucleotide addition efficiency (Lizano *et al.*, 2008) and specificity (Li *et al.*, 2002; Cho *et al.*, 2007) during the addition of

CCA to the 3' end of tRNA. Based on the multiple roles proposed for Arg204, further experiments were performed to determine whether this phenotype was due to arginine playing a role in either the enzyme's structural stability, nucleotide incorporation activity, or both.

4.3 Substitution of arginine 204 by Ala, Glu, or Gln suggests its primary role is not in defining the enzyme's overall structural integrity

4.3.1 Secondary structure

Purification of native and variant tRNA nucleotidyltransferase proteins was developed using glutathione-S-transferase affinity chromatography. All of the proteins were isolated to a similar level of purity (Fig. 3-3). The purified proteins were analyzed by far-UV circular dichroism (CD) and fluorescence spectroscopy to determine if their higher order structures were still intact, and to determine their stability.

According to one proposed function of the arginine in motif D (Li *et al.* 2002), this residue interacts with the first acidic residue in motif D (Asp200 in *C. glabrata*) during the addition of the first two CMPs (Fig. 1-6 left hand side), as well as during the addition of the terminal AMP (Fig. 1-6, right hand side). In addition to this, Asp200 may also interact with a tyrosine residue (Tyr135 in the *C. glabrata* enzyme) in the flexible loop region (Fig. 1-4), in order to orient arginine 204 during AMP addition (Toh *et al.*, 2009). As no nucleotides were present during the CD studies, one must look at the crystal structures without nucleotide bound in order to see which interactions may be altered by substitutions to arginine 204. According to the *B. stearrowthermophilus* (Li *et al.*, 2002) and *H. sapiens* (Augustin *et al.*, 2003) crystal structures resolved without nucleotides (PDB files: 1MIV and 1OU5, respectively), the hydrogen bonding pattern is the same as predicted in the models of the *C. glabrata* enzyme (Figures 1-10 and 4-1).

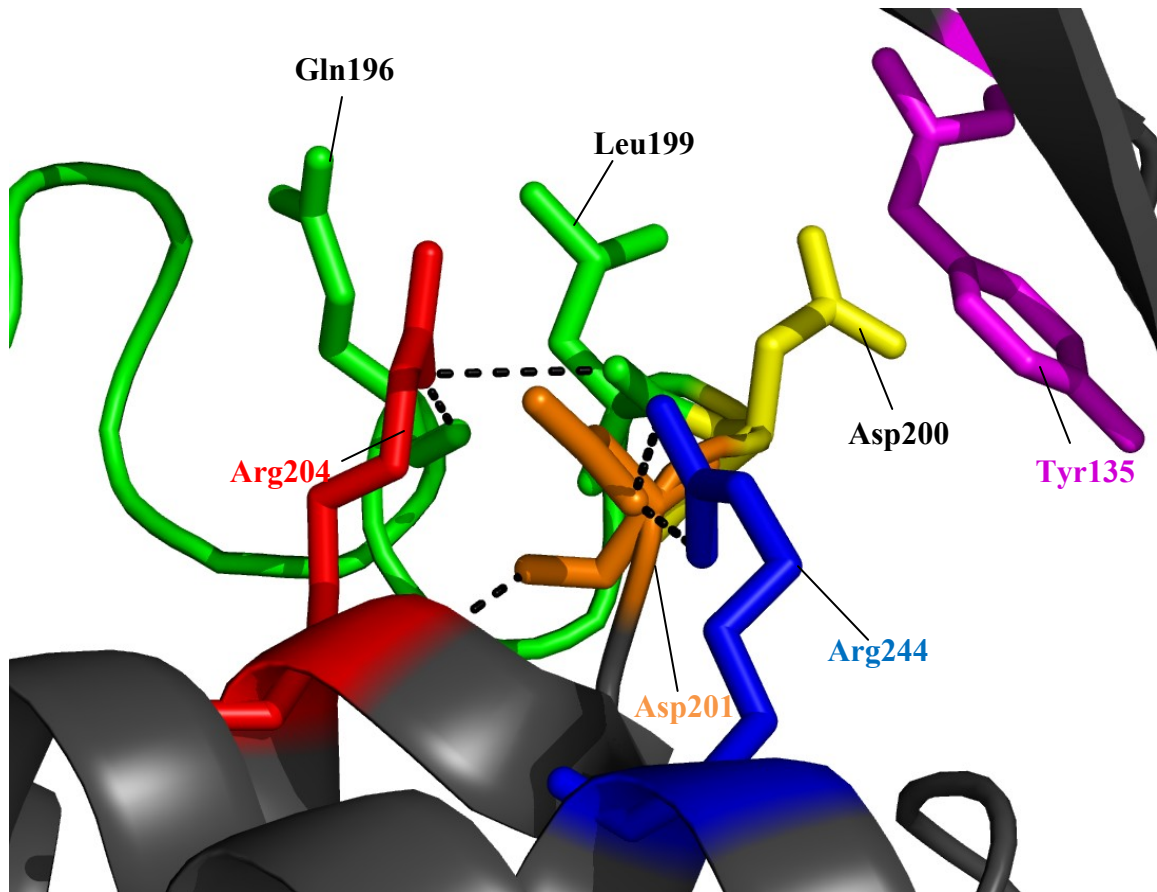


Fig. 4-1 Close-up of *C. glabrata* tRNA nucleotidyltransferase model without substrate bound showing Tyr135. *C. glabrata* tRNA nucleotidyltransferase. Arg204 (red), Arg244 (blue), Asp201 (orange), Tyr135 (pink), Gln196 and Leu199 residues (green) are labeled and displayed as sticks. The loop stabilized by Arg204 and Arg244 is shown in green (viewed with PyMol, see Fig. 1-4 for details).

From this model, Arg204 does not interact with Asp200 when no nucleotide is present, but instead seems to hold Asp200 in close proximity by interacting with the main chain of nearby residues (Gln196 and Leu199). In addition to this, Arg244 interacts with Asp201, aiding Arg204 in holding Asp200 in close proximity. Both of these interactions may be stabilizing the helix containing Arg204. Finally, Tyr135 may be able to interact with Asp200 through hydrophobic interactions as suggested by (Toh *et al*, 2009), or possibly by hydrogen bonding.

According to its CD spectrum, the native enzyme showed a typical α -helical signal at 208 nm and 222 nm (Fig. 3-5), in good agreement with the α -helical nature demonstrated by the tRNA nucleotidyltransferases whose crystal structures have been solved (Li *et al.*, 2002; Augustin *et al.*, 2003; Tomita *et al.*, 2004; Toh *et al.*, 2009) and consistent with previous experiments in our lab (Arthur, 2009). In all of these crystal structures, the arginine corresponding to arginine 204 in the *C. glabrata* tRNA nucleotidyltransferase was found at the N-terminal end of an α -helix. The CD spectra of the variant enzymes showed minor to major differences (alanine < glutamine < glutamate) as compared to the native enzyme suggesting that altering this amino acid did affect the structure of the protein and that introducing different amino acids at position 204 could affect the structure of the enzyme differently.

Of the variants, the alanine substitution demonstrated a signal most similar to the native enzyme, showing only a slight decrease in overall signal (Figures 3-4 and 3-5). Due to the location of position 204, this substitution should not destabilize an alpha helix as alanine has the highest helical propensity of all amino acids (Bryson *et al.*, 1995). This suggests that the decrease in signal may be due to small local changes caused by alanine's short side chain, and the inability to form ionic and/or hydrogen bonds to nearby residues.

The glutamine substitution resulted in a slightly decreased overall signal, although this change was greater than that seen for the alanine variant. While this amino acid is shorter than arginine and lacks a charge, it is able to hydrogen bond. So, the change that is observed although minor, may result from glutamine's lower helical propensity (as compared to alanine; Bryson *et al.*, 1995), and/or its possible inability to hydrogen bond

with nearby residues due to it being shorter than arginine. This will be addressed further when discussing the results of the enzyme assays.

Finally, the glutamate substitution resulted in a CD spectrum demonstrating the largest change compared to that of native enzyme. The curve showed the same general character as the native enzyme (both minima), but had a highly decreased signal at 222 nm, indicating a loss in helicity (Creighton, 1989). Changing a positively charged arginine 204 residue into a negatively charged glutamate (at physiological pH) may actually stabilize the helix as its location at the N-terminus has a net positive dipole (Hecht et al., 1990). In contrast, it seems like this substitution results in the destabilization of the enzyme structure due to repulsive negative charge interactions with nearby aspartate residues (positions 200 and 201). In addition, this charge repulsion may affect any possible interaction between Asp200 and Tyr135 (shown in close proximity, Fig. 4-1) of the flexible loop region, further altering the enzyme's structure due to its highly flexible lever-like function (Neuenfeldt *et al.*, 2008; Toh *et al.*, 2009; Betat *et al.*, 2010). Overall, it may be this flexibility which can propagate the loss of helicity observed for the glutamate substitution.

4.3.2 Tertiary structure

Fluorescence spectroscopy was used to probe changes in the tertiary structure of the proteins. Analysis of the protein sequence with the ProtParam tool (Gasteiger *et al.*, 2006) revealed that the protein has 8 Trp, 19 Tyr, and 25 Phe residues. The location of some of these in the protein can be seen on Fig. 4-2.

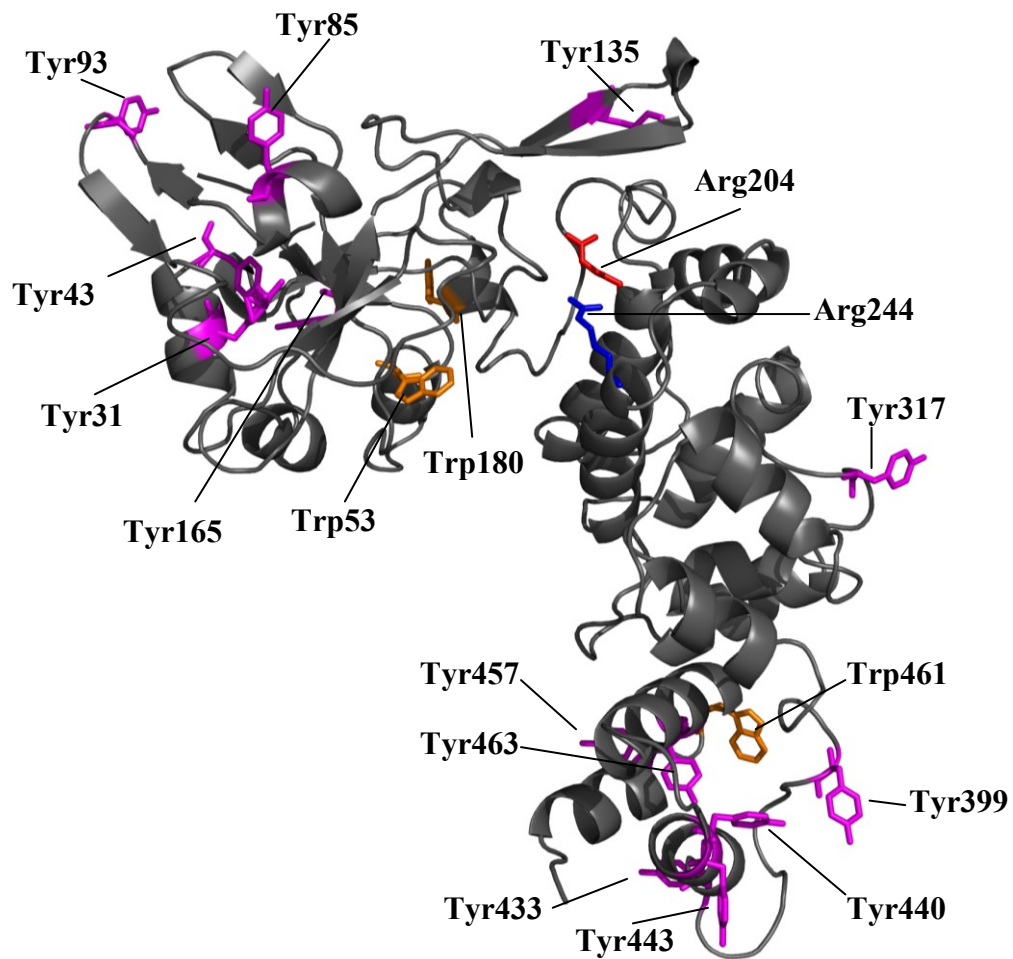


Fig. 4-2 Model of *C. glabrata* tRNA nucleotidyltransferase showing fluorophores. *C. glabrata* tRNA nucleotidyltransferase. Arg204 (red), Arg244 (blue), Trp (orange), and Tyr (pink) residues are labeled and displayed as sticks (viewed with PyMol, see Fig. 1-4 for details).

Although 8 tryptophans are in the primary sequence (Fig. 1-2), only three are visualized because the model is not of the full length peptide. Analyzing both Fig. 4-2 and the primary sequence, 4 of 8 Trp residues are located in the Head and Neck domains, while the other 4 Trp residues are in the Tail domain of the enzyme. Due to this, substitutions resulting in changes of the active site (between the Head and Neck domains) may be

reflected by changes in fluorescence as 50% of the Trp residues are in close proximity. It is likely that large changes in secondary structure will ultimately result in changes of the enzymes tertiary structure.

Based on the fluorescence results (Table 3-2), the alanine variant was the most similar to the native enzyme in both fluorescence shift and intensity (Figures 3-7 and 3-8). This suggests that although a small blue shift along with a small loss of intensity does exist, this is not major and therefore there is not a large change in tertiary structure for this variant. In contrast, both the glutamate and glutamine variants show a slight red shift (greater for glutamate) as well as a large decrease in fluorescence intensity (also larger for glutamate). These results are consistent with secondary structure changes as the alanine substitution results in the smallest change of the variants compared to the native enzyme, while the glutamate substitution results in the largest change. The slight change observed in shift for all three variants is very small, suggesting tryptophan residues are in an environment of similar polarity as the native enzyme. On the other hand, the large decrease in intensity observed for the glutamine and glutamate variants, suggests that quenching of tryptophan residues occurs through energy transfer to another residue. Considering that 50% of the Trp residues are located in the Head and Neck domains of the enzyme, the large decrease in fluorescence observed (approximately 50%) may be consistent with movement of the flexible loop region acting as a lever in causing an extensive movement of the enzyme domains.

4.3.3 Thermal stability

To further understand the effects of these substitutions on the structure of the enzyme, thermal denaturation of the native and variant proteins were carried out. Thermal denaturation was measured as a function of the change in CD signal at 208 nm versus temperature.

All of the resulting curves except the one belonging to the glutamate variant demonstrated a two-state cooperative unfolding process (Creighton, 1993) without any intermediates (Fig. 3-6). This suggests that the glutamate substitution may have resulted in a protein with an intermediate (or partially unfolded) structure corresponding to the profile observed at the start of its thermal denaturation curve. This intermediate structure is also consistent with the loss in helicity of the variant as suggested by CD data. Moreover, all of the variant proteins had a melting temperature (T_m) which was higher (Table 3-1) than the native protein as also observed for the variant enzymes analyzed by Arthur (2009). Among the single variants, the alanine variant had the largest increase in T_m (2.8°C higher than native) while the R204E and R204Q variants showed an increase in T_m of 1.6°C as compared to native. The increase in melting temperature observed for the alanine variant may be due to alanine being uncharged and its high helical propensity (as mentioned previously). For this reason, alanine cannot destabilize the positively charged N-terminus of the alpha helix (Hecht *et al.*, 1990) as arginine would in the native protein. The melting temperature increase resulting from the glutamine substitution may also be due to this amino acid having greater helical propensity (Bryson *et al.*, 1995) than arginine (but lower than alanine). In addition, this variant also demonstrated a large change in tertiary structure as compared to the native enzyme and alanine variant. This

may suggest that the enzyme has taken a new conformation, possibly rendering it more stable than the native enzyme. Finally, the glutamate substitution may be increasing the melting temperature due to its negative charge being able to stabilize the N-terminus of the helix containing position 204. This would be rather unlikely since this variant demonstrated a great loss in helicity as measured by CD spectroscopy. Furthermore, this loss in helicity is consistent with the loss in cooperativity observed during its unfolding process, as this partially unfolded variant may be explained by an intermediate.

Observing the curve for this variant (Fig. 3-6), after initial unfolding of this possible intermediate, the curve seems to merge with that of the other two variants. Since the glutamate variant showed a change in tertiary structure (along with the similar change by the glutamine variant), it can be suggested that the melting temperature increase observed for the glutamate variant (and the glutamine variant), may also be due to the enzyme having an increasingly stable structure due to the observed change in tertiary structure.

4.3.4 Summary

Overall, biophysical characterization through CD and fluorescence spectroscopy has determined that the arginine 204's primary role in maintaining a functional protein is not in defining the structural integrity of *C. glabrata* tRNA nucleotidyltransferase.

Although the glutamate and glutamine variants show greater changes in structure, these changes are not required for the loss of activity as all of the variants (including the Ala variant) show a loss of function as indicated by the cell death phenotype (Fig. 1-9). In addition, the CD spectra of the variants were still those of folded proteins and, in fact, also demonstrated increased melting temperatures. It can be said that arginine 204's

primary role is not in maintaining the overall structural integrity of tRNA nucleotidyltransferase.

4.4 Substitution arginine 244 to Ala, in combination with arginine 204 to either Glu or Gln does not significantly alter the higher order structure of the enzyme

Similarly to the single variant proteins, variants with two substitutions were also purified and analyzed by far-UV circular dichroism (CD) and fluorescence spectroscopy to determine if the higher order structures were still intact, and to determine their stability. According to the CD spectra (Figures 3-4 and 3-5), both double variants (R244A-R204E and R244A-R204Q) showed a typical α -helical signal at 208 nm and 222 nm, in good agreement with the results in section 4.3.1. The spectra for these variants were more similar to the native spectra than were those of the single variants. In addition to this, fluorescence spectroscopy (Figures 3-7 and 3-8) also showed similar spectra (with only a slight red shift) as compared to the native spectra (Table 3-2). Taken together, these data suggest that the changes resulting from substitution at position 204 may be balanced or canceled out by changes at position 244. The thermal denaturation data for these variants (Table 3-1) is two-state cooperative and shows an increase of 4.4°C compared to the native enzyme. Furthermore, a minimum 1.6°C increase in melting temperature was observed for the single variants at position 204 and an increase of 4.2°C was seen for the R244K variant (Arthur, 2009). Taken together, these results show that the Arg204 mutations do not stabilize the enzyme further. Moreover, to explain how the R244A mutation balances the structural changes caused by R204 mutations, the active site model (Figures 1-10 and 4-1) must be consulted. This model shows Arg244 interacting with Asp201 in the *C. glabrata* enzyme, suggesting that it may play a role

along with R204 in holding both aspartate residues (200 and 201) in position . If the single variants (R204E and R204Q), do indeed lead to a loss of interaction with the protein's flexible loop region (Tyr135, as described by a change in tertiary structure in section 4.3.2), this could possibly result in the flexible loop region moving away from Asp200. At this point, since Arg244 would still be interacting with Asp201, this may cause a strain by pulling Asp200 away from the flexible loop, propagating the observed change in tertiary structure. In contrast, changing arginine 244 to alanine may result in a loss of interaction with Asp201 and therefore Asp200 is no longer being pulled away from the flexible loop in the double variants. This mechanism would result in a variant protein structure which is more similar to the native enzyme (as observed by the CD and fluorescence data).

Overall, biophysical characterization through CD and fluorescence spectroscopy has determined that the higher order structure is not significantly altered by substitutions of arginine 204 to Glu or Gln, in combination with arginine 244 to alanine. The substitution of Arg244 to alanine resulted in a more native-like structure compared to the single Arg204 variants. Further studies will determine whether the reconstitution of structure in the double variants can result in native-like activity.

4.5 Ability of native and variant enzymes to use specific tRNA substrates

To address why plasmid shuffling experiments (Fig. 1-9) resulted in cells which were not viable, tRNA substrates with differing 3' ends (-N, -NC, -NCC, and-NCCA) were utilized for *in vitro* enzyme assays. For these experiments, the tRNA substrates were

prepared using radioactive GTP, and used for monitoring CTP and/or ATP addition under differing conditions.

4.5.1 tRNA-NCC substrate

When using the tRNA-NCC substrate, the native enzyme was able to efficiently extend to position 76 when supplied with both ATP and CTP, or each nucleotide individually (lanes 3, 4, and 5, Fig. 3-13, Table 3-6) during two minute assays. When both nucleotides were supplied to the alanine and glutamine variants, they demonstrated similar results (approximately 84.6% and 90.8% of the product corresponding to the size of tRNA-NCCA, respectively). In contrast, the glutamate variant did not show any product corresponding to complete extension. When these variants were then supplied with either CTP or ATP alone, an increased selectivity for ATP over CTP incorporation was observed (compared to the native enzyme). These data suggest that substitutions to Arg204 may either allow for an increase in specificity for AMP or a decrease in CMP incorporation efficiency, or both. Previous experiments have demonstrated that arginine (corresponding to Arg204) to alanine substitutions in the *E. coli* and *H. sapiens* enzymes resulted in reduced AMP incorporation to the tRNA-NCC substrate (Lizano *et al.*, 2008). From these substitutions it was observed that the *H. sapiens* enzyme was less affected in AMP incorporation (Lizano *et al.*, 2008), suggesting that the *C. glabrata* enzyme is more similar to the *H. sapiens* enzyme than the *E. coli* enzyme (as our *C. glabrata* variants demonstrated native-like efficiency). This is also consistent, with the predicted model of the *C. glabrata* enzyme in Fig. 1-4 being based on similarities to the *H. sapiens* crystal structure over all of the other available crystal structures. In addition to this, both *C. glabrata* and *H. sapiens* are more closely related evolutionarily as they are both

eukaryotes, while *E. coli* is a prokaryote. Furthermore, in order to clarify whether Arg204 mutations result in a decreased CMP addition efficiency, increase in AMP specificity, or both, reactions over a longer period of time were performed, with both ATP and CTP, or either nucleotide alone.

Two hour reactions using both nucleotides (Figures 3-29 to 3-34) demonstrated how the native enzyme was once again effective, extending within two minutes. Consistent with the standard assay data, both the alanine and glutamine variants showed full extension after only two minutes. In contrast to the standard assay data, the glutamic acid variant showed partial extension (approximately 20% taking heterogeneity into account) after four minutes and no further extension by two hours. The reduced ability of the R204E variant to extend the template efficiently is consistent with the biophysical data, as it has undergone major changes in secondary and tertiary structure. From this, it is clear that these changes affect nucleotide incorporation. However, perhaps the other substitutions (alanine, glutamine) affect specificity. To address this possibility, the enzymes were only supplied with either nucleotide over the two hour reaction period.

With CTP alone (Figures 3-36 to 3-41), only the native enzyme was able to extend the entire starting template to a size corresponding to tRNA-CCC after two minutes, while the alanine variant showed extension starting at two minutes (21.5% of product) and leveled after two hours (47.4% of product). No activity was observed for any of the other variants. These data suggest that the glutamate and glutamine variants have lost the ability to incorporate CMP to position 76 *in vitro* (as the native enzyme can). With ATP alone (Figures 3-42 to 3-47), the native enzyme and the glutamine

variant were both able to extend the tRNA-NCC template to 100% tRNA-NCCA after two minutes, while the alanine variant took four minutes. The glutamic acid variant only extended 47.1% of the template after two hours. Taken together, the R204E substitution definitely affects incorporation efficiency, but still demonstrates a preference for ATP over CTP. The other two variants demonstrate increased specificity, but without significant incorporation efficiency effects. In addition, arginine 204 is required for effective CMP misincorporation *in vitro*. Taken together all of these data suggest that arginine 204 is not essential for either efficient or accurate nucleotide addition at position 76. However, the data shown here do not completely disprove the classical binding method with ATP through the EDxxR motif (Li *et al.*, 2002) although it may suggest that the bond contributed by arginine 204 to ATP is not essential (Fig. 1-6), and that the single bond between Asp201 and ATP is sufficient for proper incorporation. Further experiments with substitutions to other EDxxR motif residues, or in with R244 will be needed in order to clarify the main role of R204 at position 76.

4.5.2 tRNA-NC substrate

To address the role that R204 plays for incorporation at positions 75, the native and variant enzymes were tested with the tRNA-NC substrate under standard conditions (Fig. 3-12 and Table 3-5). As observed with the tRNA-NCC assays, the native enzyme efficiently extended the tRNA-NC substrate to a size corresponding to position 76. In contrast, the alanine and glutamine variants were less efficient in extending to a size corresponding to extension to position 76 (only 24.3% and 19.3% of the final product, respectively). Since 16% of the initial template had a size corresponding to tRNA-NC+1 (Template, Table 3-5), and these variants demonstrated efficient extension of tRNA-NCC

to tRNA-NCCA (above), this suggests that misincorporation occurs and causes the enzyme to abort further extension (Lizano *et al.*, 2008; Arthur, 2009). In addition, the misincorporated nucleotide was not added efficiently as the alanine and glutamine variants respectively did not extend 22.8% and 45.1% of the initial tRNA-NC substrate at the end of the two minute reaction. Overall, all of the variant enzymes demonstrated reduced incorporation efficiency in adding one nucleotide to the tRNA-NC substrate, as well as increased misincorporation of AMP in place of CMP. Time course assays were used to distinguish between these two factors. .

During the time course assays using both ATP and CTP (Figures 3-23 to 3-28), none of the variants were able to fully extend to a band corresponding in size to 100% tRNA-NCCA (position 76) after two hours. The alanine variant showed full extension to at least position 75 within two minutes (62.0% of product), but did not extend more than 38% of the product to position 76 after two hours. Similarly, the glutamine extend 44% of the template to position 76 after two hours, and only showed product corresponding to at least position 75 after 60 minutes. Moreover, the glutamic acid variant showed addition after 10 minutes and left 31.0% of the tRNA-NC substrate un-extended after two hours. Overall, the R204A enzyme was the only variant which did not demonstrate a decrease in addition of only one nucleotide to the tRNA-NC substrate (compare Figures 3-23 to 3-26). However, all of the variants demonstrated a build-up of tRNA-NCA product, suggesting that misincorporation is occurring (blocking further extension). Taken together, these results confirm that Arg204's main role at position 75 is to ensure the proper nucleotide is incorporated. In addition, Arg204 may also play a role in nucleotide incorporation efficiency as demonstrated by the R204E and R204Q variants. These data

are consistent with the biophysical data, as both the R204E and R204Q variants demonstrated changes from the native enzyme's structure. Previous experiments are also consistent with these data as the Arg to Ala substitution in the *B. stearothermophilus* enzyme, resulted in a dramatic loss of specificity at this position (Cho *et al.*, 2007). In addition, the same substitution in the *E. coli* and *H. sapiens* enzymes demonstrated a reduced level of nucleotide incorporation (Lizano *et al.*, 2008).

4.5.3 tRNA-N substrate

During standard assays, the native enzyme efficiently generated product corresponding to full extension to position 76 (Fig. 3-11). The alanine variant showed apparent extension of approximately 13.7% of the substrate to position 76, and approximately 33.3% extension position 75. Since some of the starting template (approximately 21.5%) was heterogeneous at position 74, suggests that the substrate was either not extended efficiently, or that it was extended by two nucleotides along with its heterogeneous counterpart. Since the alanine variant demonstrated no efficiency problems for addition to tRNA-NC until position 75, it can be suggested that the tRNA-N substrate is not extended efficiently by this variant. The other variants (R204E and R204Q) showed no significant extension. Since none of the variant enzymes can efficiently extended to position 76, the *in vivo* observation of cell death is confirmed as these variants would not be able to undergo the aminoacylation required to carry out protein synthesis. These results imply that the arginine residue at position 204 plays a vital role in nucleotide addition at position 74; however, its role in specificity is not clear. Time-course experiments would help determine whether arginine 204 is involved in assuring CMP is added to position 74 or not.

Time course assays with the tRNA-N substrate (Figures 3-17 to 3-22) showed that none of the variants could generate a significant amount of product corresponding to position 76. The alanine variant demonstrated product corresponding to extension to at least position 75 after 15 minutes. In addition, some product corresponding to position 76 was also seen after only two minutes. At the two hour time point, product corresponding to position 76 only represented 34.4% of the total template. These data are once again consistent with tRNA-NC data, as a buildup of tRNA-NCA represents a loss of specificity and increased misincorporation at position 75. Moreover, the glutamine variant demonstrated product corresponding in size to extension to position 75, starting at the 10 minute time point and generated a larger product only after 30 minutes. As the reaction goes to two hours, more of the products corresponding to positions 75 and 76 are observed, further suggesting that arginine 204 is important of efficient nucleotide incorporation. Further confirming arginine 204's role in incorporation is observed as the glutamic acid variant only demonstrated minimal extension after two hours. Previous experiments have demonstrated that the arginine residue in the EDxxR motif is important CMP specificity (Cho *et al.*, 2007) and nucleotide incorporation efficiency (Lizano *et al.*, 2008) at this position. Although our data suggest that incorporation is definitely affected, they are not sufficient to confirm whether misincorporation occurs when extending the tRNA-N substrate. Further experiments would be needed (*i.e.*, experiments with labeled nucleotides) to assess a role of Arg204 in ensuring CMP addition. Taken together, regardless of whether misincorporation occurs or not, nucleotide incorporation is definitely dramatically altered in the variants at position 74. Experiments with Arg204 and Arg244 double variant enzymes will further help to define the role of Arg204 in CTP

binding as suggested by its classical EDxxR motif role (Li *et al*, 2002), and will also help to clarify the role of Arg244 in CTP binding as suggested by Arthur (2009).

4.5.4 Ability of the double variants to use the three tRNA substrates

Previous experiments (Arthur, 2009) where arginine 244 in the *C. glabrata* enzyme was substituted to alanine, lysine, or methionine resulted in cell death. Nucleotide incorporation assays using the tRNA substrates with differing 3' ends determined that these substitutions resulted in a loss of nucleotide addition at position 74, a reduction of specificity at position 75, and an increase in specificity at position 76. In this study, variants substituted at position 204 (with glutamate or glutamine) were similarly tested in conjunction with the R244A substitution. The experiments were performed in order to determine whether both Arg 204 and Arg244 work together for nucleotide addition efficiency and/or specificity at all three tRNA 3' end positions.

4.5.4.1 tRNA-NCC substrate

During tRNA-NCC assays under standard conditions, only the R244A-R204Q variant demonstrated activity (Fig. 3-16). In addition, this variant was also alone in showing activity when supplied with ATP alone over a two minute reaction. Furthermore, it was unable to add CTP at this position. When comparing lanes 6 and 7 in Fig. 3-16 and the percentages in Table 3-9, it was observed that the addition occurring for this variant is mostly due to AMP incorporation. Although activity was observed, it was very inefficient (Table 3-9). In order to verify whether more efficient incorporation could occur during longer assay times, time course assays at position 76 were performed using both nucleotides and either nucleotide alone.

Time course assays with both nucleotides (Figures 3-33 and 3-34, Tables 3-26 and 3-27) demonstrated that only the R244A-R204Q could extend to position 76, leaving behind only 21.5% of the initial heterogeneous starting template (consistent with standard assay data). Furthermore, it was determined that the R244A-R204Q variant was able to add AMP at this position (Fig. 3-41 and Table 3-33), but not CMP (Fig. 3-47, Table 3-39).

Overall, the R244A-R204Q variant demonstrated decreased nucleotide addition efficiency and increased ATP specificity over CTP. Since the R244A mutation alone had previously resulted in increased specificity and no loss of efficiency (Arthur, 2009), while the R204Q mutation alone demonstrated the same, it can be suggested that ATP cannot bind as efficiently in the double variant. In addition, the R244A-R204E variant did not demonstrate any addition to position 76 under any conditions, while the R204E variant showed increased specificity and decreased efficiency (section 4.5.1). Taken together, these results suggest that both arginines may be involved in keeping the binding pocket at a specific size while orienting both Asp200 and Asp201 during AMP addition to position 76. In addition, Arg204's interaction with the nucleotide would not be as important (compared to Asp201's) as arginine is not required for proper incorporation. This would be consistent with Asp200 interacting with Tyr135 in the flexible loop region (Neuenfeldt *et al.*, 2008; Toh *et al.*, 2009) while coordinating Arg204 during the specificity shift from CTP to ATP. In addition, Arg244's role in stabilizing motif D's helix-turn structure would also agree with the above suggestions (Li *et al.*, 2002; Betat *et al.*, 2010). Overall, these data demonstrate that all three mutations (R244A, R204E, and R204Q) alone result in decreased CMP incorporation as CTP would not be able to form proper interactions

due to its size (smaller than ATP), and the increased binding pocket size. In addition, these data are also consistent with the R204E change resulting in repulsive effects, further increasing the binding pocket size and resulting in the loss of AMP incorporation efficiency observed in the R244A-R204E variant (as the pocket would now also be too large for efficient ATP binding).

4.5.4.2 tRNA-NC substrate

No significant addition was observed for either variant to position 74 during standard assays or with either nucleotide alone (Fig. 3-15). In contrast, time courses with both nucleotides and tRNA-NC (Figures 3-27 and 3-28, Tables 3-20 and 3-21) demonstrated some activity. After two hours, the R244A-R204E variant demonstrated 23.8% addition of one nucleotide, while the R244A-R204Q variant showed 28.3% extension by one nucleotide and 17.0% extension by two.

Considering the single R204 variants demonstrated a loss in both efficiency and specificity at this position, while the R244A substitution resulted in a decrease in CMP specificity (Arthur, 2009), it can be suggested that Arg204 is involved in binding, while Arg244 may only be playing a supporting role. The double variant data here are consistent with these roles as both variants show a dramatic decrease in efficiency. It is plausible that if one substitution negatively affects specificity (R244A), while the other negatively affects both efficiency and specificity (R204 substitution), that the observed loss in efficiency can occur.

4.5.4.3 tRNA-N substrate

During standard tRNA-N assays, the double variants did not show any nucleotide incorporation (Figures 3-14). In addition, no incorporation was observed when they were supplied with only ATP or CTP. Similarly, time course assays with both nucleotides resulted in no significant extension after two hours. As the R244A substitution had resulted in a complete loss of nucleotide incorporation, while the R204 variants generally demonstrated a reduction in incorporation, these data suggest that Arg244 may actually bind CTP at this position. If Arg244 were to indeed bind CTP for addition to the tRNA-N substrate, Arg204 would play a supporting role in either binding pocket size and/or orientation of Asp201. This would not be consistent with the classical EDxxR motif suggested by Li *et al.* (2002), but would support a mechanism proposed by Arthur (2009) where Arg244 would form Watson-Crick-like bonds with CTP at position 74.

4.5.5 Ability of the enzymes to extend further than tRNA-NCCA

All of the enzymes (native, single and double variants) were given the full-length template as a substrate and provided with both nucleotides (Fig. 3-35). The reaction was performed over two hours and was monitored at the 30 minute and 120 minute marks. None of the enzymes were able to extend the full length tRNA to a position greater than 76. Previously, substitutions to residues R194, M197, and E198 in the *B. stearothermophilus* enzyme (corresponding to R244, V247, and E248 in the *C. glabrata* enzyme) had resulted in polynucleotide addition (Cho *et al.*, 2007). Of these residues, only R244 was substituted (double variants) in this study and no polymerase activity was observed. This was consistent with what was also observed for Arthur (2009). Since

R204 is not known to be involved in limiting the 3' end to CCA, the results observed here for the single variants are also consistent with previous studies.

4.5.6 Ability of the enzymes to utilize GTP or UTP

In order to determine whether the enzymes are able to use either GTP or UTP as a substrate *in vitro*, 30 minute reactions were performed with all three tRNA substrates and either GTP or UTP as the only nucleotide. The native enzyme, the R204A variant, and the R204Q variants were the only enzymes to demonstrate activity.

Looking at assays with the tRNA-N substrate supplied with only GTP, none of the enzymes were able to incorporate GMP at position 74 (Fig. 3-48, Table 3-40). In contrast, the native enzyme was able to incorporate up to two GMPs with products at positions 75 and 76 when supplied with the tRNA-NC substrate (Fig. 3-49, Table 3-41). The alanine variant also showed activity with this substrate, incorporating one GMP. Moreover, for addition to position 76 (Fig. 3-50, Table 3-42), the native enzyme and the alanine variant showed a band corresponding to full length extension. None of the other variants demonstrated any measurable activity.

Assays in the presence of UTP alone showed that the native protein could add either one or two nucleotides to the tRNA-N substrate (Figures 3-51, Table 3-43) depending on if it was able to add one nucleotide to the heterogeneously 3' extended portion of the initial substrate or not. In addition, the alanine variant demonstrated a band corresponding to the size of the product extended by one nucleotide, while the glutamine variant also demonstrated a band of for the tRNA-NU product. For the tRNA-NC substrate (Figures 3-52, Table 3-44) the native enzyme and both the alanine and

glutamine variants all demonstrated bands corresponding to tRNA-NCU. Finally at the terminal position (Figures 3-53, Table 3-45), all three could once again extend to tRNA-NCCU, with the glutamine variant being the least efficient of the three.

What is of particular interest here is the activity shown by the native enzyme. It has been cited that the apparent specificity of the enzyme depends on assay conditions (Cho *et al.*, 2003). The authors have stated that under their standard conditions (1: 100 ratio of protein to tRNA, 200 μ M nucleotides), class I and class II CCA adding enzymes faithfully add CCA. They also report very weak incorporation of UTP only when CTP is omitted, UTP and enzyme levels are high, or the assay is prolonged. In addition, Yue *et al.* (1996) have also demonstrated the inability of their native enzymes to incorporate UTP or GTP into tRNA-N and tRNA-NC. The UTP data observed for the *C. glabrata* enzyme support what had previously been seen as high levels of UTP and enzyme were used, CTP was excluded, and the assays were prolonged (400 μ M UTP, 30 minutes, and approximately 1: 5 ratio of protein to tRNA). Our native enzyme also demonstrated incorporation of GTP to the tRNA-NC and tRNA-NCC substrate. In addition, the enzyme could add up to two GMP molecules, while only the alanine variant could add one GMP. Adding to this, GTP incorporation has never been reported as a substrate for a native tRNA nucleotidyltransferase enzyme. Finally, it has been reported that a R157A mutation in the *B. stearrowthermophilus* enzyme (corresponding to R204A in the *C. glabrata* enzyme) readily added single C, A, U, or G to tRNA-N or tRNA-NC substrates (Cho *et al.*, 2007). The data observed throughout the study is consistent as the R204A variant has shown the ability to add all of the nucleotides. Finally, the double variant enzymes are unable to add UMP and GMP to any of the tRNA substrates, further confirming that both

arginines are indeed involved in defining the shape/size of the binding pocket. Overall, although some differences are observed for the variant enzymes (compared to the native enzyme), these experiments are preliminary and further investigation is needed to form better conclusions about the role of Arg204 in incorporating UMP and GMP *in vitro*.

4.6 Linking biophysical and enzyme assay data

Results from activity assays for the native enzyme, along with all of the variant enzymes have suggested the roles of arginines 204 and 244 during nucleotide addition at each position of the tRNA 3' end requiring extension. When using the tRNA-N substrate, Arg244 may bind CTP (with Asp201) through Watson-Crick-like interactions (Arthur, 2009), while Arg204 would help orientate Asp201 for proper CTP binding and/or control binding pocket size so ATP is excluded. Moreover, when adding to tRNA-NC, Arg204 may now bind CTP as in the classical EDxxR model (Li *et al.*, 2002) while Arg244 orients Asp201. Finally, when using the tRNA-NCC substrate, the main roles of both arginine residues may be in keeping the binding pocket at a specific size while orienting both Asp200 and Asp201 during AMP addition (see Fig 4-1 to visualize all of the residues involved and their proximity to each other). Furthermore, these suggested roles are supported by linking biophysical data with nucleotide incorporation data. In order to facilitate this process, the obtained nucleotide incorporation data and biophysical data are summarized in Tables 4-1, 4-2, and 4-3 and 4-4.

Enzyme	Substrate	
	tRNA-N	
	Activity	Specificity for CTP
R204	+++++	+++++
R204A	+++	?
R204E	+	?
R204Q	++	?
R244A-R204E	-	-
R244A-R204Q	-	-

Table 4-1 Summary of nucleotide incorporation results when the native and variant tRNA nucleotidyltransferase enzymes were supplied with the tRNA-N substrate.

Enzyme	Substrate	
	tRNA-NC	
	Activity	Specificity for CTP
R204	+++++	+++++
R204A	+++	+
R204E	+	+
R204Q	++	+
R244A-R204E	-	-
R244A-R204Q	-	-

Table 4-2 Summary of nucleotide incorporation results when the native and variant tRNA nucleotidyltransferase enzymes were supplied with the tRNA-NC substrate.

Enzyme	Substrate	
	tRNA-NCC	
	Activity	Specificity for ATP
R204	+++++	-
R204A	+++++	++++
R204E	++	+++
R204Q	+++++	+++++
R244A-R204E	-	-
R244A-R204Q	+++	+++++

Table 4-3 Summary of nucleotide incorporation results when the native and variant tRNA nucleotidyltransferase enzymes were supplied with the tRNA-NCC substrate.

Enzyme	Biophysical observations	
	Secondary Structure	Tertiary Structure
R204	-	-
R204A	Slightly less similar to R204	Similar to R204
R204E	Large change	Large change
R204Q	Small change	Large change
R244A-R204E	Similar to R204	Similar to R204
R244A-R204Q	Similar to R204	Similar to R204

Table 4-4 Summary of biophysical results compared to the native enzyme.

When analyzing Tables 4-1, 4-2, and 4-3, a general pattern is observed. The order from best to worst activity of the variant enzymes is as follows: R204A, R204Q, R204E, R244A-R204Q, and R244A-R204E. Without taking the double variant enzymes into account, the order suggested above correlates well with the changes observed in the biophysical data from that of the native enzyme (Table 4-4).

As the R204A variant was most similar to the native enzyme, this suggests that the differences observed in nucleotide incorporation are mostly due to a specific role for that amino acid in substrate binding or catalysis and not to a major structural role for this amino acid. This is consistent with changes in nucleotide efficiency and specificity observed for the same arginine to alanine substitution in *E. coli* and *H. sapiens* tRNA nucleotidyltransferases by Lizano et al. (2008). In addition, these results would be in tune with arginine 204's suggested role (above).

The second most similar variant was R204Q as it demonstrated a small change in secondary structure and a large change in tertiary structure. This variant was able to extend until position 75, although it took longer than the R204A variant. This suggests that along with a slight loss on efficiency, the glutamine side chain may also have a

reduced specificity for nucleotide incorporation such that misincorporation is increased. Since this variant worked at its best for addition to the tRNA-NCC substrate and its worst for addition to the tRNA-N substrate, it is plausible to think that the observed change in tertiary structure results in an enzyme with an altered confirmation (possibly involving Tyr135 of the flexible loop region) such that the nucleotide binding pocket is arranged to prefer ATP binding over CTP. This would be supported by a change in Watson-Crick like interactions due to the glutamine side chain, a larger binding pocket size due to glutamine being shorter than arginine, as well as this variant's enhanced ability for AMP incorporation at position 76.

Thirdly, the R204E variant demonstrated large changes in both the secondary and tertiary structure. In addition, it was the least efficient of the single variants while still demonstrating some ability to incorporate AMP at position 76. This is consistent with the change in tertiary structure resulting in an enzyme which prefers ATP, as described above for the R204Q variant. In addition, the loss of efficiency for AMP incorporation at position 76 is most probably due to the added effects of having a negative change in the active site causing repulsion and less efficient binding.

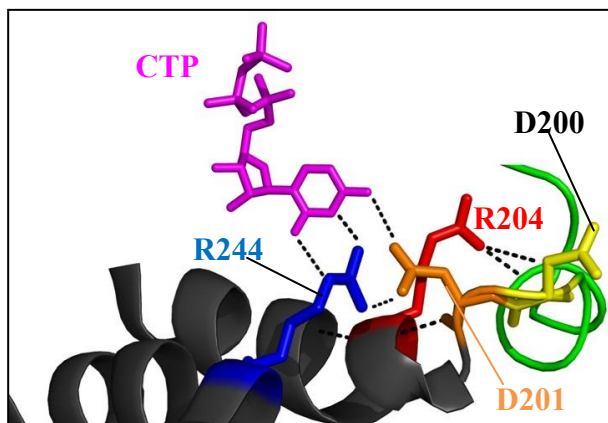
In conclusion, the double variant enzymes demonstrated the least activity, while keeping secondary and tertiary structures most similar to the native enzyme. As suggested in section 4.4, the Arg244 substitution balances out the structural changes resulting from the Arg204 substitution. Since both arginine residues are in close proximity, and are known to interact with other residues in close proximity, it seems as though the substitution to Arg244 relieves a previous strain. As arginine 244 may stabilize the helix-

turn structure of motif D (Li *et al.*, 2002; Betat *et al.*, 2010), changing Arg244 would result in a loss of interaction with neighboring residues (most probably Asp201), ensuring a native-like structure. So why do the two simultaneous substitutions result in practically inactive enzymes? The answer is simple: both arginine 204 and arginine 244 work together during nucleotide incorporation at all three positions. Details of their interplay are proposed in section 4.7

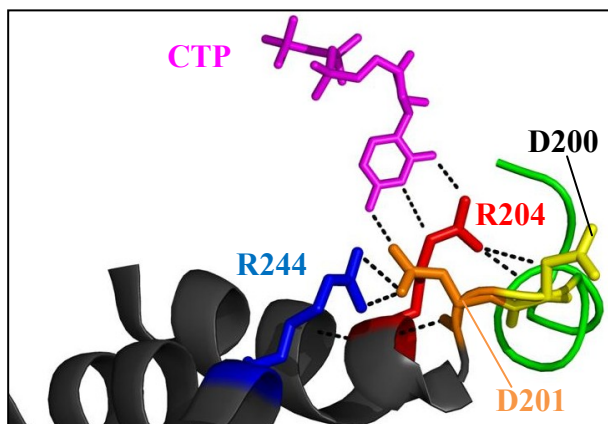
4.7 An updated proposed mechanism involving arginines 204 and 244

It has been suggested that arginine 244 may be involved in recognizing substrates (Li *et al.*, 2002), facilitating the switch to ATP recognition (Cho *et al.*, 2007), and/or orienting the 3' end of tRNA during extension (Cho *et al.*, 2007). Previous experiments in our lab (Arthur, 2009) have demonstrated that Arg244 does not limit the extension of tRNA past position 76. With this information, Arthur (2009) proposed that arginine 244 in the *C. glabrata* enzyme plays multiple roles in tRNA nucleotidyltransferase depending on the tRNA substrate that requires nucleotide addition. Here, I will propose an updated mechanism involving both residues. As suggested by Arthur (2009), the first incoming CTP is recognized directly by Arg244 through Watson-Crick interactions (O2 and N3 positions of the cytidine base), causing the nucleophilic 3'OH of the tRNA primer to be in close proximity to the nucleotide phosphates during orientation by the bound divalent metal ions. I propose that in addition to this, Asp201 would also interact with the incoming cytidine base (N4). Both these interactions would result in Watson-Crick interactions that would not be appropriate for ATP, blocking its addition to position 74. In addition to this, Arg204 would help to ensure the binding pocket size is small enough to exclude ATP by orienting Asp201 through interactions with Gln 196 and/or Leu199

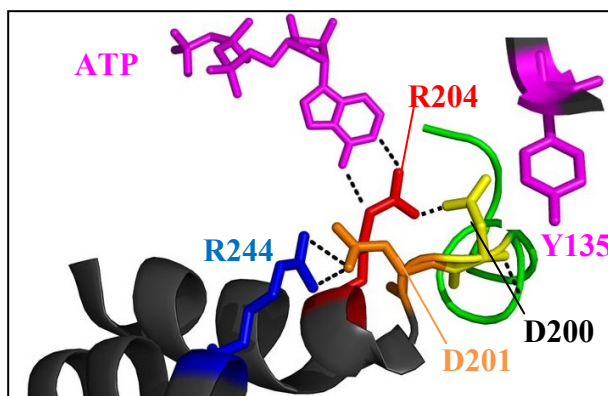
(side chain to main chain), or an ionic bond with Asp200 (Fig. 4-1). After the addition of CMP to position 74, the 3' end of the tRNA would refold to facilitate the binding of the second CTP to the (E/D)DxxR sequence of motif D (Li *et al.*, 2002; Toh *et al.*, 2008). Arthur (2009) pointed out that after this first addition, the new tRNA 3' end can now form additional interactions with Arg244 and a β -turn located opposite of the active site and Arg244 (as suggested by Tomita *et al.*, 2006). Due to this, it was suggested to the 3' end of the tRNA is now stabilized, allowing limited access to the active site, and further discriminating against the larger ATP molecule. The second CTP would bind as suggested by the crystal structure of the *B. stearothermophilus* (Li *et al.*, 2002) or *T. maritima* (Toh *et al.*, 2008) enzymes where CTP would be interacting with both Arg204 and Asp201, while Asp201 is coordinated by Arg244. Once the second CMP at position 75 is added, the tRNA 3'-end would once again refold and induce a conformational change in the enzyme. This conformational change would allow Asp200 to interact with Tyr135 (as suggested by Toh *et al.*, 2009) and cause Arg204 to rotate such that the binding pocket is now larger and suitable for ATP binding (see Fig 4-1 to visualize all the residues involved and their proximity to each other). Furthermore, this model would involve Arg244 interacting with Asp201. I propose that this interaction would be important to limit the enlargement of the active site in order to ensure a quick and seamless adaptation for the next round of CCA addition. A proposed model for nucleotide addition at all three positions is shown in Fig. 4-3.



Binding of CTP prior to addition of CMP to tRNA-N



Binding of CTP prior to addition of CMP to tRNA-NC



Binding of ATP prior to addition of AMP to tRNA-NCC

Fig. 4-3 Schematic mechanism of proposed nucleotide addition in *C. glabrata* tRNA nucleotidyltransferase. *C. glabrata* tRNA nucleotidyltransferase. Arg204 (red), Arg244 (blue), Asp201 (orange), and Tyr135 (pink) are labeled and displayed as sticks. CTP (pink) or ATP (pink) was rotated to fit the enzyme model (no substrates bound). PyMol was used to alter the configuration of Asp200 for ATP binding (viewed with PyMol, see Fig. 1-4 for details).

4.8 Conclusion

The role of arginine 204 proposed in this study is consistent with what is already known for this conserved residue in motif D (Li *et al.*, 2002), as well as with what previous studies with the *C. glabrata* enzyme have suggested. It has been proposed that Arg204 aids in limiting the size of the binding pocket while orienting Asp201 in order to help Arg244 discriminate against AMP addition at position 74. After addition of the first CMP, Arg204 (along with Asp201) would also directly interact with the second CTP through Watson-Crick like interactions between its side chain and the O2 and N3 positions of the cytidine base (as observed in Fig. 1-6), once again discriminating against AMP addition. Once the second CMP is added, a conformational change in the enzyme is induced by a refolding of the 3' end of the tRNA, resulting in an interaction between Asp200 and Tyr135 (Toh *et al.*, 2009). This interaction would in turn cause Arg204 to rotate such that the now larger binding pocket is suitable for ATP binding through Watson-Crick like interactions (Arg204 binds to position N1, while Asp200 binds to the N6 position). As Arthur (2009) has suggested, this proposed mechanism implies the existence of another binding site besides motif D. This is supported by addition at position 74 occurring in R204 variants, while it is prevented in R244 and R244-R204 variants (R244 must bind CTP since its variants show complete loss of incorporation at this position). In addition, ATP is the preferred substrate in both R204 and R244 variants (at least at positions 75 and 76), suggesting that both residues are involved in providing specificity to the binding pocket though size. This is also supported by the native enzyme demonstrating less of a preference for ATP at position 76 *in vitro*. Considering the interactions both arginines are involved in, substitutions may increase the binding pocket

size, to a degree in which CTP can no longer bind, whereas ATP would be able to form its regular interactions. In conclusion, the data provided here demonstrates a clear link between the two arginine residues as variants of both demonstrate loss of nucleotide specificity and efficiency.

4.9 Future work

Future experiments may strengthen the proposed mechanism that arginine 204 (and 244) may play in *C. glabrata* tRNA nucleotidyltransferase. Kinetic parameters for binding (K_M) of CTP and ATP when the enzymes are in contact with the different tRNA substrates would help us get more information. It would allow for the determination of the preferred substrate at every position in the native and variant enzymes. In order to verify that this enzyme does directly bind the first incoming CTP through Arg244, crystallization in the presence of a tRNA-N analogue and CTP would be ideal. In addition, radiolabeled CTP could be used with Arg204 and Arg244 variants to verify which residue is preferred for CTP binding at position 74. Substitutions of Asp200, Asp201, and Tyr135 may also be studied as was already done for Arg204 and Arg244 in order to clarify whether the amino acid triad is more involved in nucleotide addition at positions 75 and 76. Finally, the determination of the hydrodynamic radius (through dynamic light scattering) of the enzymes when bound to different substrates may shed some light on how the binding pocket changes in size during the specificity switch for both the native and variant enzymes.

5. References

- Arthur, J. (2009) "The role of arginine 244 in *Candida glabrata* tRNA nucleotidyltransferase" M.Sc. Chemistry thesis, Concordia University.
- Augustin, M. A., Reichert, A. S., Betat, H., Huber, R., Morl, M., Steegborn, C. (2003). Crystal structure of the human CCA-adding enzyme: insights into template-independent polymerization. *J. Mol. Biol.* 328, 985-994.
- Aravind, L., Koonin, E. V. (1999). DNA polymerase β -like nucleotidyltransferase superfamily: identification of three new families, classification and evolutionary history. *Nucleic Acids Res.* 27, 1609-1618.
- Best, A. N., Novelli, G. D., (1971). Studies with adenylyl (cytidylyl) transferase from *Escherichia coli* B II. regulation of AMP and CMP incorporation into tRNA^pCpC and tRNA^pC. *Arch. Biochem. Biophys.* 142, 539-547.
- Betat, H., Rammelt, C., Morl, M. (2010). tRNA nucleotidyltransferases: ancient catalysts with an unusual mechanism of polymerization. *Cell. Mol. Life Sci.* 9, 1447-1463.
- Bio-Rad Laboratories. (1995). Sequi-Gen® GT Nucleic Acid Electrophoresis Cell Instruction Manual. Retrieved January 5, 2011, from http://www.bio-rad.com/webroot/web/pdf/lsr/literature/Bulletin_9484.pdf.
- Bryson, J. W., Betz, S. F., Lu, H. S., Suich, D. J., Zhou, H. X., O'Neil, K. T., DeGrado, W. F., (1995). Protein design: a hierarchic approach. *Science* 270, 935-941.
- Cho, H. D., Oyelere, A. K., Strobel, S. A., (2003). Use of nucleotide analogs by class I and class II CCA-adding enzymes (tRNA nucleotidyltransferase): Deciphering the basis for nucleotide selection. *RNA* 9, 970-981.
- Cho, H. D., Verlinde, C. L. M. J., Weiner, A. M., (2007). Reengineering CCA-adding enzymes to function as (U,G)- or dCdCdA-adding enzymes or poly(C,A) and poly(U,G) polymerases. *Proc. Natl. Acad. Sci. USA* 104, 54-59.
- Creighton, T. E., (1989). Protein structure: a practical approach. IRL Press at Oxford University Press, Oxford, p.251-285.
- Creighton, T. E., (1993). Proteins: Structures and molecular properties. 2nd ed., W. H. Freeman and Company, New York, p.171-199 and p.261-328.
- Cudny H., Pietrzak, M., Kaczkowski, J., (1978). Plant tRNA nucleotidyltransferase I. Isolation and purification of tRNA nucleotidyltransferase from *Lupinus luteus* seeds. *Planta* 142, 23-27.

Current Protocols. "DNA/RNA Base Composition Calculator." Last accessed February 22, 2011. <http://www.currentprotocols.com/tools/dnarna-base-composition-calculator>.

DeLano, W. L., (2009). PyMOL Molecular Graphics System. DeLano Scientific, LLC. www.pymol.org.

Deutscher, M. P., (1972a). Reactions at the 3' terminus of transfer ribonucleic acid. III. Catalytic properties of two purified rabbit liver transfer ribonucleic acid nucleotidyltransferases. *J. Biol. Chem.* 247, 459-468.

Deutscher, M. P., (1973a). Synthesis and Functions of the -C-C-A Terminus of Transfer RNA. *Prog. Nucleic Acid Res. Mol. Biol.* 13, 51-92.

Deutscher, M. P., (1973b). Reactions at the 3' terminus of transfer ribonucleic acid. VII. Anomalous adenosine monophosphate incorporation catalyzed by rabbit liver transfer ribonucleic acid nucleotidyltransferase. *J. Biol. Chem.* 248, 3116-3121.

Deutscher, M. P., (1982). tRNA nucleotidyltransferase. In *The Enzymes*, P. D. Boyer, ed., Academic Press, New York. p.183-215.

Deutscher, M. P., (1983). *Enzymes of Nucleic Acid Synthesis and Modification, Volume II*, p168, CRC Press, Boca Raton.

Deutscher, M. P., (1990). Ribonucleases, tRNA nucleotidyltransferase, and the 3' processing of tRNA. *Prog. Nucleic Acid Res. Mol. Biol.* 39, 209-240.

Gasteiger, E., Hoogland, C., Gattiker, A., Duvaud, S., Wilkins, M. R., Appel, R. D., Bairoch, A., (2005). Protein Identification and Analysis Tools on the ExPASy Server; (In) John M. Walker: *The Proteomics Protocols Handbook*, Humana Press pp. 571-607.

Gibson, T. J., Higgins, D. G., (2007). ClustalW and ClustalX version 2. *Bioinformatics* 23, 2947-2948.

Hanic-Joyce, P. J., Joyce, P. B. M., (2002). Characterization of a gene encoding tRNA nucleotidyltransferase from *Candida glabrata*. *Yeast* 19, 1399-1411.

Holm, L., Sander, C., (1995). DNA polymerase β belongs to an ancient nucleotidyltransferase superfamily. *Trends Biochem. Sci.* 20, 345-347.

Hou, Y. M., (2000). Unusual synthesis by the *Escherichia coli* CCA-adding enzyme. *RNA* 6, 1031-1043.

Joyce, C. M., Steitz, T. A., (1994). Function and structure relationships in DNA polymerases. *Annu. Rev. Biochem.* 63, 777-822.

- Just, A., Butter, F., Trenkmann, M., Heitkam, T., Morl, M. Betat, H. (2008). A comparative analysis of two conserved motifs in bacterial poly(A) polymerase and CCA-adding enzyme. *Nucleic Acids Res.*, 36, 5212–5220.
- Kelley, L. A., Sternberg, M. J., (2009). Protein structure prediction on the web: a case study using the PHYRE server. *MJE Nature Protocols* 4, 363-371.
- Kim, S., Liu, C., Halkidis, K., Gamper, H. B., Hou, Y. M., (2009). Distinct kinetic determinants for the stepwise CCA addition to tRNA. *RNA* 15, 1827–1836.
- Li, F., Xiong, Y., Wang, J., Cho, H. D., Tomita, K., Weiner, A. M., Steitz, T. A., (2002). Crystal structures of the *Bacillus stearothermophilus* CCA-adding enzyme and its complexes with ATP and CTP. *Cell* 111, 815-824.
- Lim, K., Ho, J. X., Keeling, K., Gilliland, G. L., Ji, X., Rüker, F., Carter, D. C., (1994). Three-dimensional structure of *Schistosoma japonicum* glutathione S-transferase fused with a six-amino acid conserved neutralizing epitope of gp41 from HIV. *Protein Sci.* 3, 2233–2244.
- Lizano, E., Scheibe, M., Rammelt, C., Betat, H. Morl, M., (2008). A comparative analysis of CCA-adding enzymes from human and *E. coli*: Differences in CCA addition and tRNA 30-end repair. *Biochimie*, 90, 762–772.
- Martin, G., Keller, W., (1996). Mutational analysis of mammalian poly(A) polymerase identifies a region for primer binding and a catalytic domain, homologous to the family X polymerase, and to other nucleotidyltransferases. *EMBO J.* 15, 2593-2603.
- McGann, R. G., Deutscher, M. P. (1980). Purification and Characterization of a Mutant tRNA Nucleotidyltransferase *Eur. J. Biochem.* 106, 321–328.
- Milligan, J. F. & Uhlenbeck, O. C. (1989). Synthesis of small RNAs using T7 RNA polymerase. *Methods Enzymology* 180, 51-62.
- Neuenfeldt, A., Just, A., Betat, H., Morl, M., (2008). Evolution of tRNA nucleotidyltransferases: a small deletion generated CC-adding enzymes. *Proc. Natl. Acad. Sci. USA*, 105, 7953–7958.
- Oh, B., Pace, N. R., (1994). Interaction of the 3'-end of tRNA with ribonuclease P RNA. *Nucleic Acids Res.* 22, 4087-4094.
- Pain, R. H., (2004). Determining the Fluorescence Spectrum of a Protein. *Curr. Protoc. Protein Sci.* 38, 7.7.1-7.7.20.
- Peattie, D.A., (1979). Direct chemical method for sequencing RNA. *Proc. Natl. Acad. Sci. USA* 76, 1760-1764.

- Pleiss, J. A., Derrick, M. L., Uhlenbeck, O. C., (1998). T7 RNA polymerase produces 5'-end heterogeneity during in vitro transcription from certain templates. *RNA* 4, 1313–1317.
- Rether, B., Gangloff, J., Ebel, J. P., (1974). Studies on tRNA nucleotidyltransferase from baker's yeast 2. Replacement of the terminal CCA sequence in Yeast tRNA^{Phe} by several unusual sequences. *Eur. J. Biochem.* 50, 289-295.
- Sambrook, J., Maniatis, T., Fritsch, E.F., (1989). *Molecular Cloning* 2nd Ed., Cold Spring Harbor Laboratory Press, Cold Spring Harbor.
- Schürer, H., Lang, K., Schuster, J., Morl, M., (2002). A universal method to produce in vitro transcripts with homogenous 3'ends. *Nucleic Acids Res* 30, e56.
- Seth, M., Thurow, D. L., Hou, Y-M., (2002). Poly(C) synthesis by Class I and Class II CCA-adding enzymes. *Biochemistry* 41, 4521-4532.
- Shan, X., (2005). Characterization of a temperature-sensitive mutation that impairs the function of yeast tRNA nucleotidyltransferase. M.Sc. Chemistry thesis, Concordia University, Montreal.
- Shi, P. Y., Weiner, A. M., Maizels, N., (1998a). A top-half tDNA minihelix is a good substrate for the eubacterial CCA-adding enzyme. *RNA*, 4, 276–284.
- Shi, P. Y., Maizels, N. and Weiner, A. M., (1998b). CCA addition by tRNA nucleotidyltransferase: polymerization without translocation. *EMBO J.* 17, 3197–3206.
- Sikorski R.S., Hieter, P., (1989). A system of shuttle vectors and yeast host strains designed for efficient manipulation of DNA in *Saccharomyces cerevisiae*. *Genetics* 122, 19-27.
- Steitz, T. A., (1998). A mechanism for all polymerases. *Nature* 391, 231–232.
- Steitz, T. A., Smerdon, S. J., Jager, J., Joyce, C. M., (1994). A unified polymerase mechanism for nonhomologous DNA and RNA polymerases. *Science* 266, 2022–2025.
- Toh, Y., Takeshita, D., Numata, T., Fukai, S., Nureki, O., Tomita K., (2009). Mechanism for the definition of elongation and termination by the class II CCA-adding enzyme. *EMBO J.* 28, 3353-65.
- Tomita, K. and Weiner, A. M., (2001). Collaboration between CC- and A-adding enzymes to build and repair the 3'-terminal CCA of tRNA in *Aquifex aeolicus*. *Science* 294, 1334-1336.

Tomita, K., Fukai, S., Ishitani, R., Ueda, T., Takeuchi, N., Vassylyev, D. G., Nureki, O., (2004). Structural basis for template-independent RNA polymerization. *Nature* 430, 700-704.

Tomita, K., Ishitani, R., Fukai, S., Nureki, O., (2006). Complete crystallographic analysis of the dynamics of CCA sequence addition. *Nature* 443, 956-960.

Walker, J. M., (2002). *The Protein Protocols Handbook*. Humana Press, p. 57-67.

Wong, C., Sridhara, S., Bardwell, J. C. A., Jakob, U., (2000). Heating greatly increases speed of Coomassie Blue staining and destaining. *Biotechniques* 28, 426-432.

Yamada, Y. M., Ohki, H., Ishikura, H., (1983). The Nucleotide sequence of *Bacillus subtilis* tRNA genes. *Nucleic Acids Res.* 11, 3037-3045.

Yue, D., Maizels, N., Weiner, A. M., (1996). CCA-adding enzymes and poly(A) polymerases are all members of the same nucleotidyltransferase superfamily: Characterization of the CCA-adding enzyme from the archaeal hyperthermophile *Sulfolobus shibatae*. *RNA* 2, 895-908.

Yue, D., Weiner, A. M., Maizels, N., (1998). The CCA-adding enzyme has a single active site. *J. Biol. Chem.* 273, 29693-29700.

Zhu, L., Cudny, H., Deutscher, M. P., (1986). Mutation in *Escherichia coli* tRNA nucleotidyltransferase that affects only AMP incorporation is in a sequence often associated with nucleotide-binding proteins. *J. Biol. Chem.* 261, 14875-14877.